



Diploma thesis

Ring-opening polymerization started by photobase generators

conducted at the

Research Group Polymer Chemistry and Technology
Institute of Applied Synthetic Chemistry (IAS)
Technische Universität Wien

under supervision of

Senior Scientist Dipl.-Ing. Dr.techn. Patrick **Knaack**
Univ. Prof. Dipl.-Ing. Dr. techn. Robert **Liska**

by

Olja Dragojevic, BSc

01618791

Olja Dragojevic, BSc



Die approbierte gedruckte Originalversion dieser Diplomarbeit ist an der TU Wien Bibliothek verfügbar
The approved original version of this thesis is available in print at TU Wien Bibliothek.

Danksagung

An erster Stelle möchte ich mich herzlichst bei **Prof. Robert Liska** bedanken, der mir die Möglichkeit gegeben hat, meine Diplomarbeit in seiner Forschungsgruppe durchführen zu dürfen. Vielen Dank, nicht nur für die Gelegenheit, meine Diplomarbeit in einem so spannenden Fachgebiet verfassen und dabei viel Neues erlernen zu können, sondern auch für deine Unterstützung und Hilfe während meiner Arbeit.

Ein riesengroßes Dankeschön möchte ich meinem Betreuer **Dr. Patrick Knaack** aussprechen. Danke, Patrick, dass du mich so herzlich in die Arbeitsgruppe aufgenommen hast und mit deinem umfangreichen Wissen, deiner Geduld und deiner Hilfsbereitschaft auf meinem Weg begleitet und bestmöglich gefördert hast. Vielen Dank, dass du dir immer Zeit genommen hast, um mich zuzuhören und mit deinen Ideen meine Arbeit in die richtige Richtung getrieben hast.

Ebenso möchte ich **Larissa Alena Ruppitsch** herzlich danken für ihre großartige Unterstützung und Betreuung während meiner Bachelorarbeit. Danke, dass du mir das spannende Gebiet der Polymerchemie gezeigt hast und mir immer zur Seite gestanden bist!

Ein herzliches Dankeschön auch an **Klaus**, der mir beim Einstieg in die Thematik meiner Diplomarbeit eine große Hilfe war. Danke, Klaus, dass du dein Wissen mit mir geteilt, mich in die Thematik eingeführt und mir bei meinen ersten Schritten geholfen hast.

Ein riesiges Dankeschön an alle Mitglieder der **FBMC-Gruppe!** Ich möchte mich für die wunderschöne und unvergessliche Zeit bedanken. Danke die für wunderbare Zeit, eure große Hilfsbereitschaft, die gute Zusammenarbeit und die unzähligen schönen Momente, die meine Zeit im Labor unvergesslich gemacht haben.

Besonders danke an das **H45** – Klaus, Carola, Toni, Theresa, Tina und Miri – mit denen ich meine gesamte Arbeitszeit sehr genossen habe. Danke für die freundliche Arbeitsatmosphäre und eure helfenden Hände. Vielen Dank auch an **Kathi, Stefan und Davide** für eure wertvollen Ratschläge und hilfreiches Feedback während meiner Arbeit. Ein ebenso herzliches Dankeschön gilt **Dagmar, Jürgen, Walter und Heinz** für die zuverlässige organisatorische Unterstützung. Vielen Dank, dass ihr alle unterstützt und dafür sorgt, dass der Arbeitsalltag reibungslos abläuft.

Am Ende möchte ich mich von tiefstem Herzen bei meiner **Familie** bedanken. Danke, **Vanja**, dass du mich in allen Lebenslagen bedingungslos unterstützt, an mich glaubst und mir immer zur

Seite stehst. Deine Unterstützung bedeutet mir mehr, als Worte ausdrücken können. Ich freue mich sehr, auf das was kommt! Ein besonderer Dank geht an meine Eltern, **Darija und Miroslav**, für ihre unermüdliche Unterstützung während all der Jahre meines und dafür, dass sie mir stets ermöglicht haben, meinen eigenen Weg zu gehen. Ebenso danke ich meiner Schwester **Maja**, die mir immer den Rücken freigehalten, mich bestärkt und ermutigt hat. Ohne deine Unterstützung, Motivation und deinen Glauben an mich wäre dieser Weg nicht derselbe gewesen.

DANKE!

Abstract

Using light to start chemical reactions has become a powerful tool in modern chemistry, and its application to polymer and materials science has led to the well-known field of photopolymerization. This technology has been used extensively in radical-initiated curing for the past few decades, especially in adhesives, coatings, and more recently, in 3D printing. However, in recent years, the focus has increasingly shifted from radical to ionic photopolymerization. These ionic approaches, which rely on either cationic or anionic mechanism, have a number of significant benefits, such as enhanced control over polymer architecture and access to classes of polymers that were previously unavailable in 3D printing. Such features of ionic photopolymerization excite the use of this technology for emerging high-precision applications, including additive manufacturing.

At the heart of any photochemical reaction is the photoinitiation system. In this regard, photobase generators (PBGs) have become increasingly popular as promising alternatives to both radical and photoacid initiators. Compared to radical initiators, PBGs offer the significant advantage of being more controlled, while in contrast to photoacid generators, they avoid problems such as metal corrosion. These features broaden their applicability to highly sensitive areas, like electronics and automotive technologies, and at the same time make PBGs effective tools for facilitating the ring-opening polymerization of cyclic compounds, which happens to be the central focus of this work.

Therefore, the experimental work of this thesis focused on PBG-mediated ring-opening polymerization reaction of cyclic esters and amides. In the first part, the polymerization behavior of ϵ -caprolactone, ϵ -caprolactam, and 2-azetidinone was evaluated using different photobase generators. Hereby, particular attention was given to the temperature-dependent reactivity to evaluate its potential for applications in 3D printing at elevated temperatures.

The study also included the synthesis of N-substituted and N-unsubstituted 2-azetidinone derivatives, which were subsequently exposed to photoinduced ROP experiments under different conditions. Finally, the optimization of monomer conversion and polymerization kinetics was carried out by changing the reaction temperature, PBG concentration, and the amount of co-initiator.

Kurzfassung

Die Verwendung von Licht zur Auslösung chemischer Reaktionen hat sich zu einer leistungsstarken Strategie in der modernen Chemie entwickelt, und ihre Integration in die Polymer- und Materialwissenschaften hat das etablierte Forschungsfeld der Photopolymerisation begründet. Seit Jahrzehnten wird diese Technologie erfolgreich in radikal-initiierten Härtungsprozessen eingesetzt, insbesondere bei Beschichtungen, Klebstoffen und neuerdings auch im 3D-Druck. In den letzten Jahren hat sich die Aufmerksamkeit jedoch zunehmend auf die ionische Photopolymerisation verlagert. Diese ionischen Ansätze, die entweder auf kationischen oder anionischen Mechanismen beruhen, bieten mehrere Vorteile, darunter verbesserte Kontrolle über die Polymerarchitektur sowie Zugang zu zuvor unzugänglichen Polymerklassen im 3D-Druck. Solche Eigenschaften machen die ionische Photopolymerisation besonders attraktiv für neuartige, hochpräzise Anwendungen, einschließlich der additiven Fertigung.

Im Mittelpunkt jedes photochemischen Prozesses steht das photoinitiierende System. In diesem Zusammenhang haben Photobasengeneratoren (PBGs) zunehmende Aufmerksamkeit als vielversprechende Alternativen zu Photoradikalgeneratoren (PRG) und Photosäuregeneratoren (PAG) gewonnen. Im Vergleich zu PRGs bieten PBGs den Vorteil einer besseren Kontrolle, während sie im Gegensatz zu PAGs Probleme wie Metallkorrosion vermeiden. Diese Eigenschaften erweitern ihre Anwendbarkeit in sensiblen Bereichen, beispielsweise in der Elektronik- und Automobiltechnik, und machen PBGs zugleich zu effektiven Initiatoren für die Ringöffnungspolymerisation zyklischer Verbindungen.

Daher fokussierte sich diese Arbeit auf die PBG-vermittelte Ringöffnungspolymerisation von zyklischen Estern und Amiden. Im ersten Teil der Arbeit wurde das Polymerisationsverhalten von ϵ -Caprolacton, ϵ -Caprolactam und 2-Azetidinon untersucht, indem verschiedene PBGs verwendet wurden. Besonderes Augenmerk lag hierbei auf der temperaturabhängigen Reaktivität, um das Potenzial für Anwendungen im 3D-Druck bei erhöhten Temperaturen zu bewerten. Die Studie umfasste außerdem die Synthese von N-substituierten und N-unsubstituierten 2-Azetidinon-Derivaten, die anschließend photoinduzierten ROP-Experimenten unterzogen wurden. Abschließend wurde die Optimierung des Monomerumsatzes und der Polymerisationskinetik durch Anpassung der Reaktionstemperatur, der PBG-Konzentration und der Menge des Co-Initiators durchgeführt.

Table of Contents

Introduction		1
Additive Manufacturing		1
Photopolymerization		5
Ionic Photopolymerization		7
Photobase Generators		10
Ring-Opening Polymerization of Cyclic Amides (Lactams)		13
Ring-Opening Polymerization of Cyclic Esters (Lactones)		19
Objective		22
State of the Art		23
Results and Discussion	R&D	Exp.
1. Reactivity Study of ϵ -Caprolactone	29	65
1.1 Photobase Screening	29	65
1.2 Cationic Reference Systems based on Photoacid Initiation	34	65
2. Reactivity Study of ϵ -Caprolactam	38	66
2.1 Photobase Screening	38	66
2.2 ATR-FTIR Characterization	39	66
3. Reactivity Study of 2-Azetidinone	41	66
3.1 Photobase Screening	41	66
3.2 Optimizing the Model System	44	67
3.2.1 Temperature Screening	44	67
3.2.2 PBG Concentration Screening	46	67
3.2.3 Co-Initiator Concentration Screening	46	67
3.3 Gravimetric analysis	49	67
4. Reactivity Study of 2-Azetidinone Derivatives	50	68
4.1 N-Substituted 2-Azetidinone Derivative	51	68
4.1.1 Synthesis of 1-Benzyl-4-Methyl-2-Azetidinone	51	
4.1.2 Synthesis of 1-Benzyl-2-Azetidinone	52	68
4.1.3 Photo-DSC Study of 1-Benzyl-2-Azetidinone	53	70
4.2 N-Unsubstituted 2-Azetidinone Derivative	55	70
4.2.1 Synthesis of 4-Methyl-2-Azetidinone	55	
4.2.2 Synthesis of 3-Methyl-2-Azetidinone	56	70
4.2.3 Photo-DSC Study of 3-Methyl-2-Azetidinone	57	72
4.2.4 Optimizing the Model System	59	72
4.2.4.1 Temperature Screening	59	72

4.2.4.2 PBG Concentration Screening	61	72
4.2.4.3 Co-Initiator Concentration Screening	62	72
4.2.5 Gravimetric Analysis	64	72
Conclusion		74
Materials and Methods		77
Abbreviations		81
Literature		83

Introduction

Additive Manufacturing

Additive Manufacturing Technologies (AMTs), which were initially known as Rapid Prototyping (RP) and are currently generally referred to as 3D printing, were first introduced in the early 1980s and have continuously evolved since then and significantly influenced conventional manufacturing methods.¹ Unlike conventional subtractive or formative manufacturing techniques, additive manufacturing is based on a fundamentally different idea of building objects by adding material layer by layer. In addition to reducing material waste, this method also makes the production of extremely complex and customized geometries quite affordable.²⁻⁴

The manufacturing process starts with the creation of a digital representation of the object either by computer aided design (CAD) software or sometimes by 3D scanning of a real object (Figure 1, a). After that, the design is stored as a standard transformation language (STL) file and is virtually divided into two-dimensional layers by slicing software (Figure 1, b). These layers serve as instructions for the 3D printer, which constructs the object through a computer-guided, layer-by-layer process, with temporary support structures incorporated to stabilize any overhanging parts (Figure 1, c). Once the 3D printing is done, the post-processing techniques are usually employed to get the desired final properties of the part.^{5,6}

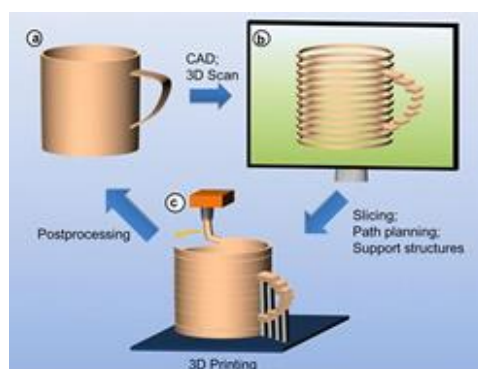


Figure 1: Principle of additive manufacturing technologies⁶

Conventional manufacturing methods can be divided into two main categories: formative and subtractive. Formative techniques, such as injection moulding, forging, and casting, use mechanical forces to shape materials without changing their overall volume.⁷ For instance, injection molding is the process which uses pre-formed mold cavities to shape molten

thermoplastic into the desired product form.^{8,9} These are typically large-scale production methods, as the cost per unit decreases with higher production volume, unlike additive manufacturing, where costs remain relatively constant regardless of quantity.¹⁰ On the contrary, subtractive manufacturing refers to the removal of material from solid blocks to achieve the desired geometric shape. This is usually achieved by mechanical operations such as milling, drilling, and turning, which are in most cases performed with computer numerical control (CNC) machines. Although this method provides high precision, it results in a large amount of waste material and generally requires more energy and time, especially if the geometries are complex. Despite the fact that both formative and subtractive are widely used, they still have significant drawbacks. The main disadvantage is the reliance on specialized tooling like molds or dies that lead to a higher initial production cost. In addition, technical and physical limitations of the mold design or tool access may cause situations where it is very difficult or even impossible to manufacture complex or highly customised geometries.²⁻⁴

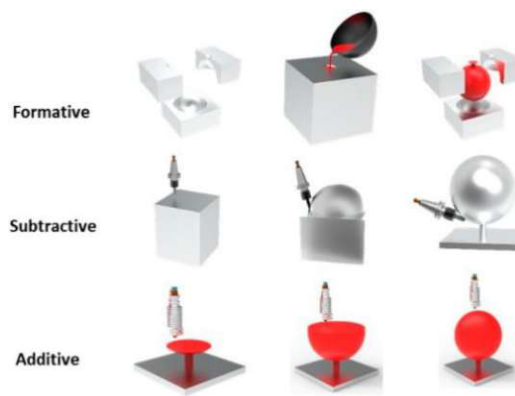


Figure 2: Types of manufacturing techniques¹¹

Most of these limitations are overcome by Additive Manufacturing Technologies (AMTs), which use a radically different production strategy. AMTs work on the principle of creating three-dimensional structures from digital 3D models layer by layer instead of removing material from a solid block or using molds. Therefore, the direct manufacture of parts with complex geometric features, for instance, internal cavities and undercuts, is feasible without the use of special tools or molds. Moreover, since only the required quantity of material is used during the manufacturing process, AMTs thus reduce material waste. For this reason, additive manufacturing is not only more economical for small production runs, such as single-piece, customized prototypes, but also more environmentally friendly. The other benefit

is design flexibility because changes to a part can be done directly in the virtual model without the need to change physical tools or equipment.⁶

Since their initial development, AMTs have made significant progress and evolved from experimental research tools into the methods of industrial manufacturing that are extensively applied now. Today, they are utilized across a broad spectrum of industries, including aerospace,^{12–15} automotive,^{15–17} consumer goods,¹⁸ and even medical sector.^{19–21} Their ability to fabricate both extremely large structures, such as building components, and microscale features used in electronics and photonics, demonstrates the versatility of these technologies.²

As the use of AMTs has expanded, so has the variety of methods available. These methods can be classified based on different parameters, such as the material state (solid, liquid, or gas), the type of manufacturing process (such as curing, dispensing, sintering, or binding), or the purpose of the printed prototype (visual, functional, material, or production prototype).²²

Additive manufacturing methods that use liquid materials, such as photopolymers that are hardened by light, are called liquid-based AM. These technologies are highly precise and can produce very fine details, often surpassing other AM methods in terms of resolution.⁶ Among liquid-based additive manufacturing methods, one of the earliest and most extensively utilized techniques is Stereolithography (SLA). It operates by exposing photopolymers to ultraviolet (UV) light, which starts a photopolymerization reaction that eventually leads to the hardening of the material and the formation of a polymer network.^{23,24} SLA is one of the first developed AM technologies and the term was first introduced by Chuck Hull in a patent from 1984.²⁵ Over time, stereolithography has been divided into two principal versions based on the light source: Laser Stereolithography (L-SL) and Digital Light Processing (DLP). Both methods use a vat filled with photocurable resin and are therefore classified as vat photopolymerization techniques. L-SL forms each layer by scanning the resin surface with a focused laser beam along the x-y plane, selectively curing areas layer-by-layer to build the part. DLP-SL, however, uses a mirror-based system to direct light from an LED source to the resin, projecting the entire layer pattern at once. While this greatly reduces printing time, it may result in slightly lower resolution due to limitations in projector pixel density. After each layer is cured, the platform is moved along the z-axis in both methods, thus new resin can fill the gap for the next layer. The process generally operates in a top-down setup, where the light source is located

underneath the vat, and the printed part is gradually lifted up. However, some systems, especially those based on DLP, can also work in a bottom-up approach, where the object is formed as it moves downward into the resin. While this method reduces resin consumption, it can make the separation of the cured layer from the transparent base of the vat more difficult.^{6,22,26}

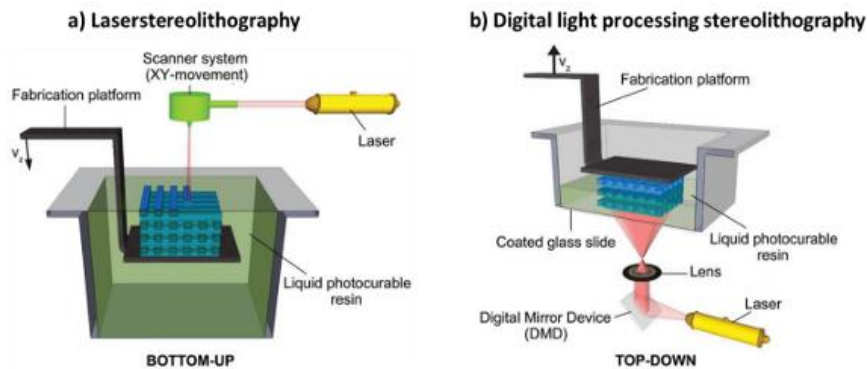


Figure 3: Different SLA-setups: a) Laserstereolithography in a bottom-up approach. b) Digital light processing stereolithography in a top-down approach²⁶

A significant innovation in vat photopolymerization is Hot Lithography, first introduced by Cubicure in 2017. This method essentially broadens the features of conventional SLA and DLP technologies by using elevated temperatures up to 140 °C, during the layer-by-layer printing process. In most cases, a bottom-up setup is employed with a transparent resin vat, and either a laser-based (L-SL) or digital light processing (DLP) system is used for photopolymerization.²⁷ The application of heat, often provided by infrared sources, improves monomer mobility and substantially increases reaction kinetics, thereby allowing the processing of resins that have a high-viscosity or are of low-reactivity and cannot be easily processed at room temperature. Consequently, Hot Lithography extends the variety of materials that can be printed, allowing for the processing of challenging formulations such as epoxy resins,²⁸ phenolic compounds,²⁹ cyanate esters,³⁰ and cyclic carbonates.³¹ In addition to extending material compatibility, this process imparts better mechanical and thermal performance to the printed parts. Research has shown that components created by Hot Lithography can exhibit a higher degree of monomer conversion, greater tensile strength, and better storage modulus than the ones produced at ambient conditions. Such enhancements make Hot Lithography a promising technology for the fabrication of tougher and more durable components, while also increasing the application potential of additive manufacturing in industries utilizing high-performance polymers.³²

Photopolymerization

Over the past years, researchers have been paying more and more attention to photopolymerization, the process of using light to start polymerization reactions. This light-induced method allows for rapid and precise synthesis of polymeric materials, thus ranking it as one of the most promising techniques in modern chemistry. Since its introduction in the 1960s, photopolymerization has been recognized as a key technology in many industries, particularly in additive manufacturing and 3D printing, due to its ability to produce extremely complex structures. Its efficiency and versatility have also influenced the development of advanced manufacturing processes, such as coatings and other high-precision applications.^{33,34}

Contrary to thermal operating technologies that require high temperatures to form initiating species, light-induced polymerization is a process that can be started by irradiation, thus allowing the reaction to be started and stopped on demand. Besides that, replacing conventional mercury lamps with LEDs as UV irradiation source leads to a further decrease in energy consumption during the curing process.^{35,36} Furthermore, photopolymerization reactions are usually performed in bulk, so the use of solvents is greatly minimized or completely eliminated, and the volatilization of organic compounds is also avoided. From a practical perspective, the light-induced nature of photopolymerization provides both precise spatial control by directing a focused light beam to specific areas, and temporal control by switching the light on, i.e. it allows the high control over time and space of polymerization even at large scales. Such a feature is particularly important, as it enables the production of materials with highly detailed structures.^{33,37} In addition, photopolymerization provides the rapid curing capability, thus a shorter production time and lower costs. Due to these unique features, photopolymerization has been recognized as a technology of growing interest, especially in fields like coatings, 3D printing, photolithography, etc.³⁷

Photopolymerization is a general term for a process that transforms liquid organic precursors or monomers into solid polymers by a chemical reaction induced by light absorption. A photocuring process requires only three elements: a monomer, a photoinitiator (PI), which is selected depending on the monomer's functional groups and the polymerization class they belong to, and a suitable light source. The photoactive species, also known as the photoinitiator, absorbs light during the photopolymerization reaction and changes into an

excited state, generating a highly reactive species. This step is called the initiation of the polymerization process, which is then followed by gradual addition of monomers and oligomers to form a growing polymer chain (Figure 4).^{37,38}

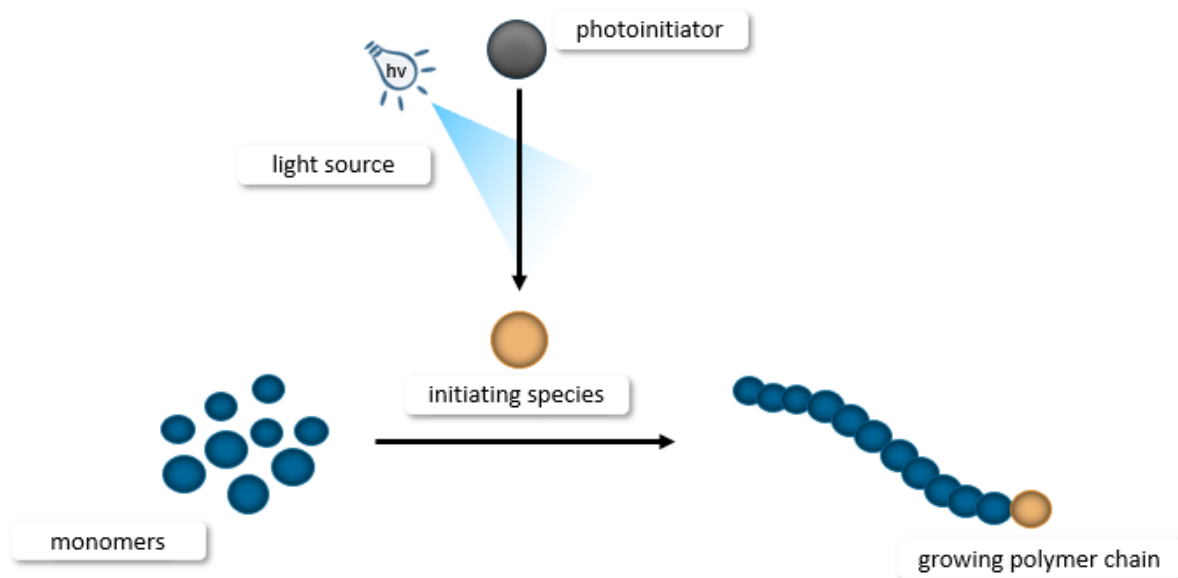


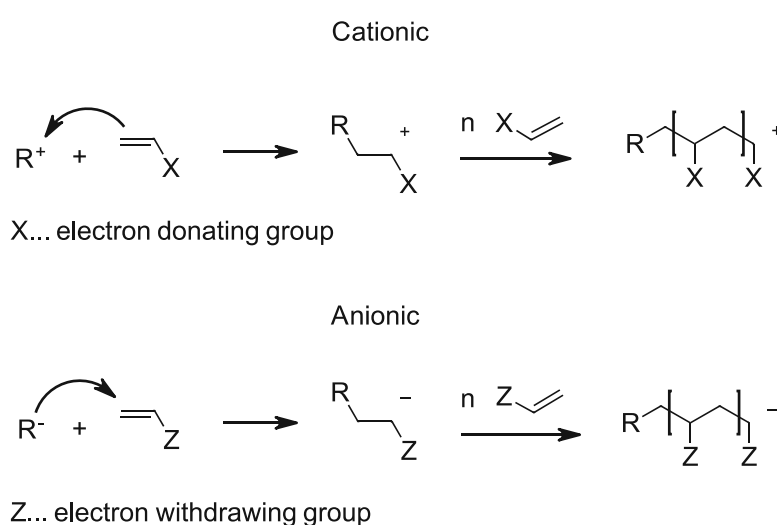
Figure 4: Graphical representation of a photopolymerization reaction

As already mentioned, the photoinitiator (PI) is an essential element in a photosensitive formulation. The ability of a photoinitiator to absorb light is related to specific structural motifs in its molecular structure, namely chromophores. Chromophores allow the photoinitiator to capture light at a particular wavelength, initiating the conversion of the light energy into the chemical energy.³⁹

Depending on the structure of the photoinitiator, the resulting species may be radicals, ions (cations or anions), acids, or bases, which are then capable of initiating free radical, cationic, or anionic polymerization. Ionic polymerization reactions, in particular, have the big advantage of insensitivity towards oxygen compared to free radical polymerizations, and typically lead to lower shrinkage of materials after curing.⁴⁰

Ionic Photopolymerization

Ionic photopolymerization begins with the generation of cationic or anionic species depending on the chemical properties of the monomer, as opposed to free radical polymerization (FRP), where the initiator generates reactive radical species. In general, monomers having electron donating groups in their structure tend to undergo cationic initiation, whereas those with electron withdrawing groups are more prone to anionic initiation. Nevertheless, there are also certain monomers like cyclic esters, which can polymerize through both cationic and anionic mechanisms.^{41,42}



Scheme 1: General mechanism of anionic and cationic polymerization⁴²

In addition to allowing the polymerization of a broader spectrum of monomers, ionic photopolymerization provides several distinct advantages over free radical polymerization (FRP). These advantages include insensitivity towards oxygen, which otherwise acts as an inhibitor in FRP and therefore, an inert atmosphere is not necessary during the ionic curing process. Moreover, various cyclic monomers are able to be polymerized through either cationic or anionic ring-opening routes, which results in the materials having reduced shrinkage after being cured. In addition, ionic polymerization technique is known to have "living" nature, meaning that the chain-ends remain active and continue to grow when more monomer is supplied. In contrary to free radical polymerization, there is almost no termination reaction during polymerization caused by the recombination of two polymer chains, which ensures high efficiency and conversion.⁴²⁻⁴⁴

Since the initiation reaction begins with the absorption of light by the PI, it is necessary to choose an initiating system that aligns with the available light source. Hence, photoacid generators (PAGs) and photobase generators (PBGs) can be used as highly effective initiators for cationic or anionic polymerization processes.³⁴

Cationic photoinitiation begins with the release of a super acid from a photoacid generator. Upon light absorption, PAGs transition into an excited singlet state. As this state is very unstable, they follow either homolytic or heterolytic decomposition process resulting in the generation of reactive intermediate species. Regardless of the decomposition pathway, the produced intermediates subsequently abstract protons from a hydrogen donor in the surrounding reaction mixture to generate super acids, which initiate the cationic polymerization reactions.^{45–47}

This super acid is a strong Brønsted or Lewis acid, and the most commonly used PAGs are salts composed of diaryliodonium or triarylsulfonium cations paired with non-nucleophilic anions.^{48,49} The ions in a PAG salt have clearly separated roles and influence the cationic photopolymerization process differently. The cation carries the chromophoric group, undergoes photodecomposition process and determines all photochemistry related properties such as absorption maximum or thermal stability. On the other hand, the anion influences the strength of the generated super acid and determines all polymer chemistry related properties, including initiation efficiency. Among these, perfluorometallates are highly interesting, for example SbF_6^- , AsF_6^- , PF_6^- , and BF_4^- .⁵⁰

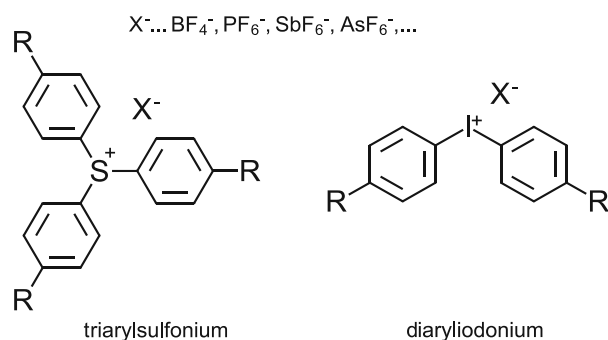


Figure 5: Examples of onium salts with different cations

As already mentioned, cationic photopolymerization expands the range of accessible monomers, as many compounds can be readily activated by a cationic initiating species, including epoxides, lactones and cyclic ethers such as oxetanes. The ring-opening

polymerization of epoxides and ϵ -caprolactone, in particular, has become feasible with the use of PAGs, thus opening numerous avenues for printing new materials with specialized properties.^{34,51}

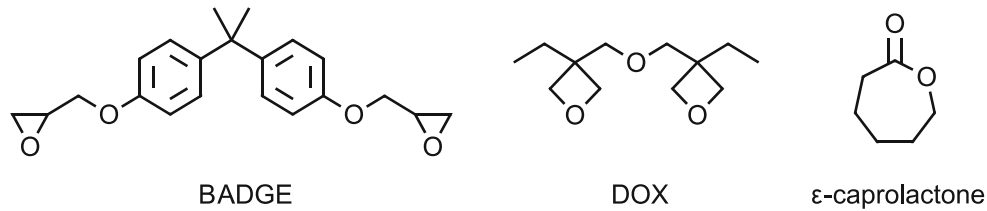


Figure 6: Structures of some common monomers suitable for the cationic photopolymerization, e.g. bisphenol-A-diglycidylether (BADGE), 3,3'-[oxybis(methylene)]bis[(3-ethyl)oxetane] (DOX), ϵ -caprolactone

As a counterpart to photoacid generators, photobase generators (PBGs) can be utilized to initiate anionic polymerization under light exposure. Nevertheless, the PBGs development has advanced significantly slower compared the well-established PAGs, resulting in limitations of their industrial applications. This is primarily due to challenges related to the strength of the liberated base and the efficiency of its release. Hence, industrial use of anionic photopolymerization remains restricted, preventing the extensive use of many potentially valuable monomers in large-scale processes.^{34,51}

Photobase Generators

Photobase generators are photoactive compounds capable of generating a base when irradiated with light. The released base can be employed as an initiating species for photo-induced anionic polymerizations, as well as thiol-Michael, thiol-isocyanate, epoxy polymerization, and thiol–thiol reactions.^{52,53}

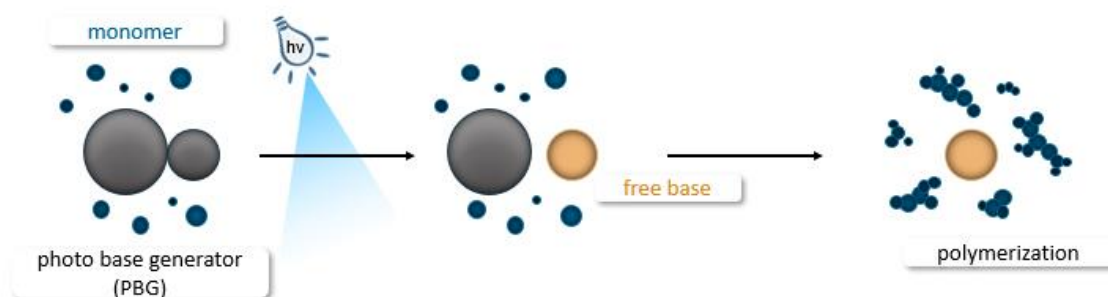
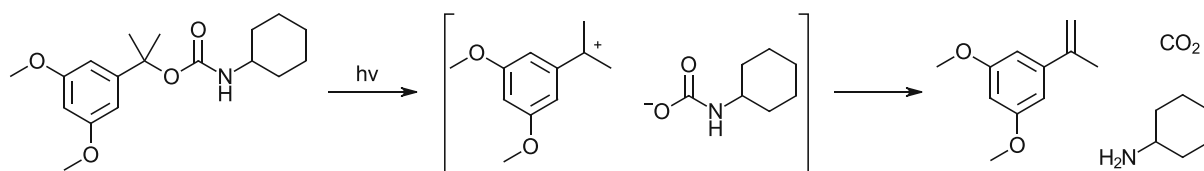


Figure 7: Irradiation of a photobase generator and generation of a free base that further initiates photopolymerization

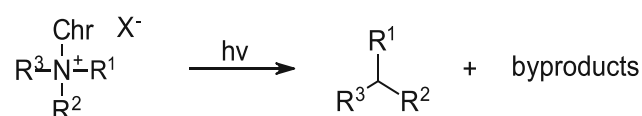
Although still less explored and developed than photoradical generators (PRGs) or photoacid generators (PAGs), PBGs offer several notable advantages, including their insensitivity to oxygen. In other words, they can be used in air, which is a very important feature when compared to free radical polymerization. Moreover, PBGs do not undergo corrosive interactions with metallic substrates, making them especially well-suited for applications in industries that depend on metals, such as automotive and electronics.^{45,53}

The concept of organic photobase generators was first introduced in 1990 by Cameron and Fréchet.⁵⁴ For their work, they used a photosensitive carbamate capable of releasing basic amines when exposed to light. Carbamates, which are primary or secondary amines protected with a photolabile group, undergo photodecarboxylation when irradiated, thus resulting in the release of free amines. However, the released primary and secondary amines are usually weak bases and therefore not highly effective in initiating anionic polymerizations. Therefore, increasing efforts have been dedicated to developing PBGs capable of cleaving stronger bases, including tertiary amines, phosphazenes or even carbenes.⁴⁵



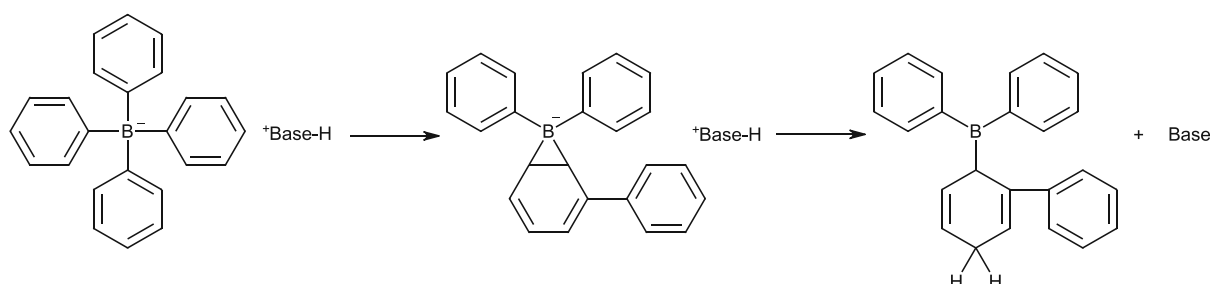
Scheme 2: Photosensitive carbamate compound and generation of a primary amine *via* UV light, reported by Cameron and Fréchet⁵⁴

Besides carbamates, quaternary ammonium salts (QAs) are an important class of compounds that can be used for base generation. First reported by Sarker et al. in 1998 and further developed in the early 2000s, these compounds enabled the release of tertiary amines for the first time, thereby significantly expanding the applicability of photobase generators to a broader range of bases.⁵⁵ Upon irradiation, a quaternary amine bonded to a chromophore undergoes C-N bond cleavage to release the corresponding amine, which is able to enact as initiator. However, a number of QA-based compounds have exhibited low thermal stability and stability in organic solvents, as well as poor solubility.⁴⁵



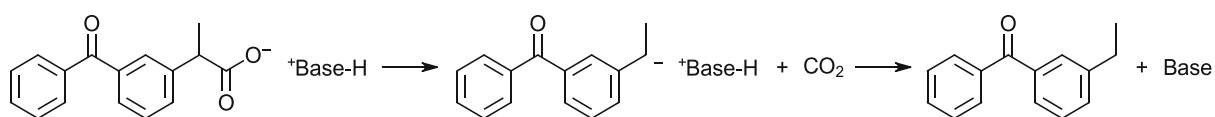
Scheme 3: Generation of a tertiary amine upon irradiation from a quaternary ammonium salt, reported by Sarker et al.⁵⁵

Significant progress in the development of photobase generators (PBGs) was made by the introduction of a novel activation mechanism based on photoinduced deprotonation. In 2008, Sun et al. introduced salts comprising a protonated, inactive base that gets activated only through photoinduced deprotonation.⁵⁶ In particular, borates that undergo structural rearrangement upon irradiation have been found to be very efficient anions, due to their tolerance toward strong bases, such as phosphazenes and carbenes.^{45,56}



Scheme 4: Photodecomposition mechanism of a borate-based PBG⁴⁵

This approach was further advanced by Arimitsu et al.,⁵⁷ who introduced carboxylate containing chromophores that release the base through deprotonation as well, but in this case through photodecarboxylation rather than structural rearrangement. This innovation was a tremendous step forward, as the chromophore structure could be altered to optimize photochemical properties, thereby increasing quantum yield and extending absorption to longer wavelengths. One of the best-known and most widely used carboxylate-based PBGs are the salts of ketoprofen, which undergo photodecarboxylation reactions with a high quantum yield upon irradiation.^{45,57}



Scheme 5: Mechanism of a base generation *via* photodecarboxylation of a carboxylate-based PBG⁴⁵

Together, these developments have broadened the scope of possible PBGs, as well as their overall applicability in polymerization techniques in recent years, and several PBGs have even become commercially available.^{45,58}

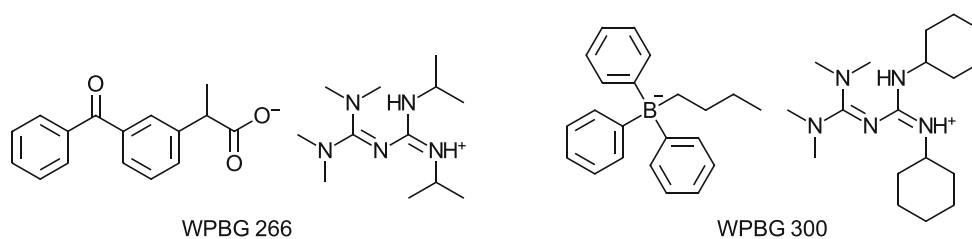


Figure 8: Examples of commercially available PBGs

Ring-Opening Polymerization of Cyclic Amides (Lactams)

In general, lactams are considered one of the largest classes of monomers that are used in the group of polymerizable heterocyclic compounds. They are especially valuable for creating polyamides and copolyamides with a variety of adjustable properties because of their capacity to go through ring-opening polymerization (ROP). The chemistry of polyamides has gone through a significant change in the last ten years as a result of the major improvements in ROP techniques and a wide range of available monomers, which have allowed for precision in the control of polymer structure and their functionalities. Today, ROP of lactams is still the main method for synthesizing polyamides and copolyamides.^{59,60}

The nitrogen or carbon substituents on lactam can be used to provide the structural variations of these compounds far beyond their basic industrial application for the synthesis of aliphatic polyamides, such as PA6 derived from ϵ -caprolactam. This allows for the creation of many analogues with specific properties and opens up new avenues for specialized applications.⁵⁹ These include different bicyclic and bridged ring systems, dilactams, and heteroatom-modified lactams. Interestingly, β -lactams are the basic structural motif of many important antibiotics such as carbapenems, cephalosporins, and penicillins. Substituted β -lactams, which constitute one of the most important components for the synthesis of bioactive β -polypeptides, have also shown their relevance outside the field of conventional polymer applications.^{59,61}

When it comes to polymerization, the kinetics and thermodynamics of the ring-opening process can be significantly influenced by the exact position, number, and size of substituents on the lactam ring, particularly at the nitrogen or carbon atoms. From a kinetic point of view, C-substituted lactams are generally less reactive than unsubstituted ones. The main reason of this decrease in reactivity is mainly due to the steric hindrance and the electronic effects. The large substituents near the reactive site may make it difficult for nucleophiles to attack, while electron-donating substituents may modify the amide moiety's electron density and thus make it less nucleophilic. These factors may prevent the transition state formation or its stabilization, which would slow the ring-opening process in comparison to unsubstituted lactams. Because of the conformational changes they introduce, substituents on the lactam ring have the ability to change the enthalpy and entropy of ring-opening polymerization. The growing polymer chain may have new intramolecular interactions due to the presence of the substituents that mostly decreases the enthalpy of polymerization. In regard to entropy, the

substitutes may decrease entropy by decreasing the mobility of the chain in the polymer backbone. The mentioned factors have especially great effect in the case of small ring lactams, whose conformational freedom is already limited. These effects can therefore cause the equilibrium to move in favour of the monomer, decreasing the thermodynamic favorability of polymerization and favouring ring closure over chain propagation.^{59,62,63}

Substitution at the nitrogen atom introduces a distinct set of challenges for ring-opening polymerization. Most significantly, because N-substitution prevents the formation of a lactam anion, the monomer is no longer appropriate for anionic ROP. As a result, anionic mechanisms are unable to produce polymers made from specific N-substituted monomers, such as 2-pyrrolidone and 2-piperidone. For these lactams, other initiation methods such as cationic or acidolytic polymerization are necessary. The ability of cis-lactams to undergo polymerization is influenced by N-substitution to a greater extent than by C-substitution. N-substituents, particularly those possessing electron-donating properties, interfere with the resonance stabilization of the amide bond, thereby decreasing reactivity, mainly in smaller, more strained rings. The effect of N-substitution is also dependent on the size of the ring. It is most significant in smaller rings and gradually diminishes as the ring expands. For instance, while four-membered N-substituted 2-azetidiones remain sufficiently strained and reactive to undergo polymerization, five-, six-, and seven-membered N-substituted lactams generally do not polymerize. Interestingly, for larger lactams with ring sizes ranging from eight to thirteen members, N-substitution does not necessarily prevent polymerization, particularly when using acidolytic or hydrolytic initiation methods.^{59,64}

The ring-opening polymerization of lactams can follow different pathways depending on the reaction conditions and the monomer structure. Among these, cationic, anionic, and hydrolytic ROP methods have been the most extensively explored ones. Each pathway has a different mechanism of initiation and propagation, thus enabling the tailored polymer structures and properties that are suitable for specific industrial and scientific applications.^{59,60}

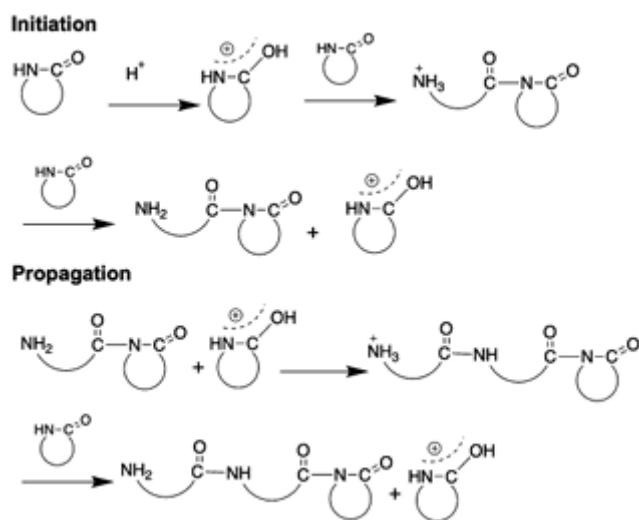
Even if cationic ring-opening polymerization (CROP) is by far less prevalent than anionic one in industrial applications, it is still the most relevant method when it comes to the polymerization of N-unsubstituted and N-substituted lactams, thus giving access to polymers that are difficult to obtain in other ways. For this purpose, a variety of initiators have been investigated, among

them strong protic inorganic acids, Lewis acids, metal halides, carbenium ions, and various acyl derivatives.⁶⁰

The cationic ring-opening polymerization (CROP) of lactams has a rather complex mechanism and depends on the nature of the initiation system as well as the structural features of the monomer, mainly the type of substitution.⁶⁰ This type of polymerization is performed under strict anhydrous conditions to prevent the occurrence of side reactions. Under these conditions, the species that plays a key role in the initiation and propagation is a lactam cation generated upon acid coordination with the monomer.⁵⁹

The lactam molecule's protonation behaviour is, in fact, a key component of this process. Protonation may take place either at the nitrogen atom or at the carbonyl oxygen atom in unsubstituted lactams. In tautomeric equilibrium, a small but significant amount of protonated nitrogen species is also present, although protonation on oxygen is thermodynamically favored. This N-protonated form is less stable due to the lack of resonance stabilization, however, it has significantly increased acylation character. Therefore, it can simply initiate the polymerization process by attacking the nitrogen atom of the lactam molecule. Then, the neutral lactam molecule attacks the N-protonated lactam species, which is a highly electrophilic center. The monomer is fast acylated due to this interaction resulting in the formation of the aminoacyl-lactam cation in the form of an ammonium salt. From a mechanistic point of view, this process is considered to involve a number of consecutive steps. The first one is the formation of a bond between the nitrogen atom of the attacking lactam and the electrophilic carbon of the protonated monomer. Ring opening is then facilitated by an internal proton transfer from one nitrogen atom to the other. The reactive aminoacyl intermediate is finally generated by a second proton transfer, this time from a hydroxyl group to an ammonium nitrogen. After the formation of the reactive aminoacyl intermediate, chain propagation proceeds through repeated acylation reactions. These occur when the neutral amine end group, which is a strong nucleophile, attacks additional protonated lactam monomers. Thus, the polymer chain is lengthened by the addition of new units. This propagation step uses proton transfer equilibria to continuously regenerate the reactive species necessary for chain growth and it is, therefore, similar to the initiation step. The impact of termination and side reactions can be reduced by carefully choosing initiators and managing

reaction parameters like temperature and solvent system, even though they may happen, especially when there is trace moisture or other contaminants present.^{59,60}



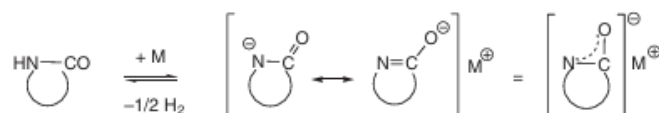
Scheme 6: Mechanism of cationic ring-opening polymerization (CROP) of lactams⁶⁰

Among the available methods for lactam polymerization, anionic ring-opening polymerization (AROP) is the most extensively employed technique. Such a method is typically performed under anhydrous conditions and is only applicable to N-unsubstituted lactams that have a hydrogen atom on the amide group, as a free N-H proton is necessary for the generation of the reactive lactam anion.⁵⁹ In most cases, initiation is done by a strong, non-nucleophilic base, and a co-initiator, either one originating from the lactam or formed in situ with acylating agents, is also used.⁶⁵ One of the major benefits of AROP is its very high polymerization rate, which is a direct consequence of its very low activation energy. The process is very effective in bulk systems, where the polymerization temperature is determined by the melting point of the lactam. Furthermore, it is the only polymerization route capable of successfully converting five- and six-membered lactams, such as 2-pyrrolidone and 2-piperidone, into high-performance polyamides.^{59,60}

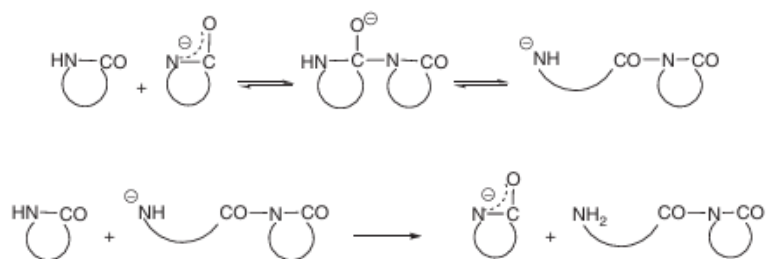
The generation of a reactive lactam anion, usually achieved by deprotonating the amide nitrogen with a strong base, starts the polymerization process. Due to the delocalization of their negative charge across the amide and carbonyl groups, the lactamate and lactam anion both exhibit resonance stabilization. The anionic species is stabilized by this delocalization, but its nucleophilic nature is not greatly diminished. The lactamate thus turns out to be the main source of the free lactam anion, which is the active species that initiates the polymerization process.^{59,65} The formed lactam anion attacks the carbonyl group of another lactam monomer

and starts the reaction, generating a tetrahedral intermediate. Consequently, an amine anion is formed, which is very reactive due to the fact that it is not resonance-stabilized as the lactam anion. An imide dimer (N-acyl lactam) is obtained when the amine anion rapidly abstracts a proton from a new monomer molecule, simultaneously regenerating a new lactam anion. Chain propagation is achieved by repeated nucleophilic attacks of the lactam anion on the endocyclic carbonyl group of the N-acyl lactam, which acts as the non-ionic growth center. During this step, the acylation of the lactam anion takes place, thus a new amide bond is created and the polymer chain is extended.⁵⁹ Propagation is much faster because of the higher electrophilicity of the N-acyl lactam and the stability of the propagating amide anion as compared to the initial stages of polymerization. Besides, the polymer amide anion may also engage in proton exchange with the unreacted monomers, thereby regenerating the lactam anion and maintaining the chain propagation.^{59,66–68}

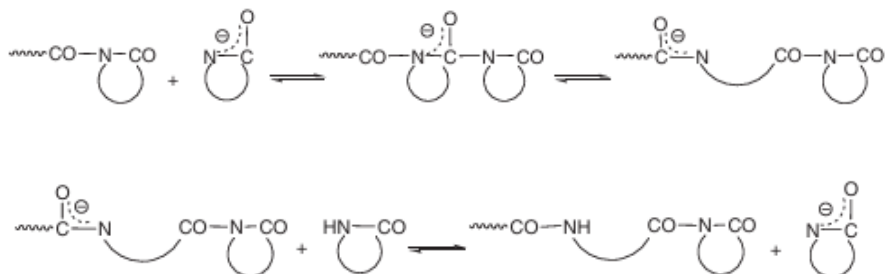
Preinitiation



Initiation

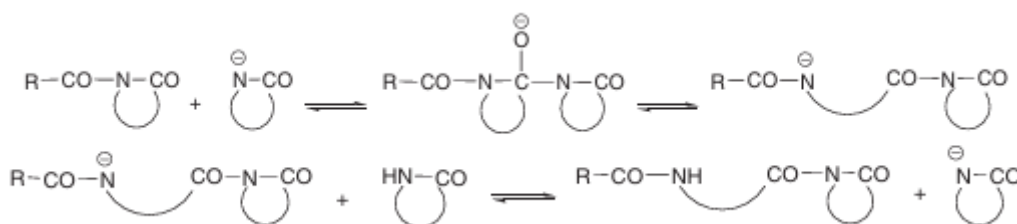


Propagation



Scheme 7: Mechanism of anionic ring-opening polymerization (AROP) of lactams⁵⁹

However, employing strong bases alone in anionic polymerization of lactams has some restrictions, as it normally needs high temperatures and the polymerization rates are slow. Unwanted side effects are more likely in these circumstances. These problems can be effectively solved by adding N-acyl lactam structures to the system. When such reactive species are present from the beginning, they significantly accelerate the initiation step and allow the polymerization to proceed at much lower temperatures. This approach also broadens the applicability of the anionic method to less reactive lactams, such as 2-pyrrolidone and 2-piperidone, for which the spontaneous formation of imide dimers is otherwise unfavorable.⁵⁹ Due to their exceptional reactivity, N-acetyl- ϵ -caprolactam, N-propionyl- ϵ -caprolactam, and N-bis-isophthaloyl- ϵ -caprolactam are among the oldest and most commonly used N-acyl lactams. The utilization of N-acyl lactam activators eliminates the need for an initial activation phase, thus permitting the immediate chain initiation as the polymerization is started.^{59,69}



Scheme 8: Introduction of N-acyl lactam activators in the AROP of lactams⁵⁹

Ring-Opening Polymerization of Cyclic Esters (Lactones)

Lactones are a significant class of monomers, which have been widely utilized in the production of polyesters that are both biodegradable and biocompatible. The most popular representatives are lactide, glycolide, and ϵ -caprolactone, whose corresponding polymers have been extensively applied in the biomedical field, including drug delivery systems, scaffolds for tissue engineering, and sutures.⁷⁰ Besides that, these materials have also attracted a lot of interest as environmentally friendly replacements for conventional petroleum-derived plastics due to their biodegradability and attractive mechanical properties.^{71–73}

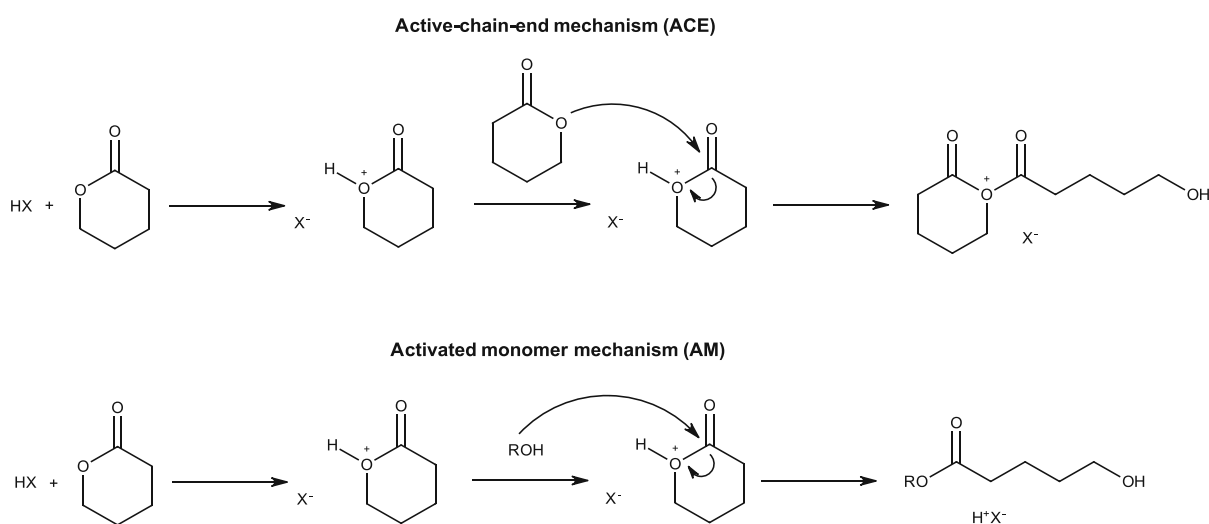
The size and the ring strain of the monomer greatly influence the reactivity of lactones in polymerization processes. As a consequence of their highly strained rings, four-membered lactones tend to polymerize easily and they can achieve full conversion even under milder conditions. Five-membered rings, such as γ -butyrolactone, on the other hand, have long been thought to be non-polymerizable because of their minimal ring strain, which makes them thermodynamically stable and resistant to polymerization.⁷⁴ Recent developments, however, have shown that its polymerization is feasible.⁷⁵ Under appropriate conditions, six-membered lactones, such as δ -valerolactone, and seven-membered ϵ -caprolactone, easily undergo ring-opening polymerization and are frequently researched and used in controlled polymerization techniques.^{76,77}

ROP remains the principal method for transforming lactone monomers into high-performance polyesters. The process relies on the cleavage of the ring structure caused by various catalysts and initiators, among them photogenerated acids and bases.⁷⁸ The choice of the polymerization pathway – whether anionic, cationic, or coordinated – greatly influences the polymerization kinetics, molecular weight distribution, end-group functionality, and stereochemical configuration.⁷⁹

The active chain end (ACE) mechanism and the activated monomer (AM) mechanism are the two main mechanistic pathways through which cationic ring-opening polymerisation (CROP) of lactones can proceed. Both pathways are started by electrophilic activation of the monomer. The reaction conditions, notably the presence of hydroxyl-functional compounds and the type of used acid catalyst, define the exact pathway.⁸⁰

In the ACE mechanism, the initiator – most often a protonic acid, Lewis acid, an alkylating, or an acylating agent – promotes polymerization through electrophilic attack on the endocyclic oxygen atom of the lactone ring. The acyl–oxygen bond is thus cleaved, and a reactive oxonium ion is generated at the growing chain end. Propagation then occurs through successive nucleophilic attacks by additional monomer molecules on this oxonium-terminated chain. However, this mechanism tends to be accompanied by undesirable side reactions. Backbiting reactions are usually caused by positive charges at the chain end, resulting in cyclic byproducts, and intermolecular chain transfers can also lead to broader molecular weight distributions as well.^{80–82}

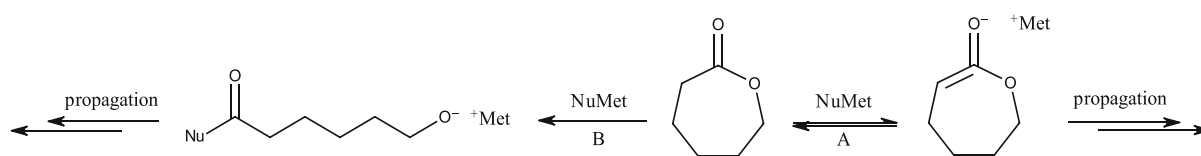
Alternatively, when the polymerization is performed with alcohols or diols, the reaction may proceed *via* the activated monomer (AM) mechanism. Here, cationic species refers to the protonated monomer instead of the growing chain end of the polymer. Propagation proceeds through nucleophilic attack of a hydroxyl group on the activated monomer, with the hydroxyl end group being regenerated in the process. One of the greatest advantages of the AM mechanism is the absence of a charged species on the propagating chain, thus the possibility of side reactions such as cyclization and backbiting is very much reduced. Therefore, AM-based CROP yields better molecular weight control, lower dispersity, and the possibility of a living polymerization behavior, especially when monomer addition is carefully controlled.^{80,82,83}



Scheme 9: Polymerization of lactones *via* ACE and AM mechanisms⁴²

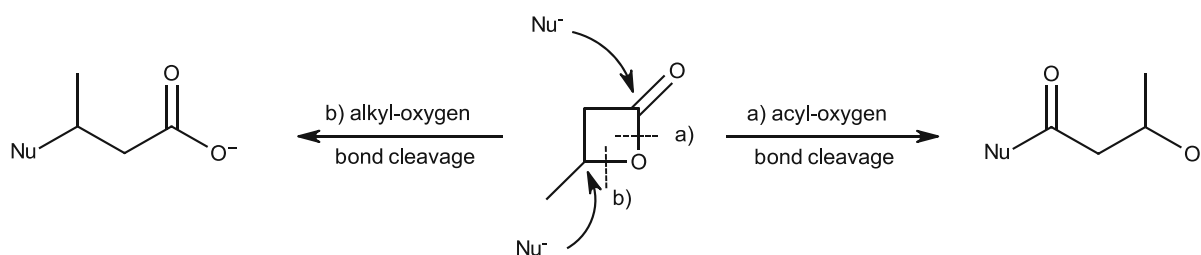
Anionic ring-opening polymerization (AROP) is a well-established and extensively studied method used to produce aliphatic polyesters from lactone monomers. Usually, the process is started by strong nucleophilic agents, typically alkali metals, their oxides, or alkali metal

naphthalenide complexes. To increase reactivity and solubility, these are often combined with crown ethers. The size and structure of the lactone ring, together with the nucleophilicity and basicity of the initiator, are the major factors that decide the reaction mechanism.⁷⁶ Bigger lactones, such as lactide and ϵ -caprolactone (ϵ CL), are generally involved in ring-opening *via* acyl–oxygen cleavage, thus an alkoxide ion is generated as the active species, which continues to propagate through successive nucleophilic attacks on additional monomer molecules. Depending on the choice of initiator, the polymerization may begin either through nucleophilic attack on the carbonyl carbon or *via* monomer deprotonation, with propagation proceeding *via* an alkoxide intermediate.^{79,84}



Scheme 10: Initiation step in the AROP of lactones *via* a) monomer deprotonation or *via* b) nucleophilic attack

On the other hand, four-membered β -lactones show a significantly different behavior, primarily due to their high ring strain and polarity. These monomers can undergo ring opening *via* attack on the carbonyl carbon or on the carbon adjacent to the endocyclic oxygen atom, resulting in the formation of carboxylate and alkoxide end groups. Although β -lactones have been the most extensively studied group of cyclic esters in AROP, their reactivity demands very precise control of reaction parameters in order to avoid side reactions.⁸⁴



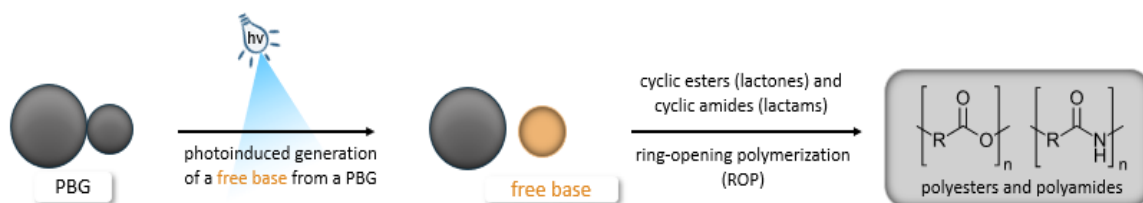
Scheme 11: Ring-opening of lactones by a) O–acyl or b) O–alkyl bond cleavage⁸⁵

Overall, AROP has a much lower probability of side reactions like backbiting compared to cationic ring-opening polymerization. Mainly, this method is appealing for the production of linear, high-molecular-weight polyesters, as it eliminates the possibility of rearrangements due to the absence of positively charged intermediates.^{82,84}

Objective

In recent years, lithography-based additive manufacturing technologies have gained considerable attention. Currently, these processes mostly rely on radical photopolymerization, employing conventional acrylates and methacrylates as monomers in combination with radical photoinitiators. However, due to the polymerization mechanism, such systems are prone to oxygen inhibition and exhibit high volumetric shrinkage. To avoid these drawbacks, anionic photoinduced ring-opening polymerization (AROP) can be employed as an oxygen-insensitive reaction that often produces materials with reduced polymerization-induced volumetric shrinkage.

The primary objective of this work is to evaluate the photoinduced polymerization reactivity of two classes of anionically curable cyclic monomers, lactones and lactams, using different photobase generators as initiators. In the initial stage of the work, a screening of three literature-known monomers should be conducted to assess their reactivity and suitability for PBG-mediated AROP reactions. The influence of polymerization temperature on both reactivity and the molecular weight of the resulting polymers should be systematically examined to provide a base for further development. Finally, reaction conditions including temperature, PBG concentration, and co-initiator concentration should be optimized.



State of the Art

Cyclic compounds, primarily cyclic esters and cyclic amides, are among the most fascinating classes of monomers, as their ring-opening polymerization allows obtaining polymers with exact structures and tailored properties, thus being very appropriate for a large range of uses. Such potential continues to inspire extensive research into their preparation and modification.^{59,86}

In ring-opening polymerization, the main driving force stems from the release of ring strain and the increased conformational freedom gained upon transformation of cyclic monomer into a linear or branched polymer – a phenomenon that has been extensively studied in the literature for a variety of cyclic compounds, both in bulk and in solution.⁸⁷

Conventional ROP of cyclic esters typically relies on metal-based catalysts, with stannous octoate being the most widely used due to its FDA approval as a food stabilizer and its non-cytotoxicity, making it suitable for biomedical applications.^{88,89} Other metal-based initiators, such as metal alkoxides, can also be employed. Yet, it is often quite difficult to remove the residual traces of their remains completely, and this makes it difficult to use them in sensitive fields such as medical or electronic industries.^{89–91} In the case of cyclic amides, conventional ROP is generally performed under acidic or basic catalysis. The literature includes different possibilities, with strong bases (e.g., sodium hydride,⁵⁹ potassium tert-butoxide^{92,93}) being usually mentioned for anionic polymerization, and strong acids like trifluoromethanesulfonic acid, phosphoric and metaphosphoric acids, or hydrochloric acid allowing cationic routes.⁵⁹

However, the use of photopolymerization to cure these monomers is still a bit rare in general, especially in the case of anionic initiators. One of the main problems of anionic photopolymerization is the scarcity of photobase generators that are both very efficient and highly reactive. Nevertheless, photoinduced ROP of cyclic esters and amides has recently attracted a lot of attention and evolved into a rapidly expanding research field due to the benefits it has over conventional ROP methods. After these improvements, research has mainly focused on developing photoinitiators, which can generally be classified into two major categories: photoacid generators (PAGs) and photobase generators (PBGs). Among them, PAGs – capable of releasing strong acids upon irradiation – have been studied more extensively.³⁴

Classical examples include sulfonium and iodonium salts that have been employed to start cationic polymerization of cyclic esters or to incorporate these monomers in crosslinked polymer networks.^{48,49}

For instance, Sangermano et al. combined the degradability of PCL with the crosslinking potential of multifunctional epoxides to prepare degradable coatings, employing a PAG-mediated photo-ROP process.⁹⁴ In another study, Barker and Dove achieved the photopolymerization of ϵ -caprolactone and δ -valerolactone using a triarylsulfonium salt, while Boyer and co-workers employed a reversible merocyanine-based, visible-light-regulated PAG to achieve temporal control over the ROP of these monomers simply by switching light on or off.⁹⁵

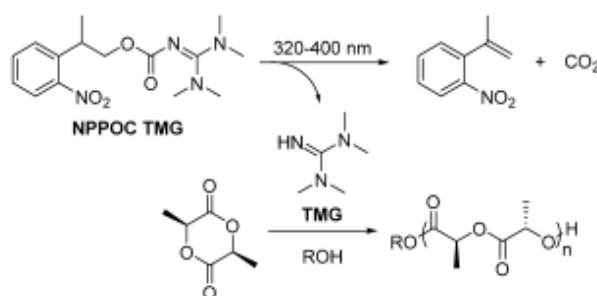
Building upon these previous reports, Mete et al. conducted a detailed study on cationic ROP of ϵ -caprolactone initiated by a sulfonium salt acting as a photoacid generator. When exposed to ultraviolet light, the sulfonium salt in their system went through photolysis and a strong Brønsted acid was released, which thus activated the monomer causing ring-opening and polymer chain growth. Also, the use of difunctional crosslinkers, such as multifunctional epoxides, was quite influential in reducing the gelation time and in the production of robust, crosslinked polymer networks. The authors suggested these materials as promising candidates for advanced coating technologies and microfabrication, since they were able to fabricate dimensionally stable materials with tunable mechanical and degradation properties. Nevertheless, these reactions still had to be carried out at elevated temperatures to obtain sufficient reactivity and the use of difunctional crosslinkers was necessary to decrease the gelation time.³⁰

With the advancement of PAG-mediated photo-ROP, the development of photobase generators (PBGs) was a great boost to anionic photoinduced ring-opening polymerization (ROP), although early reports were relatively rare. These systems, which made significant progress during the 2000s, were the subject of a detailed review by Shirai et al., who recognized their potential and at the same time highlighted the problem of the still existing shortage of highly efficient PBGs that could be used for practical ROP applications.⁹⁶

Surprisingly, despite the development of photobase generators (PBG), just a handful of UV-triggered ROP examples have been reported at the time. A major step forward was achieved in 2008, when Sun and co-workers introduced a PBG composed of a protonated TBD

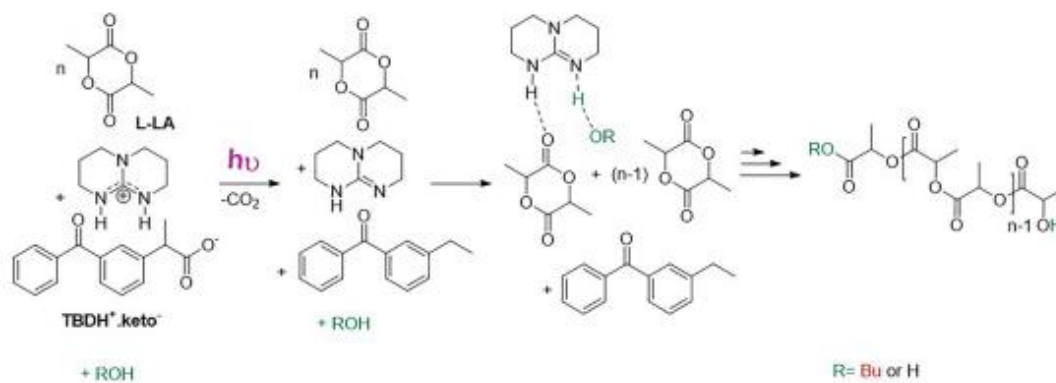
cation paired with a UV-sensitive tetraphenylborate counteranion. Upon irradiation at 254 nm, this system released free TBD, which in the presence of 1 mol% n-hexanol as an initiator enabled the bulk polymerization of ϵ -caprolactone, reaching 70 % monomer conversion after just 5 minutes of exposure, followed by post-baking at 60 °C for 8 hours. In their work, they showed that bicyclic guanidinium tetraphenylborate could be used to mediate living anionic ROP of ϵ -caprolactone. However, the process was limited by a relatively low quantum yield of 0.18 for TBD release at 254 nm.⁵⁶

A notable advancement milestone was achieved by Dove and co-workers with the development of NPPOC-protected tetramethylguanidine (NPPOC-TMG) for the photoinduced ROP of L-lactide and related lactones. The TMG base in this system was masked with a ketoprofenate group and was released upon exposure to 320–400 nm light, thus making the monomer conversion complete within 3 minutes only. In addition to being the pioneering instance of photocaged TMG in the ROP of L-lactide, the method also allowed for the exact control of molecular weight distribution.⁹⁷



Scheme 12: Photoinduced ROP of L-lactide using NPPOC-TMG, reported by Dove et al.⁹⁷

Placet et al. also devised a similar idea and reported the UV-triggered ROP of L-lactide through photocaged superbases. They activated PBG TBD-ketoprofenate upon irradiation at 254 nm in a dichloromethane solution at room temperature, thus releasing free TBD and initiating fast polymerization. This method made it possible to control the process “on-demand” and achieve full monomer conversion within 3 minutes of irradiation. In both the absence and the presence of 1-butanol as an initiator, the system produced linear PLA chains, and the use of an excess of 1-butanol relative to the photolabile catalyst gave polymers with well-defined molecular weights and narrow dispersity.⁹⁸



Scheme 13: Photoinduced ROP of L-lactide Using TBDH⁺.keto⁻, reported by Placet et al.⁹⁸

These achievements were revisited by Zivic et al.,⁴⁵ who concentrated their work on the design of organic PBGs and the difficulties arising from their use, followed by a review from Pei and co-workers that pointed out the fast development and the expanding scope of PBG chemistry and its applications.⁹⁹

The latest innovations in PBG technology have shifted the focus from harmful UV to visible-light-responsive systems, offering enhanced safety and deeper light penetration. In 2023, Yu et al. disclosed two novel BODIPY-based photobase generators, which could liberate the strong base tetramethylguanidine (TMG) upon visible LED irradiation, with a thiol-ene Michael “click” reaction serving as the activation pathway.¹⁰⁰

Most significantly, the field has even evolved toward practical applications. Honda and colleagues recently reported vat ring-opening photopolymerization method using PBGs to enable the 3D printing of fully degradable polymeric structures. This invention presented a sustainable vat-photopolymerization method that employs light-triggered base generation to convert lactone or carbonate monomers into crosslinked but degradable networks – thus allowing both high resolution and recyclability in additive manufacturing.¹⁰¹

In the past ten years, the development of PBG technology has been progressively more related to additive manufacturing applications. The combination of photo-ROP with vat photopolymerization, particularly Hot Lithography, enables the fabrication of high-resolution degradable structures with customized mechanical and degradation properties. Nevertheless, enhancements in photochemical efficiency, monomer scope, and selectivity of these systems are still quite needed to fully realize their potential for industrial-scale 3D printing.

Results and Discussion

In order to identify PBGs capable of promoting the ring-opening polymerization of cyclic monomers, a preliminary screening of various literature-known compounds was conducted. For this purpose, three different PBGs were selected due to availability (Figure 9), including two commercial PBGs (WPBG-266 and WPBG-300) from FUJIFILM Wako Chemicals Europe GmbH, which liberate an organic Brønsted superbase – a biguanide ($pK_{BH^+} = 31.8$),^{102,103} and a photobase referred to as TP, which sets P_2 -phosphazene superbase ($pK_{BH^+} = 33.5$) free.¹⁰⁴

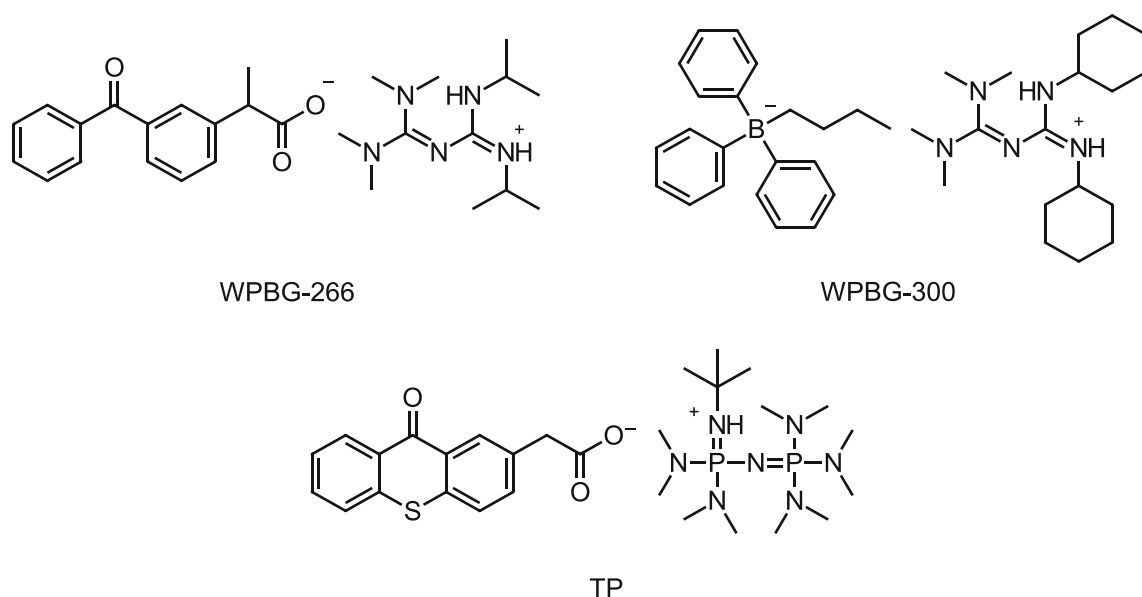
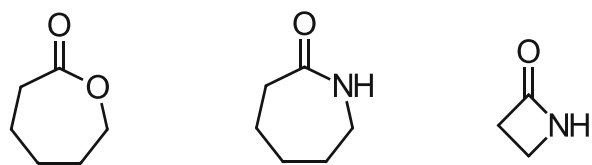


Figure 9: Structures of PBGs used in the screening of potential initiator for ROP of cyclic monomers

The primary objective of this thesis was to establish the occurrence of ring-opening polymerization of cyclic monomers upon use of different PBGs as initiators, hence, different monomers were selected and their reactivity was studied. The chosen monomers were ϵ -caprolactone, ϵ -caprolactam, and 2-azetidinone. ϵ -Caprolactone and ϵ -caprolactam were selected primarily because they are among the most frequently studied seven-membered cyclic lactones and amides, which have been deeply investigated and are generally considered to provide reproducible results. Nevertheless, seven-membered cycles normally have low ring strain, which is the reason for the limited heat evolution observed during their polymerization. Therefore, a four-membered lactam – 2-azetidinone – was selected as a promising candidate due to its significantly higher ring strain, which provides a stronger driving force for ring-opening polymerization reactions and increases the likelihood of exothermic behavior.^{86,105} An overview of investigated monomers is given below (Figure 10).



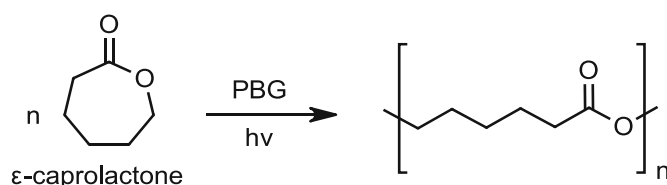
ϵ -caprolactone ϵ -caprolactam 2-azetidinone

Figure 10: Structures of cyclic monomers selected for the model system

In order to investigate the reactivity of all selected monomers and ensure a coherent analysis, photo differential scanning calorimetry (photo-DSC) was chosen as a reliable, controllable and consistent curing method. To ensure a comparable analysis of all monomers, the curing of all samples was carried out using this method, although it was expected that in not all cases an exothermic signal might be visible. The main advantage of employing the photo-DSC method to cure the samples was the ability to precisely replicate the same reaction parameters for all samples, including temperature, irradiation time and intensity. An Omnicure 2000 from Lumen Dynamics with glass fiber light waveguides was used as the light source. The curing of samples took place under N_2 -atmosphere at 25, 50, 70, 80, 90, 100 or 120 °C, with each formulation containing the respective monomer being irradiated with a spectral range of 320 – 500 nm at an intensity of $80 \pm 1 \text{ mW cm}^{-2}$. Once the desired temperature was reached, the system was equilibrated for 4 minutes before being irradiated twice for 5 minutes. Moreover, the polymerized samples were analyzed immediately after irradiation *via* $^1\text{H-NMR}$ and GPC analysis to assess the outcome of the reaction.

1. Reactivity Study of ϵ -Caprolactone

Among all lactones, ϵ -caprolactone stands out as probably the most extensively investigated and widely used, primarily due to its low cost, abundance, biocompatibility and availability from renewable sources.^{106,107} Given its well-established ability to undergo anionic ring-opening polymerization (AROP),¹⁰⁶ this seven-membered cyclic ester was selected as the first model monomer whose reactivity should be tested with three photobase generators (PBGs), namely WPBG-266, WPBG-300, and TP.



Scheme 14: ROP of ϵ -caprolactone

1.1 Photobase Screening

A photo-DSC study of ϵ -caprolactone was performed using three different photobases – WPBG-266, WPBG-300, and TP. For the formulation containing 2 mol% WPBG-266, 2 mol% benzyl alcohol were employed as a co-initiator.¹⁰² In order to facilitate rapid and complete conversion during the photocleavage of the ketoprofen anion, 0.02 mol% 9,10-dibutoxyanthracene (DBA) were utilized as a sensitizer.^{108–111} In contrast, the formulations containing either 2 mol% WPBG-300 or 2 mol% TP utilized 2 mol% N-acetylcaprolactam as the co-initiator. Moreover, as the literature suggests, DBA was replaced with 0.02 mol% isopropylthioxanthone (ITX) as the sensitizer.¹⁰³

The samples were irradiated for 300 s with 80 mW cm^{-2} (320 – 500 nm light source) and the temperature was varied between 25 °C and 120 °C. Despite attempts to monitor the exothermic behavior of the reaction *via* photo-DSC analysis, negative peak areas were observed, which were calculated from the difference between the second exposure phase and the first exposure phase. This outcome indicates that no measurable heat release occurred during the photopolymerization process and therefore calorimetric information could not be obtained. The photo-DSC curves of ϵ -caprolactone cured with 2 mol% WPBG-266 recorded at different temperatures are presented below (Figure 11).

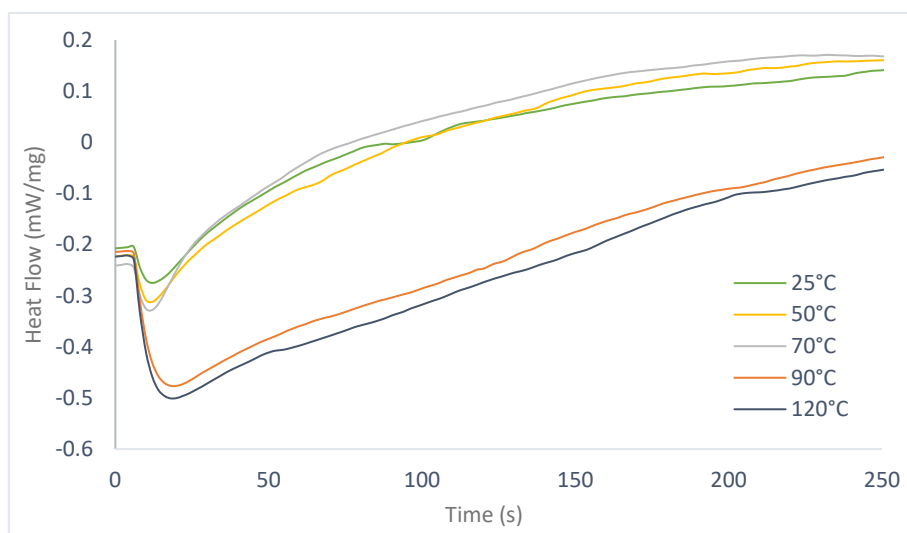


Figure 11: Photo-DSC analysis of ϵ -caprolactone cured with 2 mol% WPBG-266

In ring-opening polymerizations (ROP), the exothermic nature of the reaction is primarily driven by the release of ring strain. This strain arises from angular and torsional deformations in the monomer's cyclic structure. Normally, three- and four-membered rings exhibit significant ring strain, making them highly reactive and releasing considerable heat during polymerization.^{86,105,112} In contrast, five- and six-membered rings are less strained due to their geometry, resulting in lower reactivity. Seven-membered cycles, such as that of ϵ -caprolactone, generally exhibit similarly low ring strain, which explains the limited heat evolution observed during their polymerization.^{86,105} Consequently, the polymerization enthalpy of ϵ -caprolactone is relatively low – approximately -30 kJ mol^{-1} – and is primarily associated with the modest release of ring strain.¹¹³ Therefore, the heat released during polymerization could not be detected using photo-DSC analysis, as shown in Figure 11.

Nevertheless, $^1\text{H-NMR}$ was utilized to assess the degree of polymerization by analyzing the polymer end-groups, as well as the conversion of monomer. During photopolymerization reaction, achieving complete monomer conversion is desirable for ensuring good properties of the resulting polymer. New signals or an altered shape of existing peaks, especially broadening or shifts, are signs of polymerization. Such signs of polymerization can be found when comparing the spectra of cured samples with those of the unreacted formulation. Therefore, conversion can be determined by comparing the integral values of the emerging polymer signal at 4.0 ppm to the unreacted monomer (Figure 12).

$$\text{conversion (\%)} = 100 \cdot \frac{I_P}{I_M + I_P}$$

I_P ... polymer peak

I_M ... monomer peak

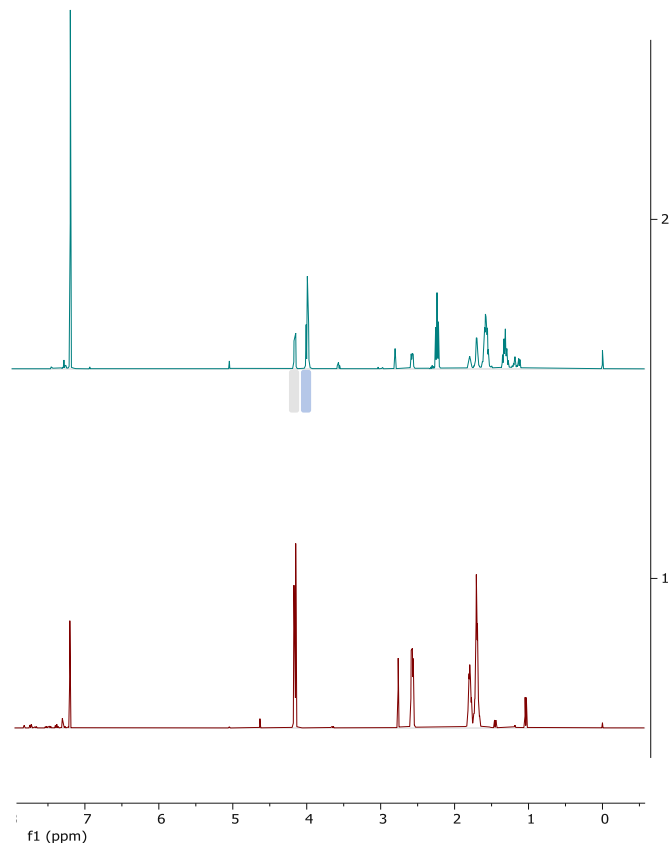


Figure 12: 1) Example of the ¹H-NMR spectra of formulation before irradiation (red curve below) and 2) after ROP reaction of ε-caprolactone cured with WPBG-266 (blue curve above), and formula used for conversion calculation (on the left)

When focusing on the area between 3.5 and 4.0 ppm of the polymerized samples, peaks attributed to terminal methylene groups can be detected (Figure 13). As the ring-opening polymerization results in the appearance of a terminal OH group, comparing the methylene protons near this group with those in the backbone can be used to estimate the degree of polymerization.

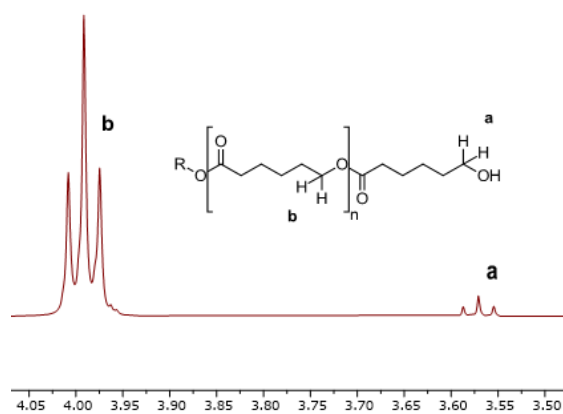


Figure 13: Example for P_n determination by the integration of the protons next to the end group and the methylene proton in the main chain

The $^1\text{H-NMR}$ results show a clear temperature dependence of the photoinitiated ring-opening polymerization of ϵ -caprolactone for all investigated photobases (Figure 14 and Figure 15).

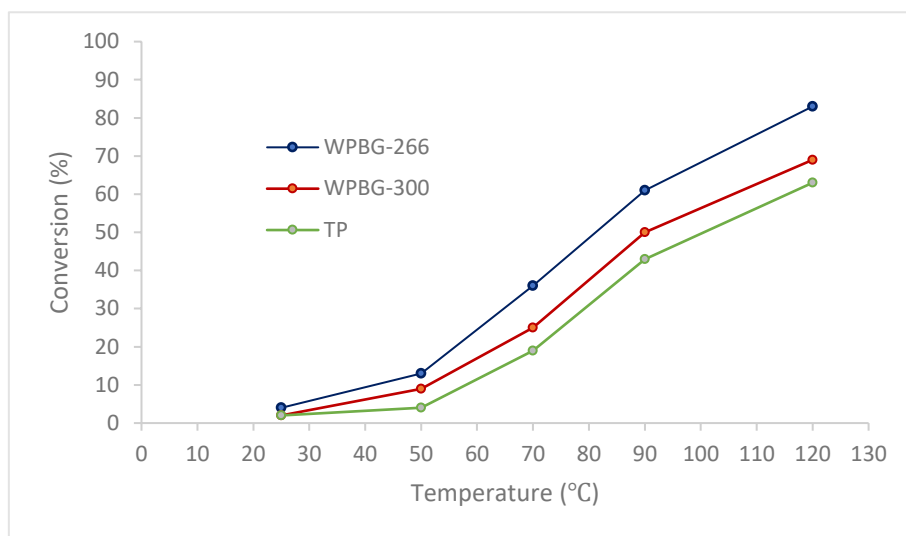


Figure 14: Conversion values of ϵ -caprolactone for samples cured with WPBG-266, WPBG-300 and TP

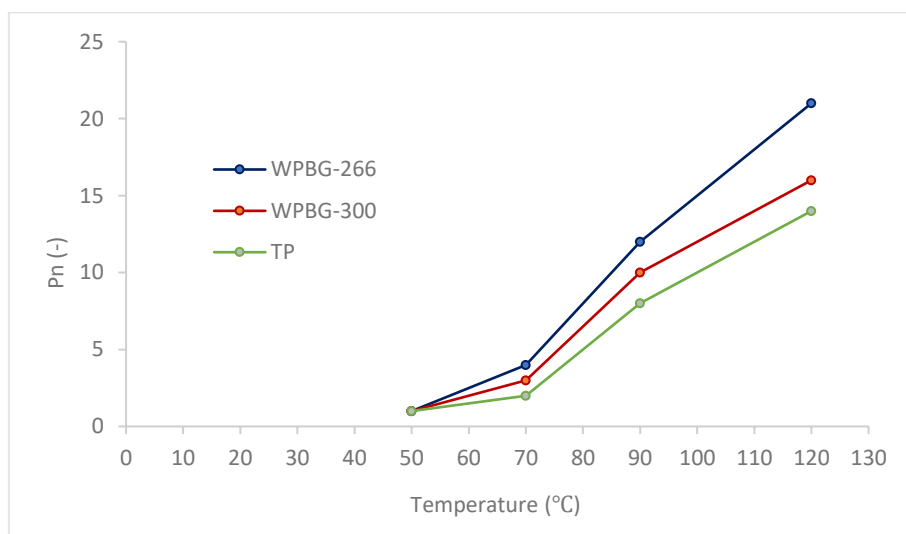


Figure 15: P_n values of ϵ -caprolactone for samples cured with WPBG-266, WPBG-300 and TP

The temperature increase revealed a clear trend of higher monomer conversions and degrees of polymerization (P_n) in all systems. This trend indicates that thermal activation is essential for facilitating the ring-opening polymerization of ϵ -caprolactone. Thus, the highest temperature of 120 °C proved to be the most suitable for the PBG-mediated ROP reactions of ϵ -caprolactone. Among the tested photobases, WPBG-266 exhibited the highest reactivity, achieving a maximum monomer conversion of 83 % as well as a degree of polymerization of 21 at 120 °C. Slightly lower monomer conversions and degrees of polymerization were

achieved at all curing temperatures when using the photobase WPBG-300 as the photoinitiator. This shows that both photobases can generate the anionic ring-opening polymerization (AROP) of ϵ -caprolactone; however, WPBG-266 was a little bit more effective under the same experimental conditions. A photobase TP followed a similar overall trend, but the final conversions and degrees of polymerization were a little lower than those with the photobase WPBG-266 and generally comparable to or slightly lower than those obtained with the photobase WPBG-300. Overall, the temperature remains the most important factor for a high monomer conversion rate in photoinitiated AROP systems with any of the three PBGs tested, as confirmed by the results.

Moreover, GPC was used to monitor any increase in molecular weight. The results obtained from the $^1\text{H-NMR}$ and GPC analyses reveal a clear correlation between curing temperature and both the monomer conversion and the molecular weight of the resulting polymers (Figure 16 and Figure 17).

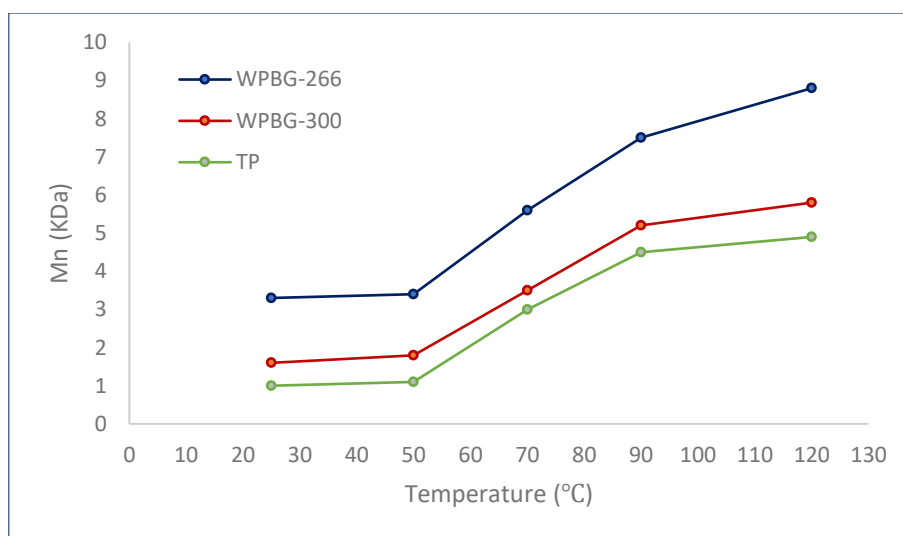


Figure 16: M_n values of ϵ -caprolactone for samples cured with WPBG-266, WPBG-300 and TP

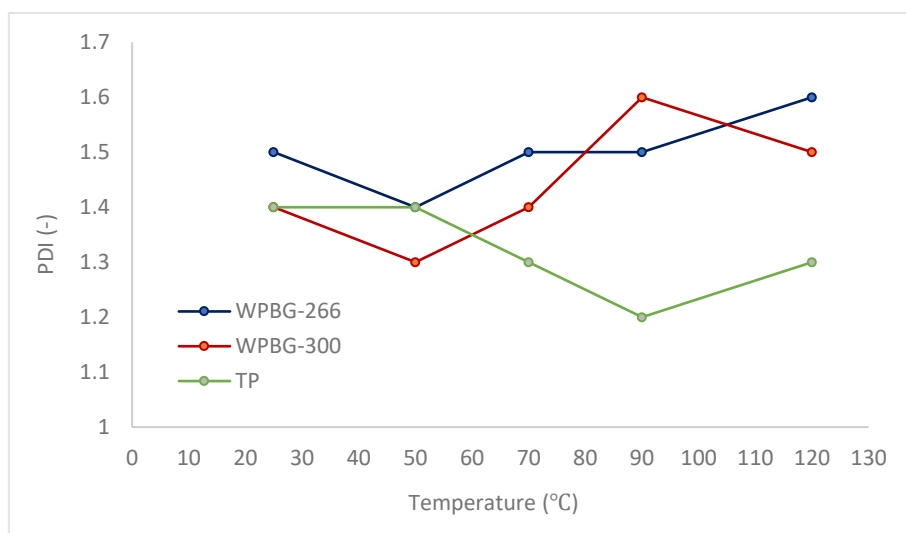


Figure 17: PDI values of ϵ -caprolactone for samples cured with WPBG-266, WPBG-300 and TP

The GPC results further confirmed the temperature dependence of PBG-mediated anionic ring opening polymerization. Only negligible molecular weights were observed at lower temperatures of 25 °C and 50 °C in all systems. Nevertheless, the polymerization was more efficient at higher temperatures in all systems studied, the molecular weights of the polymers increased, and the dispersity index (PDI) stayed at a comparatively low level, which is an indication of a controlled polymerization process. WPBG-266 gave the highest molecular weights under the same experimental conditions, whereas WPBG-300 and TP produced somewhat lower molecular weights and thus, exhibited slightly lower polymerization efficiencies. These trends in molecular weight correlated with trends in monomer conversion and degree of polymerization observed in the $^1\text{H-NMR}$ analysis, confirming that WPBG-266 provides the most efficient initiation and propagation.

1.2 Cationic Reference Systems based on Photoacid Initiation

For further reactivity studies of ϵ -caprolactone, reference systems containing photoacid generators (PAGs) as photoinitiators were prepared and compared with systems initiated by PBGs. Therefore, two PAGs were included into the reactivity studies of ϵ -caprolactone (Figure 18). The iodonium salt I-AI was expected to show good reactivity, while the sulfonium salt S-B, commercially available as Irgacure 290, was also expected to show good reactivity, but also better thermal stability.⁴²

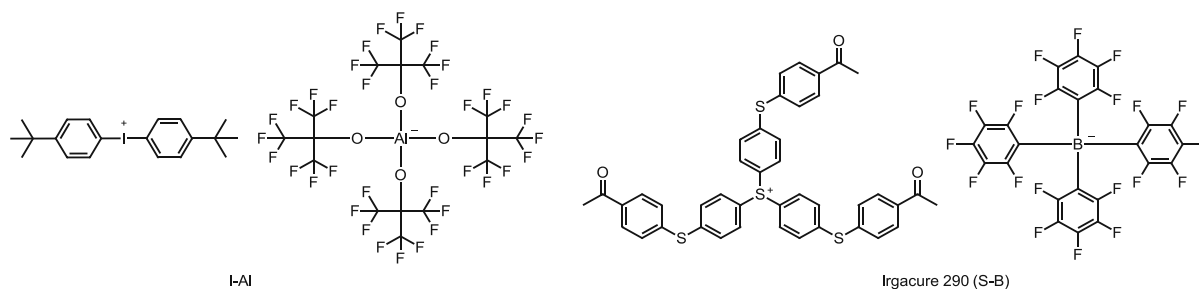


Figure 18: Structures of PAGs used for reference systems in ROP of ϵ -caprolactone

A photo-DSC study of ϵ -caprolactone was performed with either 2 mol% I-Al or 2 mol% S-B in combination with 2 mol% benzyl alcohol as a co-initiator, without the use of any sensitizer.⁴² The samples were irradiated for 300 s with 80 mW cm^{-2} , with temperatures ranging from 25 °C to 120 °C.

Nevertheless, there was no exothermic response visible, and thus, no calorimetric data could be obtained. To prepare the samples for GPC and $^1\text{H-NMR}$ analysis, the reactions were quenched with 0.3 wt% pyridine. Therefore, GPC was employed to monitor potential increases in molecular weight, and monomer conversion and degree of polymerization were further evaluated *via* $^1\text{H-NMR}$.

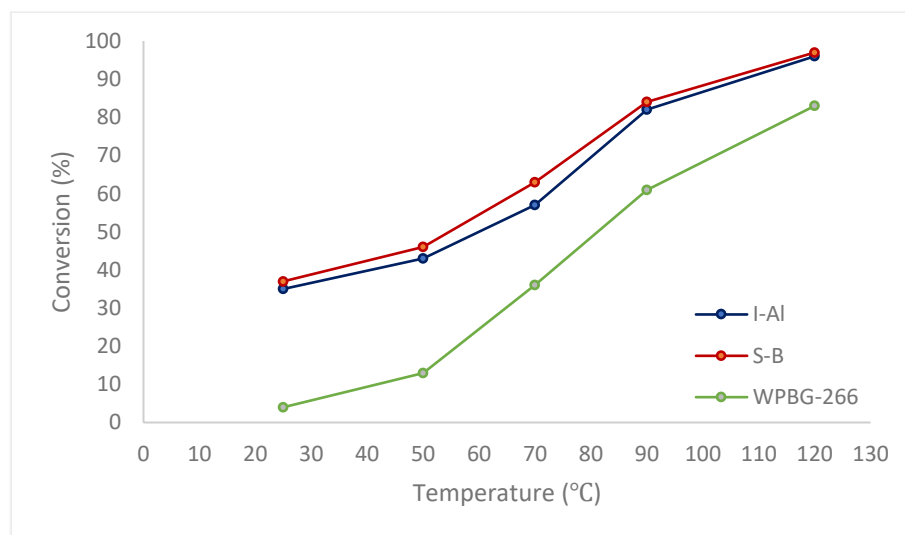


Figure 19: Conversion values of ϵ -caprolactone for samples cured with PAGs (I-Al and S-B) compared to those of samples cured with photobase WPBG-266

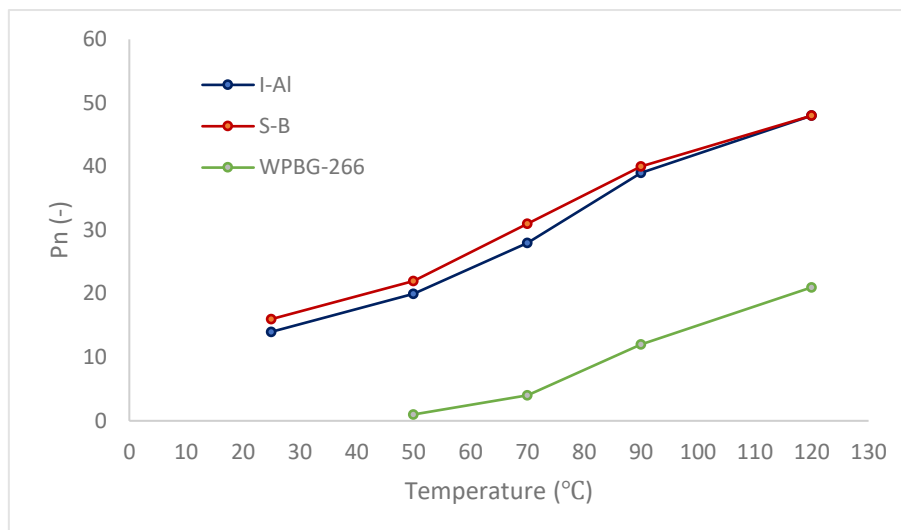


Figure 20: P_n values of ε-caprolactone for samples cured with PAGs (I-Al and S-B) compared to those of samples cured with photobase WPBG-266

The obtained ¹H-NMR results indicate that the reaction proceeds even though the photo-DSC measurements did not reveal any exothermic behavior during the photopolymerization of ε-caprolactone in the presence of I-Al or S-B and benzyl alcohol. Compared to the previously tested PBG system containing WPBG-266 as the photobase, which showed the highest reactivity among tested PBGs, photoacid generators (PAGs) enabled significantly higher reactivity of monomer across the entire temperature range. In both PAG systems, a gradual increase in conversion and degree of polymerization with temperature was observed. However, the S-B photoacid system exhibited slightly higher conversions and degrees of polymerization at all tested temperatures compared to I-Al. At the highest curing temperature of 120 °C, both systems reached nearly complete conversion up to 97 %, but S-B produced marginally higher P_n values under identical conditions. Overall, these results suggest that the S-B photoacid provides slightly enhanced polymerization efficiency compared to I-Al, although both systems showed comparable temperature-dependent behavior characteristic of PAG-initiated ring-opening polymerization.

The results obtained by GPC analysis revealed a clear trend of increasing molecular weights of the resulting polymers with increasing temperature (Figure 21 and Figure 22).

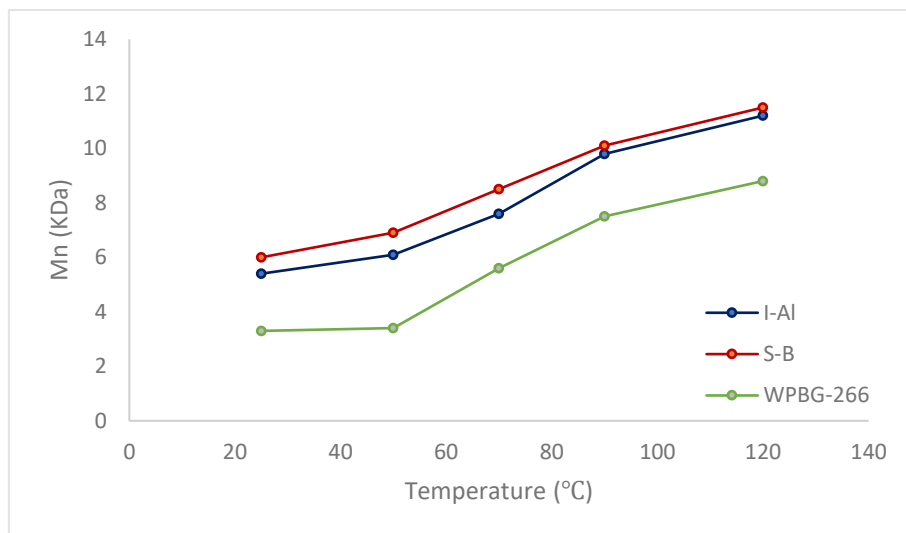


Figure 21: M_n values of ϵ -caprolactone for samples cured with PAGs (I-Al and S-B) compared to those of samples cured with photobase WPBG-266

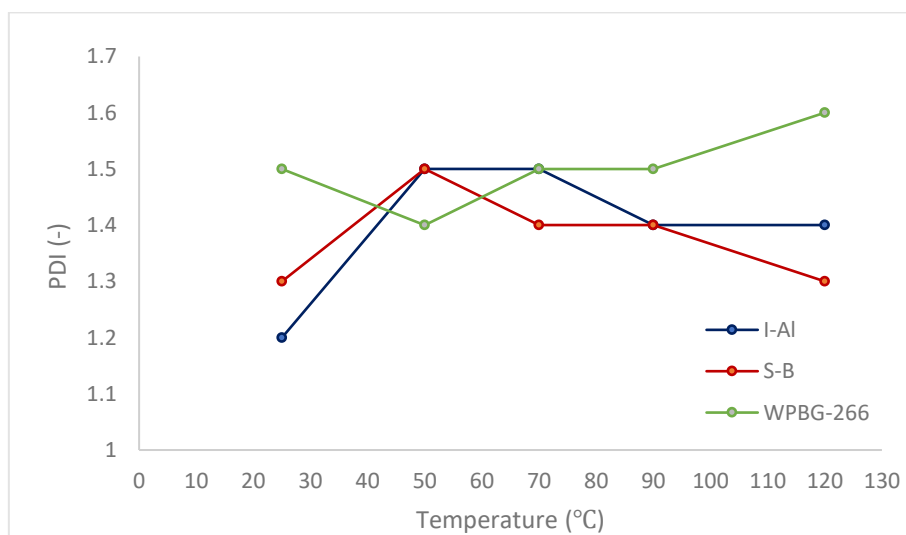
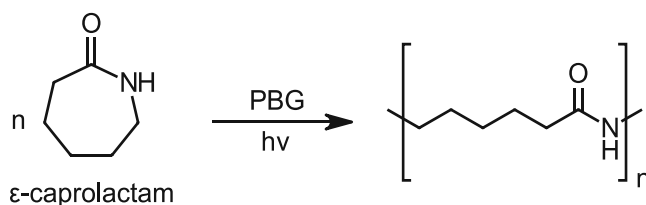


Figure 22: PDI values of ϵ -caprolactone for samples cured with PAGs (I-Al and S-B) compared to those of samples cured with photobase WPBG-266

The molecular weight increased steadily over the tested temperature range, while PDI remained in a moderate range, indicating a relatively well-controlled polymerization process. Compared to the I-Al system, the S-B system resulted in slightly higher molecular weights, confirming its somewhat higher polymerization efficiency under identical experimental conditions. On the other hand, the PBG model system containing WPBG-266 as photobase showed significantly lower conversions and molecular weights, especially at reduced temperatures. Overall, photoacid generators (PAGs), particularly S-B, showed significantly better performance, enabling not only higher monomer conversions but also the formation of polymers with higher molecular weights over the entire temperature range. This highlights their distinct advantage in the photoinitiated ring-opening polymerization of ϵ -caprolactone.

2. Reactivity Study of ϵ -Caprolactam

To investigate the potential anionic ring-opening polymerization (AROP) reaction between ϵ -caprolactam and a photobase, three previously mentioned photobase generators (PBGs) – WPBG-266, WPBG-300, and TP – were used in the photobase screening. Accordingly, the anionic ROP of ϵ -caprolactam (Scheme 15) was carried out under the same conditions as for ϵ -caprolactone, in this case at 100 °C.



Scheme 15: ROP of ϵ -caprolactam

2.1 Photobase Screening

In an attempt to evaluate the influence of different photobase generators (PBGs) on the anionic ring-opening polymerization of ϵ -caprolactam, three formulations were prepared and tested under identical irradiation and thermal conditions. In the formulation containing 2 mol% WPBG-266, 2 mol% benzyl alcohol were employed as a co-initiator, since strong organic bases such as biguanides can efficiently deprotonate alcohols, thereby generating reactive alkoxide species that initiate the anionic ring-opening polymerization of lactams in a controlled manner.^{114–116} In addition, 0.02 mol% 9,10-dibutoxyanthracene (DBA) were included as a sensitizer, thereby extending the absorption spectrum of WPBG-266 towards longer wavelengths and ensuring more efficient photogeneration of initiating species. Conversely, in the other two formulations, which contained either 2 mol% WPBG-300 or 2 mol% TP, N-acetylcaprolactam (2 mol%) was chosen as the co-initiator. Due to its structural similarity to ϵ -caprolactam, N-acetylcaprolactam provides excellent chemical compatibility within the system. More importantly, it can stabilize the developing anionic center through resonance and inductive effects, thereby improving control over chain initiation and propagation.^{114–116} For these formulations, ITX (0.02 mol%) – a more versatile sensitizer known for its broad absorption profile and efficient triplet energy transfer – was employed in order to ensure efficient photoactivation, generation of the desired base, and effective initiation of the polymerization process.¹⁰³

Since anionic ring-opening polymerization (AROP) of ϵ -caprolactam did not show any exothermic behavior in photo-DSC analysis, $^1\text{H-NMR}$ analysis was used to determine monomer conversion. Nevertheless, one interesting and unexpected detail was observed during the preparation of samples for $^1\text{H-NMR}$ analysis. Although polyamides, such as nylon 6 and nylon 6,6, are generally known for their poor solubility in common organic solvents like tetrahydrofuran (THF) and chloroform due to their high crystallinity and strong intermolecular hydrogen bonding, which create a dense and stable structure resistant to solvent penetration, all the cured samples in this case dissolved readily in both solvents at room temperature.¹¹⁷ This unusually high solubility raised the first suspicion that ring-opening polymerization (ROP) of ϵ -caprolactam might not have occurred as intended. To investigate further, $^1\text{H-NMR}$ analysis of the samples dissolved in chloroform was performed. However, no differences were observed between the spectra of the samples before and after curing, indicating that polymerization was likely unsuccessful.

Given these results – namely, the unexpected solubility of the cured samples in THF and chloroform as well as the absence of spectral changes in NMR after irradiation – additional ATR-FTIR analysis was conducted to clarify whether ring-opening polymerization (ROP) of ϵ -caprolactam had occurred.

2.2 ATR-FTIR Characterization

As previously mentioned, given the results of the NMR analysis and the results of the solubility tests of the cured samples, the first doubts regarding the success of the polymerization emerged at this stage. Therefore, ATR-FTIR spectra were used to reinforce and further support these findings (Figure 23 and Figure 24).

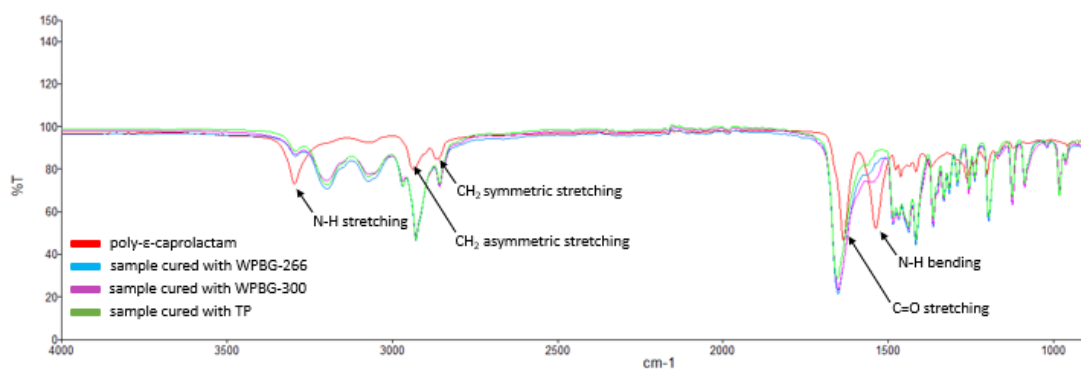


Figure 23: Comparison of ATR-FTIR spectra of poly- ϵ -caprolactam (red curve) and samples cured with different PBGs (blue, purple and green curves)

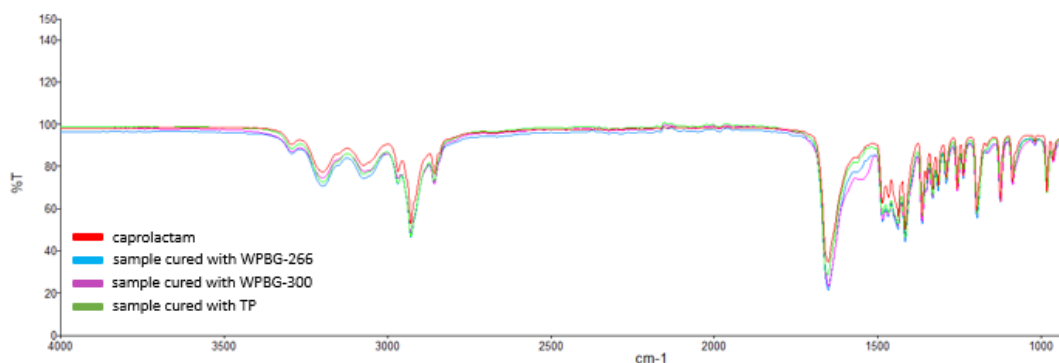
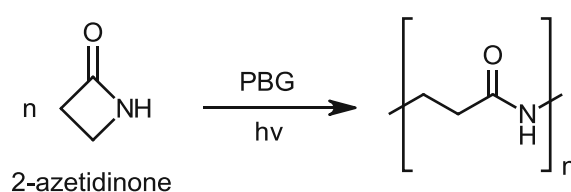


Figure 24: Comparison of ATR-FTIR spectra of ϵ -caprolactam (red curve) and samples cured with different PBGs (blue, purple and green curves)

According to the literature,^{118,119} a sign of successful polymerization and the formation of poly- ϵ -caprolactam would be N-H stretching bands at 3290-3400 cm^{-1} , CH_2 asymmetric stretching bands at 2930–2950 cm^{-1} , CH_2 symmetric stretching bands at 2850–2870 cm^{-1} , C=O stretching bands at 1635-1645 cm^{-1} as well as N-H bending at 1260-1300 cm^{-1} , as shown in Figure 23 by the red curve. After curing of the model system, the characteristic IR absorption bands of poly- ϵ -caprolactam were not detected. The absence of these bands supports the assumption that successful ring-opening polymerization of ϵ -caprolactam and subsequent formation of poly- ϵ -caprolactam did not occur during the 5-minute irradiation, regardless of the photobase generator used (Figure 23, blue, purple and green curve). In addition, Figure 24 shows an overlap between the curves of the samples cured with three different PBGs and the curve of caprolactam (red curve), which was used as a reference, further confirming that the ring opening was unsuccessful.¹²⁰

3. Reactivity Study of 2-Azetidinone

Due to the lack of detectable heat release during the anionic ring-opening polymerization of ϵ -caprolactone and ϵ -caprolactam – which can be attributed to their relatively low ring deformation – attention was turned to smaller, more strained monomers in order to enable monitoring using photo-DSC (Scheme 16). In this context, a four-membered lactam – 2-azetidinone – was selected as a promising candidate due to its significantly higher ring strain, which provides a stronger driving force for ring-opening polymerization reactions and increases the likelihood of exothermic behavior.



Scheme 16: ROP of 2-azetidinone

3.1 Photobase Screening

As previously discussed, the ring-opening polymerization of 2-azetidinone is – contrary to 7-membered cycles – exothermic and thus suitable for calorimetric analysis. Therefore, the reactivity of 2-azetidinone during anionic ROP was investigated with photo-DSC analysis. Prior to irradiation, both the sample and reference were conditioned in an isothermal phase at the selected temperature to ensure thermal equilibrium. The samples were then exposed to two successive irradiation cycles, during which heat evolution was recorded in real time, and parameters relevant to evaluate the efficiency of the photopolymerization were derived from these measurements. These parameters included the heat of polymerization (expressed as the area under the heat flow curve), which was calculated from the difference between the second and the first exposure phase, the time until a peak maximum was reached (t_{\max}), and the time required to reach 95 % of the total polymerization enthalpy (t_{95}).

However, due to the immiscibility of the TP photobase with the monomer, only two commercially available photobase generators – WPBG-266 and WPBG-300 – were used for photobase screening. As a result, two formulations were prepared: one with 2 mol% WPBG-266, 2 mol% N-acetylcaprolactam as a co-initiator, and 0.02 mol% DBA as a sensitizer,¹⁰² and another consisting of 2 mol% WPBG-300, 2 mol% N-acetylcaprolactam, and 0.02 mol% ITX

as a sensitizer.¹⁰³ A broadband UV/VIS light source (320-500 nm) with an intensity of 80 mW cm⁻² was used to trigger photopolymerization and the heat released during the polymerization was recorded. The samples were irradiated for 300 s and the measurements were performed at 90 °C. In Figure 25, the measured heat flow of the polymerization for 2-azetidinone with WPBG-266 and WPBG-300 is represented.

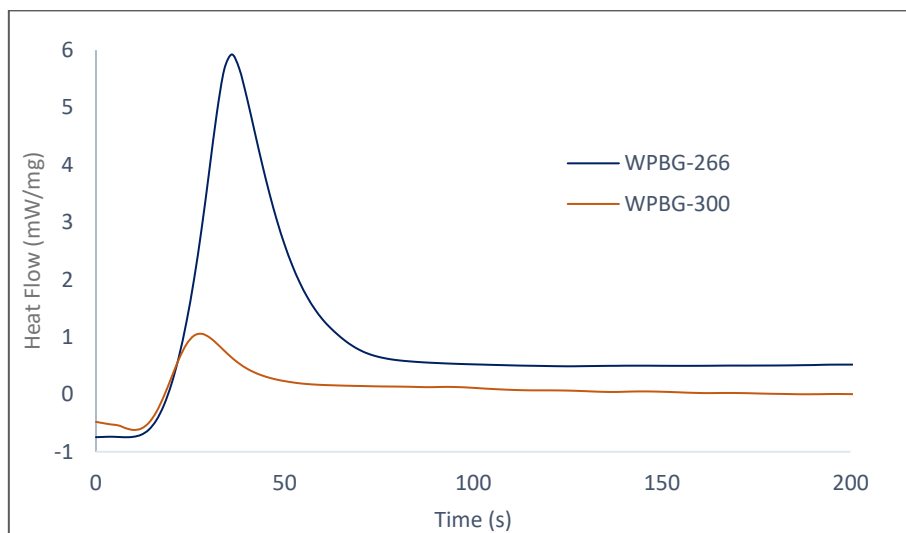


Figure 25: Photo-DSC analysis of 2-azetidinone cured with WPBG-266 and WPBG-300 at 90 °C

Table 1: Results obtained from photo-DSC analysis of 2-azetidinone with WPBG-266 and WPBG-300 at 90°C

PBG	Area [J g ⁻¹]	t _{max} [s]	t ₉₅ [s]
WPBG-266	117.4	36	66
WPBG-300	33.6	28	93

The much larger exothermic area of 117.4 J g⁻¹ for WPBG-266 compared to only 33.6 J g⁻¹ for WPBG-300 clearly indicates that WPBG-266 was significantly more reactive, thus the formulation with WPBG-266 went through ring-opening polymerization more effectively. WPBG-266 took a slightly longer time than WPBG-300 to reach maximum heat flow (t_{max}), however, this short delay was more than compensated by its overall better performance. Additionally, WPBG-266 took considerably less time than WPBG-300 to reach 95 % of total heat evolution (t₉₅), indicating that the system containing WPBG-266 reached completion of polymerization more rapidly, exhibiting both higher intensity and faster kinetics. Overall, WPBG-266 performed better than WPBG-300, thus it is the most effective photobase generator for initiating the ring-opening polymerization of 2-azetidinone under the tested conditions.

As expected for polyamides such as nylon 3, the cured samples exhibited poor solubility in common organic solvents, which posed a considerable limitation for conducting GPC analysis.¹²¹ In particular, samples cured with WPBG-266 could not be dissolved in pure tetrahydrofuran (THF), and even the use of 8 wt% hexafluoroisopropanol (HFiP) did not result in homogeneous solutions when mixed with THF. Although hexafluoro isopropanol usually significantly enhances the solubility of substances, in the case of samples cured with WPBG-266, using 8 wt% hexafluoro isopropanol did not yield success and did not produce any homogeneous solutions. Despite the good solubility in pure hexafluoro isopropanol, GPC analysis was not feasible, as the addition of small amounts of THF resulted in a precipitate. In contrast, the samples cured with WPBG-300 showed improved processability – they were easily dissolved in 8 wt% HFiP and were further diluted with THF for successful GPC analysis. The GPC results of the samples cured with WPBG-300 showed a molecular weight of 9 kDa and a polydispersity index (PDI) of 1.6.

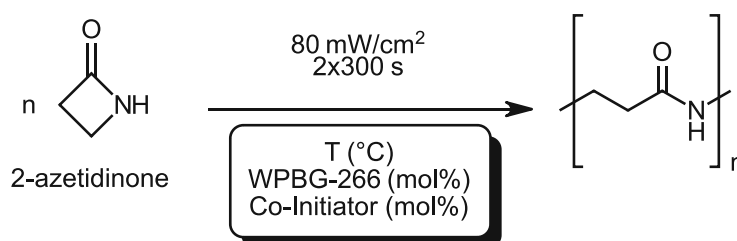
In addition to photo-DSC analysis, further characterization of the cured samples was pursued to better assess the efficiency of the polymerization process. Despite the challenges encountered with GPC, it was observed during sample handling that both samples were fully soluble in pure HFiP, a solvent known to disrupt strong hydrogen bonding in polyamides and enhance solubility.¹²² This observation was used to explore an alternative characterization approach – dynamic light scattering (DLS). Therefore, cured samples were dissolved in HFiP and subjected to DLS analysis, which allowed the measurement of the hydrodynamic radius of the polymer chains in solution, providing information about the molecular size of the polymers formed with each PBG. Sample preparation requires a particular attention because dust dramatically interferes in the DLS measurements. The entire sample preparation was therefore conducted under a thoroughly cleaned fume hood to minimize the risk of dust interference. Glass cuvettes were pre-cleaned and flushed with compressed air and the cured polymer samples were dissolved in hexafluoro isopropanol yielding concentrations of 1 mg mL⁻¹ and transferred into the glass cuvettes *via* syringe filters.

DLS measurements were performed at 25 °C and the scattering angle was set to 90° with respect to the incoming beam. The hydrodynamic radius of samples cured with WPBG-266 was found to be 0.9 nm, whereas the polymer formed using WPBG-300 exhibited a smaller radius of 0.5 nm, indicating that WPBG-266 led to the formation of larger polymer chains under the

given conditions. These results are in a very good agreement with the photo-DSC results, confirming WPBG-266 as a more suitable and efficient PBG for initiating the ring-opening polymerization of 2-azetidinone.

3.2 Optimizing the Model System

In the previous chapter, the photobase generators were established as possible initiators for the light-induced ring-opening polymerization (ROP) of 2-azetidinone. Based on preliminary results, WPBG-266 emerged as more efficient photoinitiator for this reaction and was therefore selected for further investigation. In order to find the most favorable reaction conditions for efficient PBG-mediated ROP of 2-azetidinone, several parameters were altered in a controlled manner, including temperature, PBG concentration, and the concentration of the co-initiator. All reactions were conducted in triplets on a photo-DSC device coupled with a light source emitting in the 320-500 nm range, following the procedure described at the beginning of the *Results and Discussion* chapter. Therefore, each sample was irradiated for 300 s with an intensity of 80 mW cm^{-2} .



Scheme 17: Optimization of temperature, PBG and co-initiator concentration for ROP of 2-azetidinone

3.2.1 Temperature Screening

The ring-opening polymerization of 2-azetidinone was performed in the presence of an equimolar mixture of PBG and co-initiator (2 mol% WPBG-266 and 2 mol% N-acetylcaprolactam). The irradiation intensity of the light source was set at 80 mW cm^{-2} and the samples were irradiated for 300 s. Materials obtained from the photo-DSC analysis were then dissolved in formic acid and further analyzed using NMR to provide information about the monomer conversion.

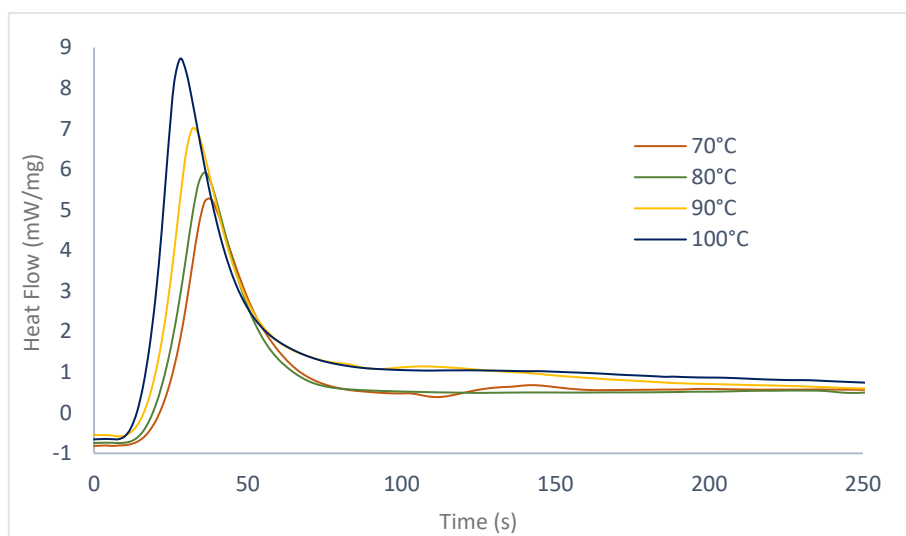


Figure 26: Temperature screening results for ROP of 2-azetidinone with WPBG-266 as initiator

Figure 26 shows the temperature screening results obtained from photo-DSC measurements.

Table 2: Summary of results for ROP of 2-azetidinone with WPBG-266 at different temperatures

T [°C]	Area [J g ⁻¹]	t _{max} [s]	t ₉₅ [s]	R _p [mmol L ⁻¹ s ⁻¹]	Conversion [%]
70	108.3	37	62	51.9	37
80	117.4	36	66	56.3	40
90	219.9	33	72	67.6	51
100	235.2	28	71	81.9	54

The observed increase in the measured photo-DSC signal results from a higher monomer conversion. Furthermore, a minimum temperature of 70 °C was required to initiate noticeable polymerization and to observe a measurable exothermic response in the photo-DSC analysis. In addition, the practical theoretical heat of polymerization was estimated by correlating the DSC-measured reaction enthalpy, expressed as the integrated exothermic area, with the NMR-determined monomer conversion. The resulting values were 20.8, 21.1, 30.7 and 31.1 kJ mol⁻¹ at 70, 80, 90 and 100 °C, respectively, showing a clear increase with temperature that correlates well with the higher monomer conversions determined by NMR. Furthermore, the time to reach maximum heat flow also decreased from 37 s to 28 s with increasing temperature, suggesting that higher temperatures accelerate the initiation of the polymerization. This trend was further confirmed by NMR analysis, which showed increasing monomer conversion with temperature. However, conversions exceeding 50 % were only achieved at 90 °C or higher. Using the theoretical heat of polymerization of 2-azetidinone (~100 kJ mol⁻¹) and applying Equation 1 presented in *Materials and Methods* chapter, the rate of polymerization R_p was determined, also showing an increase with increasing

temperature.^{123–125} Overall, the results showed that higher temperatures significantly promote the reactivity and conversion in anionic ring-opening polymerization of 2-azetidinone.

3.2.2 PBG Concentration Screening

The following screening experiments demonstrate the impact of the PBG concentration on the ROP reaction of 2-azetidinone, since the concentration of PBG can significantly affect both monomer conversion and achievable polymer chain length. All reactions were performed at 90 °C and the intensity of the incident light was set to 80 mW cm⁻². Three different formulations containing 1 mol%, 2 mol% or 3 mol% WPBG-266 were analyzed under identical photo-DSC conditions, each combined in equimolar ratio with N-acetylcaprolactam as co-initiator, as shown in Figure 27. Due to the limited availability of formic acid required for polymer dissolution prior to NMR analysis, monomer conversion was determined only for the temperature screening experiments and was therefore not calculated for the PBG concentration screening.

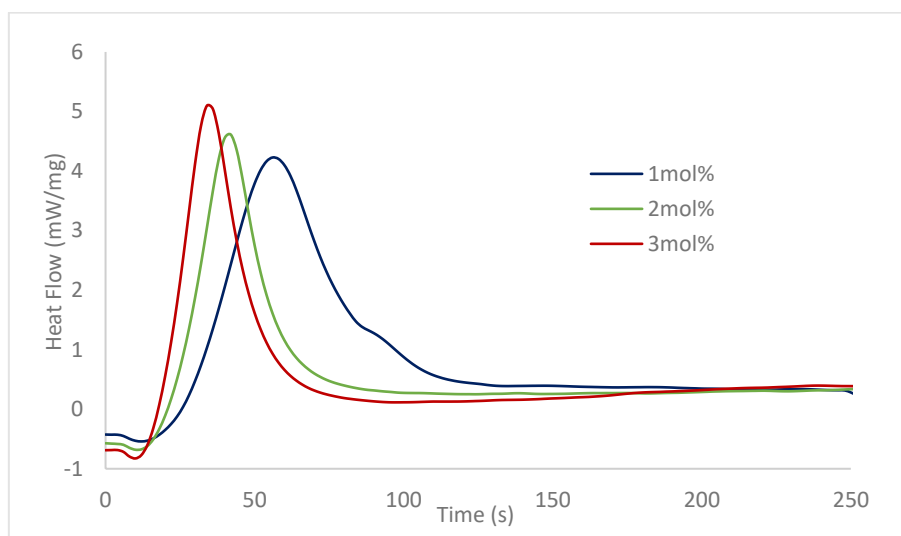


Figure 27: PBG concentration screening results for ROP of 2-azetidinone cured with WPBG-266, each in an equimolar mixture with N-acetylcaprolactam as co-initiator

The results presented in Table 3 demonstrate a clear influence of WPBG-266 concentration on the ring-opening polymerization (ROP) of 2-azetidinone.

Table 3: Summary of results for ROP of 2-azetidinone with different concentrations of WPBG-266 and N-acetylcaprolactam

Concentration [mol%]	Area [J g ⁻¹]	t _{max} [s]	t ₉₅ [s]
1	152.9	57	104
2	96.4	41	66
3	107.6	35	60

At a concentration of 1 mol% PBG and co-initiator, the highest reaction enthalpy of 152.9 J g⁻¹ was measured, accompanied by the slowest reaction kinetics, as indicated by the longest t_{max} of 57 s and t₉₅ of 104 s. This elevated enthalpy may be partly due to the slower reaction rate, which allows for greater thermal accumulation over a prolonged period. When the PBG concentration was increased to 2 mol%, a notable acceleration in polymerization was observed, with t_{max} and t₉₅ decreasing to 41 s and 66 s, respectively. The maximum heat flow was reached faster, followed by a drop in total enthalpy (96.4 J g⁻¹). The reaction proceeded even faster at 3 mol% and achieved the shortest t_{max} = 35 s, as well as t₉₅ = 60 s, with a small increase in enthalpy (107.6 J g⁻¹) compared to 2 mol%, indicating a further improvement in reaction efficiency. In general, the results show a compromise between the polymerization rate and the total thermal output, with 1 mol% producing the highest thermal output, possibly as a result of its slower kinetics, and 3 mol% providing the fastest and most effective initiation, which could be advantageous for applications requiring quick curing.

3.2.3 Co-Initiator Concentration Screening

In an attempt to further optimize the reaction conditions for the ring-opening polymerization of 2-azetidinone, the influence of different co-initiator concentrations was additionally investigated. For this purpose, N-acetylcaprolactam was employed in concentrations ranging from 1 to 3 mol%, while the PBG concentration was kept constant at 3 mol% WPBG-266 – previously identified as the most effective initiator level. All experiments were conducted at 90 °C under constant light irradiation of 80 mW cm⁻². Because formic acid, required for polymer dissolution and subsequent NMR analysis, was available only in limited quantities, monomer conversion values were evaluated exclusively for the temperature screening experiments, and therefore were not obtained for this set of experiments.

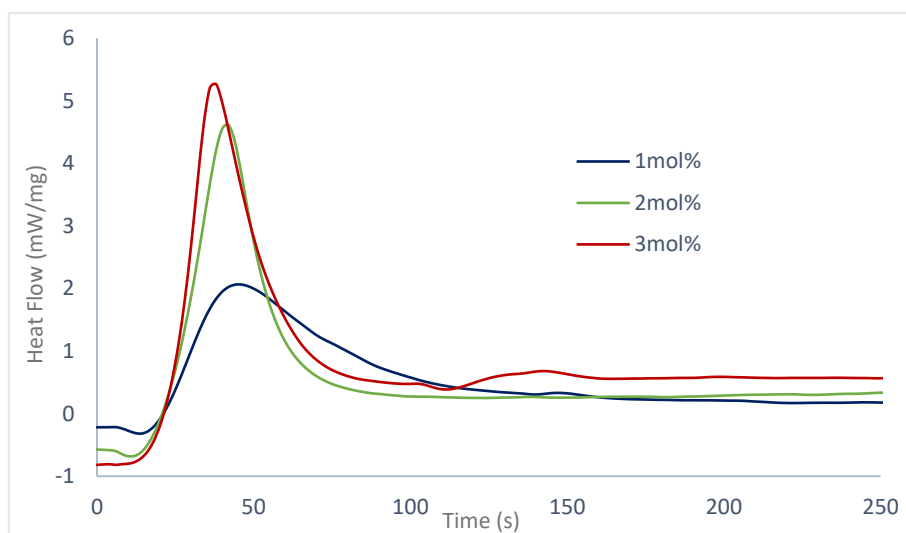


Figure 28: Co-initiator concentration screening results for ROP of 2-azetidinone with 3 mol% WPBG-266 as initiator

As summarized in Table 4, increasing the co-initiator concentration from 1 to 3 mol% resulted in significant changes in both reaction kinetics and overall enthalpy.

Table 4: Summary of results for ROP of 2-azetidinone cured with 3 mol% WPBG-266 and different concentrations of N-acetylcaprolactam

Concentration[mol%]	Area [J g^{-1}]	t_{max} [s]	t_{95} [s]
1	92.3	46	131
2	96.8	42	66
3	108.3	38	62

While concentrations of 2 mol% and 3 mol% N-acetylcaprolactam both demonstrated noticeably faster polymerization kinetics, the lowest concentration of 1 mol% of N-acetylcaprolactam produced the least favourable kinetic profile among the tested concentrations, as indicated by the longest t_{95} value. The longest $t_{\text{max}} = 46$ s and $t_{95} = 131$ s, as well as the lowest reaction enthalpy (92.3 J g^{-1}) were recorded at 1 mol% N-acetylcaprolactam, indicating slower initiation and a more prolonged reaction, which may be the result of an insufficient activation of the monomer. Increasing the concentration to 2 mol% led to the enhancement of the reaction rate so that t_{max} was shortened to 42 s and t_{95} was reduced to 66 s, while the enthalpy was slightly increased to 96.8 J g^{-1} . The most effective results were obtained at 3 mol%, with the shortest t_{max} of 38 s, the lowest t_{95} of 62 s, and a moderate increase in polymerization enthalpy (108.3 J g^{-1}) compared to the system containing 2 mol% co-initiator, indicating faster and more complete polymerization. These results suggest that 3 mol% N-acetylcaprolactam offer the most favorable balance between reaction speed and monomer conversion under the tested conditions, showing a trend in which increasing

co-initiator concentration enhances both the rate and extent of polymerization. However, the differences between using 2 mol% and 3 mol% co-initiator are rather small, with the 3 mol% variant offering a slight advantage in overall reactivity.

3.3 Gravimetric analysis

In addition to the previously described analytical techniques, gravimetric analysis was also performed as a complementary method to determine monomer conversion. After the photopolymerization reaction was completed, the conversion was determined gravimetrically by dissolving the cured samples in formic acid and precipitating in cold ethanol under vigorous stirring and centrifugation, followed by prolonged standing. Finally, the polymer precipitate was separated, washed with more cold ethanol, and dried to constant weight in a drying oven. The results presented in Figure 29 showed a good agreement between the conversion data obtained by gravimetry and conversion data using $^1\text{H-NMR}$ analysis.

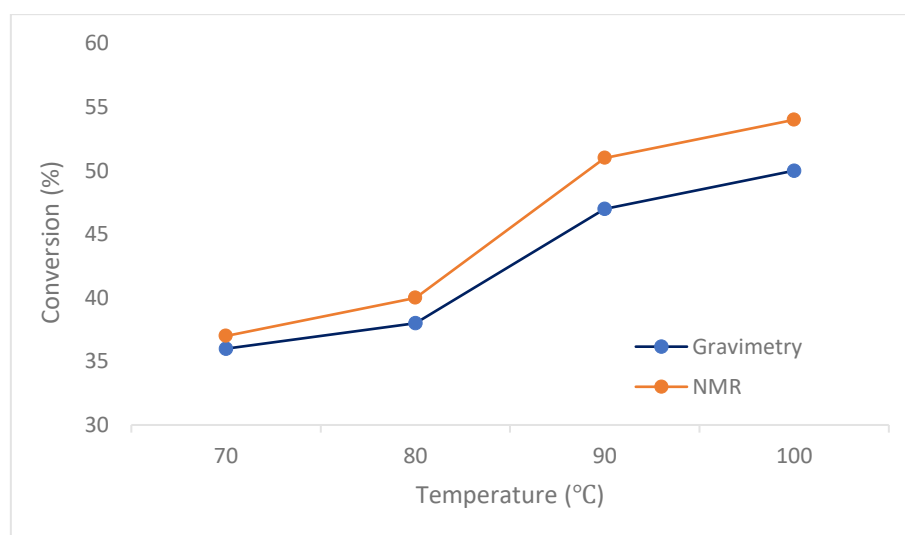


Figure 29: Comparison of monomer conversion at different temperatures calculated by gravimetric and NMR analysis

The gravimetric analysis provided conversion values that closely matched those obtained from the corresponding $^1\text{H-NMR}$ measurements, confirming the consistency of both analytical methods. As shown in Figure 29, a clear trend of increasing monomer conversion with temperature is observed in both datasets. The small differences between the two approaches are within an acceptable range and probably arise from experimental variability. In general, the results show good agreement and they support the conclusion that higher temperatures lead to higher efficiency of the photoinitiated ring-opening polymerization of 2-azetidinone.

4. Reactivity Study of 2-Azetidinone Derivatives

Since 2-azetidinone comes with the drawback of being solid at room temperature, which limits its practical applicability in certain processes such as 3D printing, this part of the diploma thesis focused on finding liquid 2-azetidinone derivatives and investigating their reactivity with the photo base WPBG-266 – the most effective photoinitiator among the three tested so far. With this in mind, we aimed to synthesize two liquid 2-azetidinone derivatives differing in the substituent attached to the nitrogen atom, a position believed to be essential for the initiation of the polymerization reaction (Figure 30).⁶³

One of the target compounds was therefore an N-substituted 2-azetidinone derivative, in which the hydrogen atom at the nitrogen position was replaced by a preferably small substituent (e.g., an alkyl or aryl group). A review of the literature revealed several 2-azetidinone derivatives suitable for this purpose. Among them, 1-benzyl-4-methyl-2-azetidinone was initially selected due to a well-described synthetic route that afforded the product in high yield, along with available data on its appearance and various analytical properties.¹²⁶ However, the synthesis of this compound was not successful. As an alternative, 1-benzyl-2-azetidinone was synthesized as a representative of N-substituted 2-azetidinone derivatives, and its reactivity with WPBG-266 was subsequently evaluated.

The second target compound was an N-unsubstituted 2-azetidinone derivative. During the literature research and compound selection process, attention was primarily directed toward methyl-substituted 2-azetidinone derivatives due to their structural similarity to the previously studied 2-azetidinone. Consequently, attempts were made to synthesize either 4-methyl- or 3-methyl-2-azetidinone. While the synthesis of 4-methyl-2-azetidinone was unsuccessful, 3-methyl-2-azetidinone was successfully obtained.

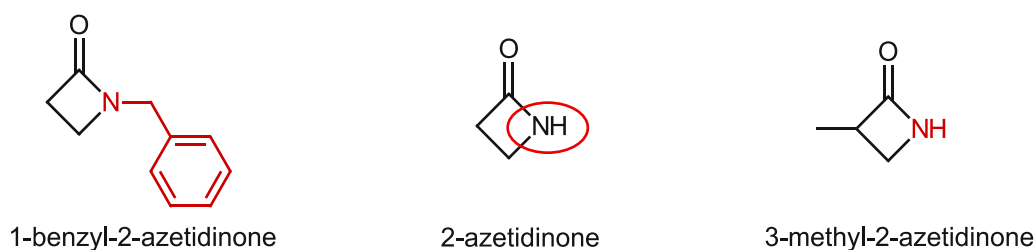


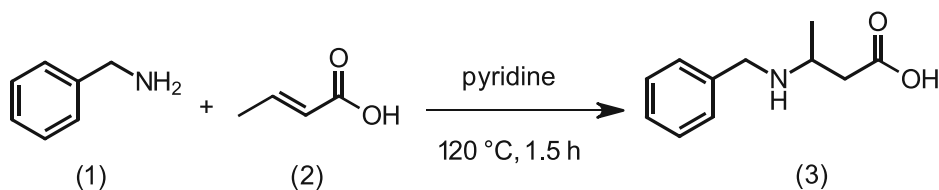
Figure 30: Structures of liquid N-substituted (1-benzyl-2-azetidinone) and N-unsubstituted (3-methyl-2-azetidinone) 2-azetidinone derivatives chosen for the reactivity investigation with WPBG-266

4.1 N-Substituted 2-Azetidinone Derivative

For the synthesis of N-substituted 2-azetidinone derivative, two synthetic procedures were attempted according to Kanwar and Sharma,¹²⁶ as represented in Scheme 18 and Scheme 19, and Fang et al. as depicted in Scheme 20 and Scheme 20.¹²⁷

4.1.1 Synthesis of 1-Benzyl-4-Methyl-2-Azetidinone

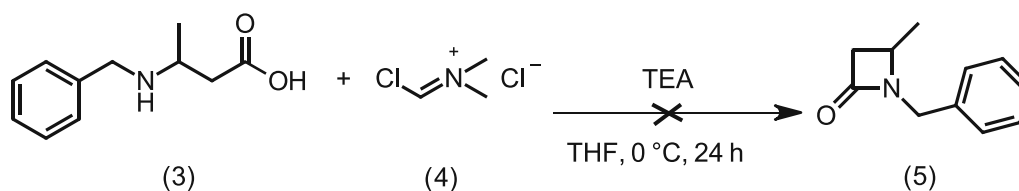
4.1.1.1 Synthesis of 3-Benzylaminobutyric acid



Scheme 18: Synthetic route to 3-benzylaminobutyric acid (3)

3-Benzylaminobutyric acid (**3**) was synthesized following the procedure previously described by Dzygiel et al.¹²⁸ In this step, benzylamine (**1**) was reacted with crotonic acid (**2**) in dry pyridine under an argon atmosphere at 120 °C. Upon cooling, the reaction mixture yielded a crystalline white β -amino acid (**3**), which was isolated by filtration and washed with acetone.

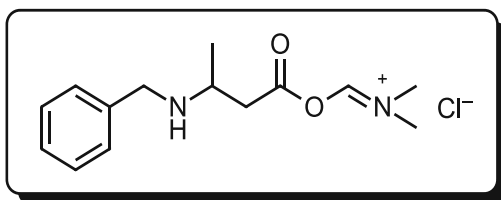
4.1.1.2 Synthesis of 1-Benzyl-4-Methyl-2-Azetidinone



Scheme 19: Synthetic route 1-benzyl-4-methyl-2-azetidinone (5)

For the second step of the reaction, a novel protocol for the cyclisation of β -amino acids reported by Kanwar and Sharma was employed.¹²⁶ In their study, (chloromethylene)dimethylammonium chloride (**4**) was introduced as an effective reagent that conveniently and efficiently mediates the amide bond formation in β -lactams *via* cyclodehydration of β -amino acids leading to β -lactam formation under mild reaction conditions. Following their procedure, a suspension of compound **3** (1 equiv.) in dry tetrahydrofuran was cooled to 0 °C, after which reagent **4** (6.45 equiv.) was added gradually over 30 min under stirring. Subsequently, triethylamine (2.1 equiv.) in dry tetrahydrofuran was added dropwise, and the reaction mixture was stirred overnight at room temperature. The

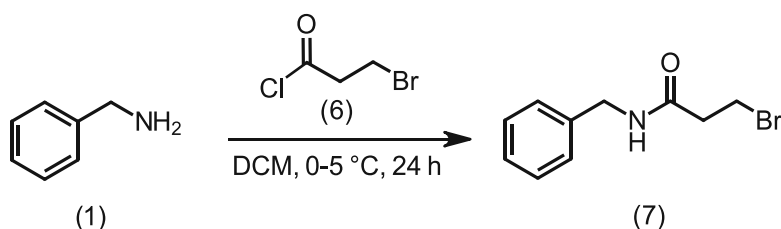
reaction control was performed with ^1H -NMR and UPLC-MS. These measurements have shown that the reaction was unsuccessful. Unfortunately, this synthetic route resulted in the formation of the compound shown below, instead of the desired monomer.



The authors further explored the effect of solvent on cyclization success, identifying dichloromethane, tetrahydrofuran, and acetonitrile as the most favorable solvents.¹²⁶ For this reason, the reaction was repeated under the same conditions with dichloromethane and acetonitrile replacing tetrahydrofuran as the solvents. Nevertheless, in both cases, the reaction resulted in the previously observed outcome, thus no solvent effect on selectivity or efficiency of the ring formation could be observed under these conditions.

4.1.2 Synthesis of 1-Benzyl-2-Azetidinone

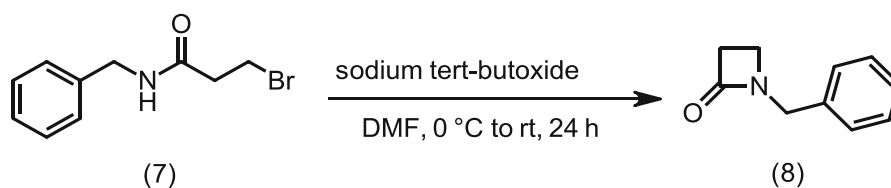
4.1.2.1 Synthesis of N-Benzyl-3-Bromopropionamide



Scheme 20: Synthetic route to N-benzyl-3-bromopropionamide (7)

The first reaction step was performed according to a procedure published by Więckowska et al.²⁶ In this step, a solution of benzylamine (**1**) in dichloromethane, precooled to 0–5 °C, was treated dropwise with a solution of 3-bromopropanoyl chloride (**6**) in the same solvent. The reaction mixture was then allowed to warm to room temperature and stirred for 24 h. After one day, extraction was performed to give white crystalline N-benzyl-3-bromopropionamide (**7**) in 52 % yield.

4.1.2.2 Synthesis of 1-Benzyl-2-Azetidinone



Scheme 21: Synthetic route to 1-benzyl-2-azetidinone (8)

In the second step, the cyclization to the corresponding β -lactam was performed following the procedure reported by Fang et al.¹²⁷ Specifically, 1 eq. of **7** was dissolved in dimethylformamide and cooled to 0 °C, after which sodium tert-butoxide (1.1 eq.) was added in a single portion. The reaction mixture was then gradually warmed to room temperature and stirred for 24 h, after which it was intentionally stopped before the standard longer reaction time, as sufficient product had already formed for further analysis. ¹H-NMR analysis confirmed the formation of the desired β -lactam (**8**). The crude product was purified by extraction and recrystallization, yielding the final compound as a slightly yellow liquid in 44 % yield.

4.1.3 Photo-DSC Study of 1-Benzyl-2-Azetidinone

A photo-DSC study of 1-benzyl-2-azetidinone was performed in the presence of 2 mol% WPBG-266 and 2 mol% N-acetylcaprolactam, which served as a co-initiator.¹⁰² To enhance the efficiency of the photoreaction, 0.02 mol% DBA was added as a sensitizer,^{108–111} promoting rapid and complete conversion during the photocleavage of the ketoprofen anion. The samples were irradiated for 300 s with 80 mW cm⁻² (320 - 500 nm light source) and the temperature was set to 70 °C.

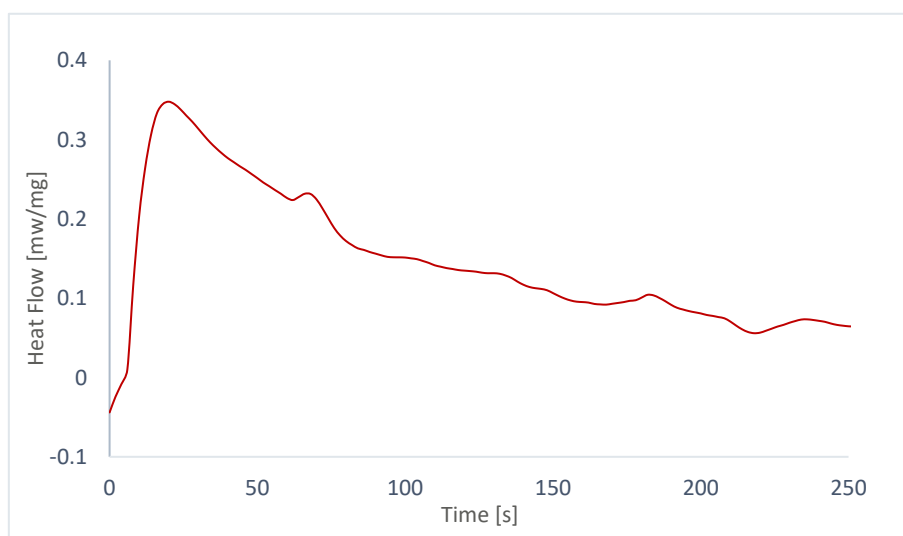


Figure 31: Photo-DSC of 1-benzyl-2-azetidinone with WPBG-266 at 70 °C

As shown in Figure 31, the photo-DSC analysis exhibited only a weak exothermic response, with a total heat release of only 8.5 J g^{-1} . Although the exothermic peak was reached rapidly at 19 s, indicating that the reaction itself proceeded fast, the overall low heat evolution suggests that ring-opening polymerization of 1-benzyl-2-azetidinone was largely ineffective under the applied conditions. This behavior can be explained by the ROP mechanism of lactams. Anionic ROP typically proceeds *via* nucleophilic attack on the carbonyl carbon of the amide group, a step strongly favored in unsubstituted 2-azetidinones due to their high ring strain and the accessibility of the lactam anion intermediate. However, N-substitution radically changes this pathway. A benzyl substituent on the nitrogen atom prevents the formation of a stable lactam anion, thus anionic ROP becomes thermodynamically and kinetically unfavorable. In addition, N-substituents like benzyl groups cause steric hindrance and alter the electronic environment around the amide bond. As a result, the resonance destabilization that is required to facilitate ring-opening is significantly reduced and the carbonyl carbon becomes much less susceptible to nucleophilic attack. Therefore, the weak exothermic response observed in the photo-DSC is not surprising. The poor reactivity is a direct consequence of the N-substitution, and the low polymerization efficiency under the applied conditions is, in fact, not surprising.^{63,129}

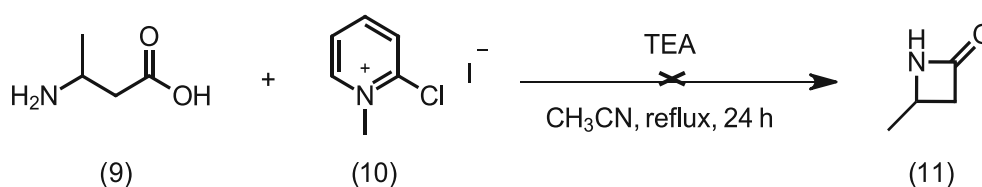
After the photo-DSC measurements, the cured samples were directly used for further investigation *via* gel permeations chromatography. Therefore, the samples were dissolved in corresponding amount of THF-solution spiked with 0.5 mg mL^{-1} butylhydroxytoluene (BHT) to achieve $2\text{-}4 \text{ mg mL}^{-1}$ solutions. The GPC results revealed a molecular weight of only 489 Da. Since the molecular weight of the monomer, 1-benzyl-2-azetidinone, is 161.2 g mol^{-1} , the detected mass corresponds to merely two to three repeating units, most likely a dimer, or at best a low oligomer. Therefore, the GPC analysis was in agreement with the photo-DSC observations, further confirming that effective ring-opening polymerization did not occur under the applied conditions.

4.2 N-Unsubstituted 2-Azetidinone Derivative

Multiple synthesis attempts were performed to synthesize N-unsubstituted 2-azetidinone derivative.

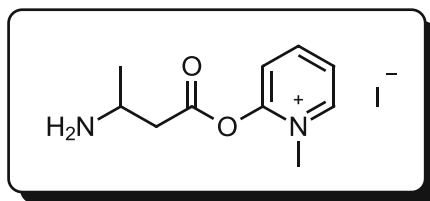
4.2.1 Synthesis of 4-Methyl-2-Azetidinone

Mukaiyama reagent (2-chloro-1-methylpyridinium iodide, CMPI), which was introduced by Teruaki Mukaiyama back in 1975, has been acknowledged as a highly efficient and convenient reagent for the activation of hydroxyl groups in carboxylic acids.^{130,131} This reagent has been extensively utilized in the syntheses of lactones,¹³² esters,¹³¹ amides,¹³³ and lactams.¹³¹ In one of the studies, Huang et al. developed a practical and efficient approach for the preparation of various β -lactams from the corresponding β -amino acids, using CMPI as a condensing reagent.¹³¹ The method offers several notable advantages, including easy handling, shorter reaction times, broad substrate scope and high product yields under mild, one-pot conditions. Encouraged by these findings and the efficiency of the method developed by Huang et al.,¹³¹ we followed their approach for the synthesis of methyl-substituted 2-azetidinone derivative. Therefore, 3-aminobutyric acid (**9**) was selected as a suitable β -amino acid precursor in our initial approach, with the aim of synthesizing 4-methyl-2-azetidinone (**11**), as depicted in Scheme 22.



Scheme 22: Synthetic route to 4-methyl-2-azetidinone (11)

The synthesis involved refluxing 3-aminobutyric acid (**9**) in a solution of CMPI (**10**) and triethylamine in acetonitrile under an argon atmosphere. Unfortunately, after solvent evaporation and drying of the residue, UPLC-MS analysis revealed that the reaction had not gone through the intramolecular nucleophilic attack of the amino group to the activated carboxylic acid moiety, which is the crucial step for β -lactam ring formation. Instead, the reaction seemed to have stopped at the intermediate stage, as shown below.



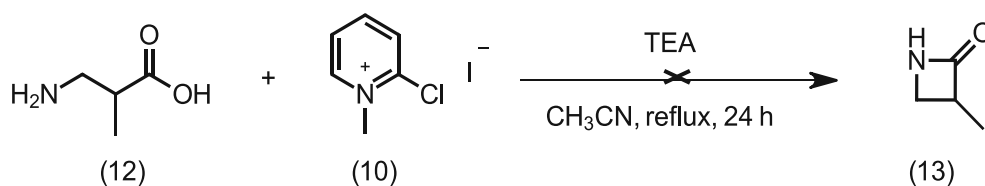
Based on the above-mentioned results, we decided to change the initially used β -amino acid with 3-amino-2-methylpropanoic acid (**12**) (Scheme 23). The reason for such a modification was the assumption that the altered reactivity of 3-amino-2-methylpropanoic acid (**12**) could lead to the formation of an alternative methyl-substituted 2-azetidinone derivative. In particular, we aimed to find out if 3-methyl-2-azetidinone (**13**) could be synthesized under the same reaction conditions.

4.2.2 Synthesis of 3-Methyl-2-Azetidinone

For the synthesis of 3-methyl-2-azetidinone (**13**), three different synthetic procedures were attempted, as shown below.

1st Attempt

As previously mentioned, the first attempt to synthesize 3-methyl-2-azetidinone (**13**) was carried out following the method of Huang et al.,¹³¹ analogous to the procedure described in the previous chapter, with the only difference being the use of 3-amino-2-methylpropionic acid (**12**) instead of 3-aminobutyric acid (**9**). However, the reaction was unsuccessful, yielding the same product as obtained in the attempt using 3-aminobutyric acid (**9**).

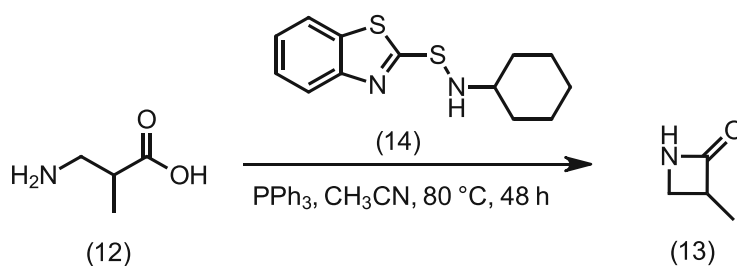


Scheme 23: First attempt towards the synthesis of 3-methyl-2-azetidinone (**13**)

2nd Attempt

In this attempt, 3-methyl-2-azetidinone (**13**) was synthesized as reported by Murayama et al.¹³⁴ Following the synthetic procedure, a suspension of 3-amino-2-methylpropanoic acid (**12**) and N-cyclohexyl-2-benzothiazolylsulfenamide (**14**) in acetonitrile was stirred with triphenylphosphine at 80°C. After the solvent was removed, the desired product was obtained

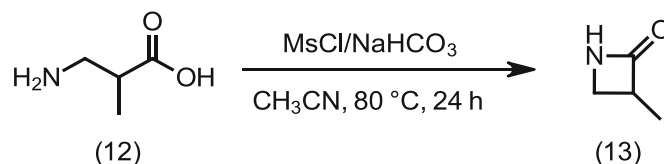
as a slightly yellow liquid in 29 % yield. The structure of the product was confirmed by $^1\text{H-NMR}$ spectroscopy.



Scheme 24: Second attempt towards the synthesis of 3-methyl-2-azetidinone (13)

3rd Attempt

Due to the low yield obtained in the previous synthetic route, another procedure (Scheme 25) was attempted, based on the method reported by Loewe et al.¹³⁵ In this attempt, 3-amino-2-methylpropanoic acid (**12**) was added to a solution of methanesulfonyl chloride in acetonitrile containing suspended NaHCO_3 . The reaction was performed at $80\text{ }^\circ\text{C}$ and for 24 h and the yield was enhanced from 29 % to 67 %.



Scheme 25: Third attempt towards the synthesis of 3-methyl-2-azetidinone (13)

4.2.3 Photo-DSC Study of 3-Methyl-2-Azetidinone

The photo-DSC measurements of 3-methyl-2-azetidinone were conducted using a formulation containing 2 mol% WPBG-266, along with 2 mol% N-acetylcaprolactam as a co-initiator,¹⁰² and 0.02 mol% DBA as a sensitizer.^{108–111} The measurements were conducted at temperature of $70\text{ }^\circ\text{C}$, with the samples being irradiated for 300 s using a light intensity of 80 mW cm^{-2} . The thermal response of the samples during photoinduced polymerization was recorded and the results are presented in Figure 32.

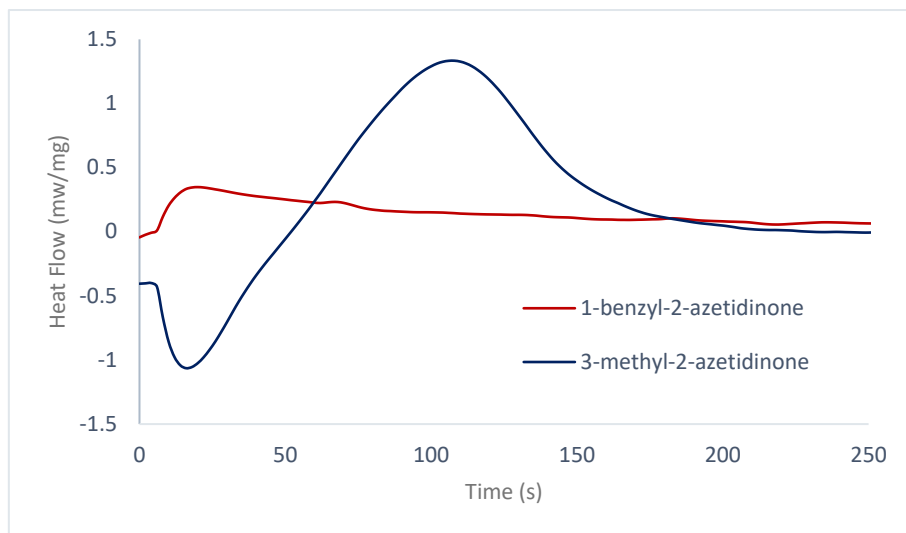


Figure 32: Photo-DSC analysis of 3-methyl-2-azetidinone cured with 2 mol% WPBG-266 at 70 °C compared to the photo-DSC results obtained for 1-benzyl-2-azetidinone cured under the same conditions

The overall shape of the recorded DSC curve of 3-methyl-2-azetidinone suggests that, although the system exhibits a brief delay at the start of irradiation, the polymerization reaction proceeds efficiently and reliably once initiated (Figure 32).

An interesting feature of the DSC curve of 3-methyl-2-azetidinone shown in Figure 32 is the initial downward deviation into the negative region before the characteristic exothermic polymerization peak appears. This initial negative signal may correspond to system equilibration or a minor thermal artifact before the actual polymerization begins. Thus, one possible explanation is the thermal equilibration of the sample and its components within the DSC crucible, which may cause transient baseline shifts, especially at elevated temperatures.¹³⁶ Additionally, the observed endothermic dip may result from non-radiative relaxation processes of the sensitizer DBA. Sensitizers like DBA can absorb photon energy and dissipate it as heat or *via* intersystem crossing to a triplet state before efficiently transferring energy to the photoinitiator system. This energy loss may briefly suppress exothermic heat flow during the induction phase.¹³⁷ Moreover, the delay in the onset of exothermic activity suggests the presence of an induction period required for the generation of reactive species through the multi-component initiation system. In systems involving electron or energy transfer between sensitizer, co-initiator, and photoinitiator, such induction periods are often necessary to establish a sufficient concentration of reactive species to initiate polymerization effectively.^{138,139}

The obtained data demonstrate a total released energy of 89.2 J g^{-1} , indicating that the photopolymerization proceeds efficiently under the applied experimental conditions. The reaction reached its maximum rate after 108 s, reflecting a relatively fast initiation phase despite not being immediate. Altogether, these results clearly confirm the relatively good reactivity and efficacy of the investigated formulation.

4.2.4 Optimizing the Model System

Given that the preliminary experiments showed promising results, where WPBG-266 showed a potential as a photoinitiator for the ring-opening polymerization of 3-methyl-2-azetidinone, further attempts were made to optimize the reaction parameters for this process. As in the case of 2-azetidinone, key reaction parameters were varied, including temperature, PBG concentration, as well as the concentration of the co-initiator, with the aim of identifying the most suitable conditions for efficient polymerization. All trials were performed in triplicate using a photo-DSC device equipped with a 320–500 nm light source. In each experiment, the samples were exposed to light for 300 s at an intensity of 80 mW cm^{-2} , in accordance with the procedure outlined at the beginning of the Results and Discussion section.

4.2.4.1 Temperature Screening

The following screening experiments demonstrate the impact of the temperature on the PBG-mediated ROP reaction of 3-methyl-2-azetidinone. The experiments employed an equimolar mixture of WPBG-266 and N-acetylcaprolactam (2 mol%). The samples were irradiated for 300 s under an irradiation intensity of 80 mW cm^{-2} . Materials obtained from the photo-DSC analysis were additionally dissolved in formic acid and analyzed using NMR to provide information about the monomer conversion.

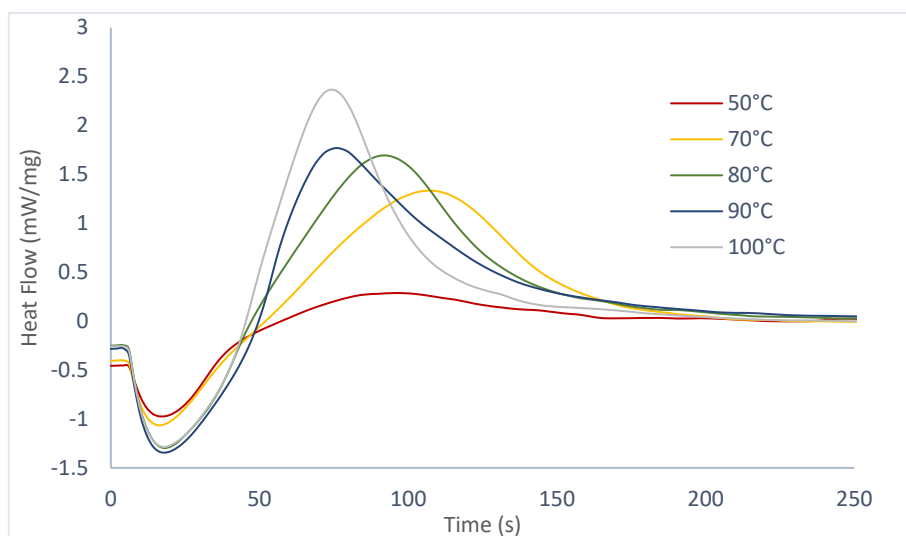


Figure 33: Temperature screening results for ROP of 3-methyl-2-azetidinone cured with WPBG-266

The results in Figure 33 and Table 5 demonstrate a trend, confirming the influence of thermal activation on the efficiency of the photoinitiated ROP process of 3-methyl-2-azetidinone when using WPBG-266 as a photoinitiator.

Table 5: Summary of results for ROP of 3-methyl-2-azetidinone cured with WPBG-266 at different temperatures

T [°C]	Area [J g ⁻¹]	t _{max} [s]	t ₉₅ [s]	R _p [mmol L ⁻¹ s ⁻¹]	Conversion [%]
50	14.5	94	157	-	-
70	89.2	108	175	17.2	27
80	101.6	92	170	21.7	31
90	105.2	77	167	22.5	33
100	110.1	74	157	30.8	37

A very weak exothermic response was observed at 50 °C, with a total heat release of only 14.5 J g⁻¹. This temperature marked the lowest point at which any exothermic behavior could be detected. However, the low heat release suggests that the extent of polymerization at this temperature was minimal. As the temperature increased, a clear trend emerged. The exothermic response became significantly more pronounced, and the total heat released increased steadily. The area under the exothermic curve rose sharply to 89.2 J g⁻¹ at 70 °C, and further increases in temperature to 80 °C, 90 °C, and 100 °C led to slight, but consistent improvements in both heat release and conversion. t_{max} values showed an inverse trend – decreasing from 108 s at 70 °C to 74 s at 100 °C – indicating that the reaction rate accelerated at higher temperatures. Additionally, the time to reach 95% of the total heat release slightly decreased, suggesting a more efficient and complete reaction process. Moreover, the rate of polymerization R_p was calculated using the theoretical polymerization enthalpy for methyl

derivatives of 2-azetidinone ($\sim 80 \text{ kJ mol}^{-1}$) and applying Equation 1 presented in *Materials and Methods* chapter, showing an increase with increasing temperature.^{123,124} Overall, the results revealed that temperature is an important parameter for promoting effective ROP in this model system. While 50 °C was the lowest temperature at which polymerization initiated, the polymerization efficiency and conversion were substantially improved at elevated temperatures, with 100 °C yielding the highest conversion and most pronounced exothermic response.

4.2.4.2 PBG Concentration Screening

With the aim to further refine the reaction conditions, the concentration of the WPBG-266 was varied between 1 and 3 mol% to evaluate its influence on the ring-opening polymerization of 3-methyl-2-azetidinone. The procedure was performed analogously to that used for 2-azetidinone. All reactions were carried out at 70°C using an equimolar mixture of WPBG-266 and N-acetylcaprolactam (ranging between 1 and 3 mol%). As the available amount of formic acid was insufficient to prepare all samples for NMR characterization, conversion analysis was performed exclusively for the temperature screening, and was not carried out for the co-initiator screening experiments.

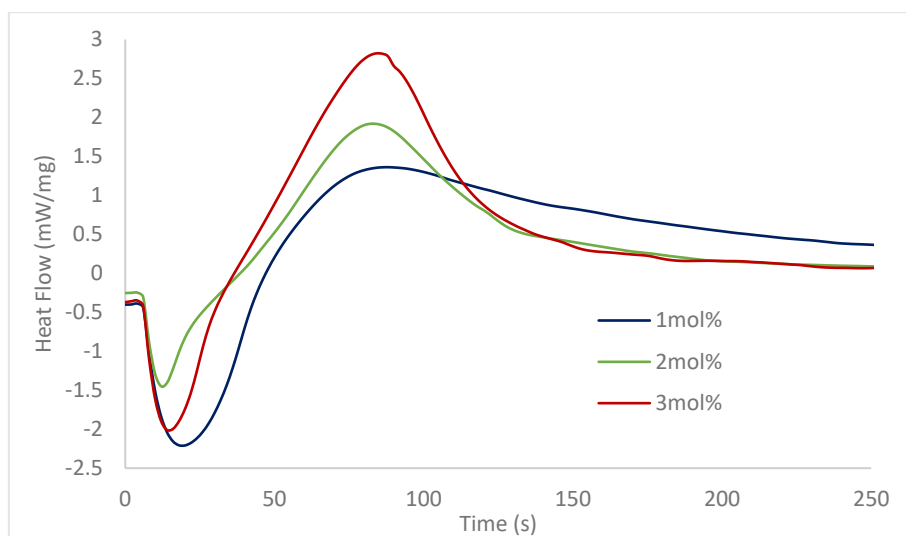


Figure 34: PBG concentration screening results for ROP of 3-methyl-2-azetidinone, each in an equimolar mixture with N-acetylcaprolactam as co-initiator

Table 6: Summary of results for ROP of 3-methyl-2-azetidinone cured with different concentrations of WPBG-266 and N-acetylcaprolactam

Concentration [mol%]	Area [J g ⁻¹]	t _{max} [s]	t ₉₅ [s]
1	112.3	88	228
2	116.1	83	167
3	166.8	85	168

The model system containing 1 mol% WPBG-2666 and 1 mol% N-acetylcaprolactam already exhibited a solid exothermic response, with a total heat release of 112.3 J g⁻¹. However, the reaction progressed relatively slowly, as reflected by prolonged t₉₅ of 228 s. Increasing the initiator and co-initiator concentration to 2 mol% resulted in a slight increase in heat release (116.1 J g⁻¹), but more importantly, the reaction proceeded faster – t_{max} decreased to 83 s and t₉₅ shortened considerably to 167 s. The most pronounced effect was observed at 3 mol%, where the exothermic area increased markedly to 166.8 J g⁻¹, indicating more efficient polymerization. The reaction remained fast, with t_{max} and t₉₅ values of 85 s and 168 s respectively, similar to those at 2 mol%, but with notably improved polymerization efficiency.

In general, these findings indicate that increasing the concentration of WPBG-266 significantly enhances the reaction rate as well as the extent of polymerization. 3 mol% WPBG-266 seems to be the most effective concentration among the tested conditions, effectively balancing initiation efficiency and polymer growth. This concentration may thus serve as a reliable baseline for further optimization in future studies.

4.2.4.3 Co-Initiator Concentration Screening

To evaluate the influence of co-initiator concentration on the ring-opening polymerization of 3-methyl-2-azetidinone, the amount of N-acetylcaprolactam was varied from 1 to 3 mol%, while maintaining the concentration of WPBG-266 constant at 3 mol%. All experiments were carried out at 70 °C under a light intensity of 80 mW cm⁻². Per formulation, triplicates were measured and one exemplary photo-DSC plot is depicted in Figure 35. Due to the insufficient amount of formic acid available for dissolving the obtained polymers prior to NMR characterization, conversion values were determined only in the temperature screening, and therefore were not obtained for this set of experiments.

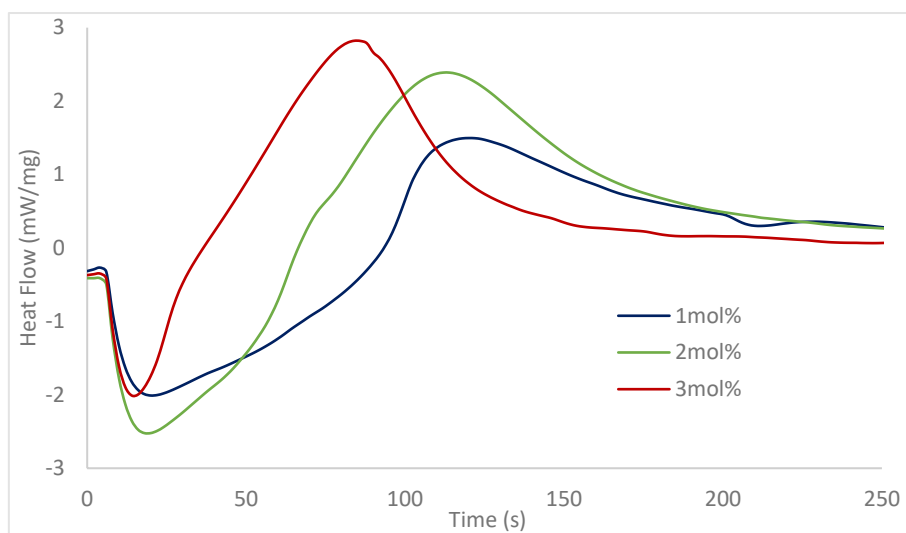


Figure 35: Co-initiator concentration screening results for ROP of 3-methyl-2-azetidinone cured with 3 mol% WPBG-266

The exothermic area of the model system containing 1 mol% N-acetylcaprolactam was relatively low and the reaction proceeded slowly. Increasing the co-initiator concentration to 2 mol% significantly enhanced the reaction, achieving a much higher heat release of 147.9 J g^{-1} , along with faster kinetics with $t_{\text{max}} = 112 \text{ s}$ and $t_{95} = 198 \text{ s}$. A further increase to 3 mol% led to an additional rise in the exothermic area, where the total heat release peaked at 166.8 J g^{-1} , and a more pronounced acceleration of the reaction, with t_{max} reduced to 85 s and t_{95} to 168 s. Table 7 summarizes the results of the analysis.

Table 7: Summary of results for ROP of 3-methyl-2-azetidinone cured with WPBG-266 and different concentrations of N-acetylcaprolactam

Concentration [mol%]	Area [J g^{-1}]	t_{max} [s]	t_{95} [s]
1	98.6	120	206
2	147.9	112	198
3	166.8	85	168

Overall, these results indicate that higher concentrations of N-acetylcaprolactam facilitate a more efficient ROP process of 3-methyl-2-azetidinone. While both 2 and 3 mol% show considerable improvements over 1 mol%, the results suggest that 3 mol% provides the optimal balance of high conversion and rapid reaction kinetics under the studied conditions.

4.2.5 Gravimetric Analysis

In order to determine the monomer conversion, gravimetric analysis was performed and the results were compared with those obtained by NMR spectroscopy. After the photopolymerization reaction was completed, cured samples were dissolved in formic acid and subsequently precipitated in cold ethanol under vigorous stirring, followed by centrifugation. The precipitate was then separated, washed with cold ethanol, and dried to constant weight in a drying oven. The conversion values obtained through gravimetric analysis were found to be in good agreement with those determined by ^1H NMR analysis.

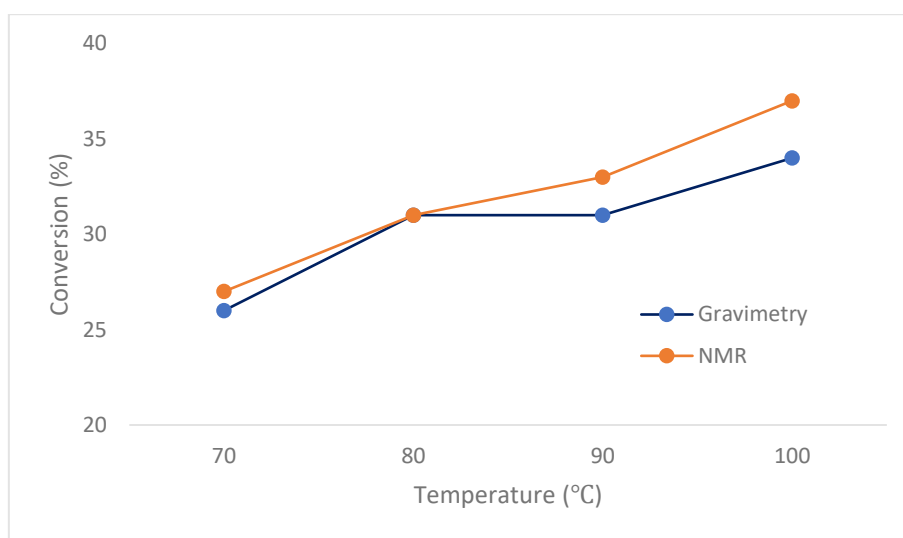


Figure 36: Comparison of monomer conversion at different temperatures calculated by gravimetric and NMR analysis

The monomer conversion values determined by gravimetric analysis and NMR spectroscopy at various temperatures revealed a consistent trend of increasing monomer conversion with rising temperature (Figure 36). The reason for such behavior is most likely due to better thermal activation that helps the release of basic species from the photobase generator and also enhances monomer diffusion in the reaction medium. Moreover, the results obtained by both analytical methods are in strong agreement across all tested temperatures, with deviations not exceeding 3 %. Therefore, this consistency supports the overall validity of the experimental findings.

Experimental Part

1. Reactivity Study of ϵ -Caprolactone

1.1 Photobase Screening

Three formulations were prepared, each composed of PBG (either WPBG-266, WPBG-300, or TP) combined with a co-initiator (benzyl alcohol or N-acetylcaprolactam) in an equimolar ratio, along with 0.02 mol% of either DBA or ITX as a photosensitizer. A completely homogenous solution was produced using a Vortex mixer and/or an ultrasonic bath. Photo-DSC analyses were carried out in triplicates using a Photo-DSC 204 F1 equipped with an autosampler from Netzsch. Measurements were performed under a nitrogen atmosphere at temperatures of 25, 50, 70, 90, and 120 °C. For each measurement, 12 ± 2 mg of the respective formulation was weighed into a 25 μ L aluminum crucible, sealed with a glass lid and exposed twice to filtered UV-light (320–500 nm) from an Exfo Omnicure 2000 Spot Curing System with a 200 W Hg lamp, maintaining a constant nitrogen flow of 20 mL min⁻¹. The light intensity at the sample surface was adjusted to 80 mW cm⁻², which is equivalent to 2 W cm⁻² at the tip of the light guide. Each sample was subjected to a 4-minute isothermal conditioning phase at the respective measurement temperature prior to irradiation. Data from the experiments were obtained by using Netzsch Proteus Thermal Analysis software, version 8.0.1.

After the photo-DSC analysis, the polymerized samples were analyzed *via* ¹H-NMR and GPC analysis. For NMR analysis, the samples were dissolved in CDCl₃, and the resulting spectra were processed using software MestreNova. For the GPC analysis, the samples in the aluminum crucibles were dissolved in THF containing 0.5 mg mL⁻¹ BHT as a flow marker. The resulting solutions were filtered through syringe filters and transferred into GPC vials for measurement.

1.2 Cationic Reference Systems based on Photoacid Initiation

CROP reactions were performed following the general procedure, employing an equimolar mixture of the respective PAG (I-AI or S-B) and benzyl alcohol as the co-initiator. All reactions were conducted in triplets on a photo-DSC device coupled with a light source emitting in the 320-500 nm range. For both systems, the reaction temperature was varied between 25, 50, 70, 90, and 120 °C. The samples were irradiated for 300 s with an intensity of 80 mW cm⁻².

Additionally, the cured samples were dissolved in either THF or CDCl_3 and prepared for further characterization using GPC and $^1\text{H-NMR}$ analysis. To this end, the reactions were quenched with 0.3 wt% pyridine.

2. Reactivity Study of ϵ -Caprolactam

2.1 Photobase Screening

Three previously described PBGs were used for the photo base screening. Accordingly, three formulations – each consisting of a PBG and a co-initiator (benzyl alcohol or N-acetylcaprolactam) in an equimolar ratio, as well as 0.02 mol% of either DBA or ITX as a photosensitizer – were irradiated at a constant temperature of 100 °C with a light intensity of 80 mW cm^{-2} , following the general procedure described in the Materials and Methods section.

2.2 ATR-FTIR Characterization

To obtain more detailed information and gain deeper insight into the efficiency of the AROP reactions of ϵ -caprolactam, ATR-IR measurements were carried out. FTIR spectra were recorded for the ϵ -caprolactam monomer, poly- ϵ -caprolactam, and after the photo-DSC measurements. ATR-FTIR measurements of the monomer, polymer and cured samples were performed in ATR mode using a PerkinElmer Spectrum 65 FT-IR Spectrometer equipped with a Specac MKII Golden Gate Single Reflection ATR System. Spectral data from the experiments were processed by using PerkinElmer Spectrum software in version 10.03.07.0112. The spectra were recorded in the wavenumber range of 4000 –1000 cm^{-1} .

3. Reactivity Study of 2-Azetidinone

3.1 Photobase Screening

Two formulations were prepared, each containing 2 mol% of either WPBG-266 or WPBG-300 in an equimolar ratio with a co-initiator (benzyl alcohol or N-acetylcaprolactam), and 0.02 mol% of DBA or ITX as a photosensitizer. Photopolymerization was initiated using a broadband UV/Vis light source (320–500 nm) with an intensity of 80 mW cm^{-2} . The samples were irradiated for 300 s and the measurements were conducted at 80 °C.

Following the photo-DSC analysis, the cured samples were subjected to DLS analysis. The samples were dissolved in hexafluoro isopropanol to a concentration of 1 mg mL^{-1} and filtered through syringe filters before being transferred into glass cuvettes. DLS measurements were conducted at $25 \text{ }^\circ\text{C}$, with the scattering angle set to 90° relative to the incident beam.

3.2 Optimizing the Model System

3.2.1 Temperature Screening

AROP reactions were carried out following the general procedure outlined in the Materials and Methods section, using an equimolar ratio of WPBG-266 and N-acetylcaprolactam, with 0.02 mol% of ITX as the photosensitizer. Experiments were conducted at temperatures of 70, 80, 90, and $100 \text{ }^\circ\text{C}$ and the samples were irradiated for 300 s using a light source with an intensity of 80 mW cm^{-2} .

3.2.2 PBG Concentration Screening

AROP reactions were investigated in accordance with the general procedure described in the Materials and Methods section, while testing different concentrations of WPBG-266, i.e. 1, 2 and 3 mol%. Equimolar mixtures of WPBG-266 and N-acetylcaprolactam were used for all measurements. All reactions were performed at $70 \text{ }^\circ\text{C}$ and the irradiation intensity was set at 80 mW cm^{-2} .

3.2.3 Co-Initiator Concentration Screening

AROP reactions were carried out in agreement with the general procedure described in the Materials and Methods section, using 3 mol% WPBG-266 whilst testing different N-acetylcaprolactam concentrations, i.e. 1, 2 and 3 mol%. The reaction temperature was kept constant at $70 \text{ }^\circ\text{C}$ and the irradiation intensity of the light source was set at 80 mW cm^{-2} .

3.3 Gravimetric analysis

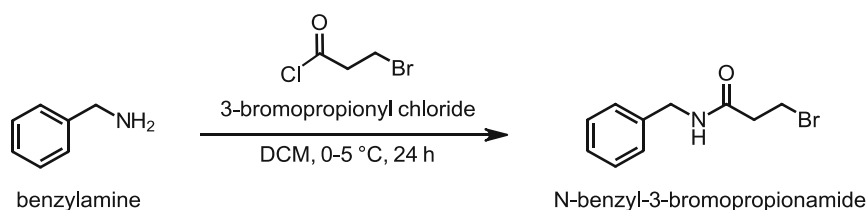
After completion of the reaction, the cured samples described in Section 3.2.1 were dissolved in formic acid and precipitated in cold ethanol under vigorous stirring. The precipitate was separated out by centrifugation and was left to stand for an extended period. The polymer was subsequently isolated, washed with an additional portion of cold ethanol, and dried in a drying oven to a constant weight.

4. Reactivity Study of 2-Azetidinone Derivatives

4.1 N-Substituted 2-Azetidinone Derivative

4.1.2 Synthesis of 1-Benzyl-2-Azetidinone

4.1.2.1 Synthesis of N-Benzyl-3-Bromopropionamide



The first reaction step was the synthesis of N-benzyl-3-bromopropionamide, which was performed according to a procedure published by Więckowska et al.¹⁴⁰ In a three-necked round-bottom flask set under an argon atmosphere, benzylamine (1 equiv., 21 mmol, 2.22 g) was dissolved in 165 mL of DCM and cooled to 0–5 °C. In a separate dropping funnel set under an argon atmosphere, 3-bromopropanoyl chloride (1.15 equiv., 24 mmol, 4.08 g) was dissolved in 80 mL of DCM and added dropwise to the stirring solution of benzylamine while maintaining the temperature at 0–5 °C. After complete addition, the stirring of the reaction mixture continued for 24 h at room temperature. Afterwards, the reaction mixture was cooled again to 0–5 °C, followed by the addition of 100 mL of a saturated solution of NaHCO₃. The organic layer was separated and further washed with saturated NaHCO₃ solution (2×100 mL), and then dried over Na₂SO₄. The drying agent was filtered off, and the solvent was evaporated under reduced pressure. The crude product was purified by column chromatography (PE:EE=1:3). The purified intermediate was obtained as white crystals with 52 % of the theory (18.2 g) and was used for the next synthesis step.

Yield: 18.2 g (52 % of the theory)

Appearance: white crystals

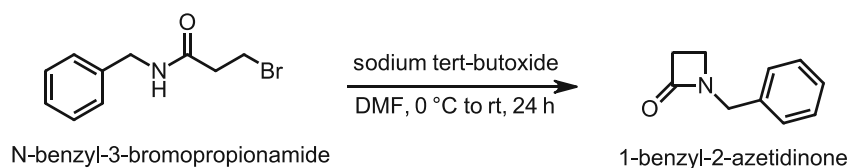
Melting point: 101.8–103.3 °C

¹H-NMR δ (ppm, 400 MHz, CDCl₃): 7.26–7.37 (m, 5H), 5.81 (s, 1H), 4.52 (d, 2H), 3.66 (t, 2H), 2.80 (t, 2H).

UPLC-MS: [M+1] 243

NMR data were in accordance with literature.¹⁴⁰

4.1.2.2 Synthesis of 1-Benzyl-2-Azetidinone



The second reaction step was conducted according to Fang et al.¹²⁷ In a three-necked round-bottom flask set under an argon atmosphere using a Schlenk technique, the intermediate N-benzyl-3-bromopropanamide (1 equiv., 62 mmol, 15.11 g,) was dissolved in 50 mL DMF and cooled to 0 °C. After cooling down to 0 °C, sodium tert-butoxide (1.1 equiv., 68 mmol, 6.55 g) was added in one portion, and the suspension was allowed to warm up to room temperature gradually. After 24 h, 30 mL H₂O were added to quench the reaction. At last, the reaction mixture was washed with ethyl acetate (2x50 mL). The organic phases were combined and the solvent was evaporated under reduced pressure. The crude product was purified by extraction using 1:1 mixture of petroleum ether and ethyl acetate. The purified product was obtained as a slightly yellow liquid with 44 % of the theory (4.3 g).

Yield: 4.3 g (44 % of the theory)

Appearance: pale yellow liquid

¹H-NMR δ (ppm, 400 MHz, CDCl₃): 7.37–7.20 (m, 5H), 4.38 (s, 2H), 3.12 (t, 2H), 2.94 (t, 2H).

UPLC-MS: [M+1] 162.20

NMR data were in accordance with literature.¹²⁷

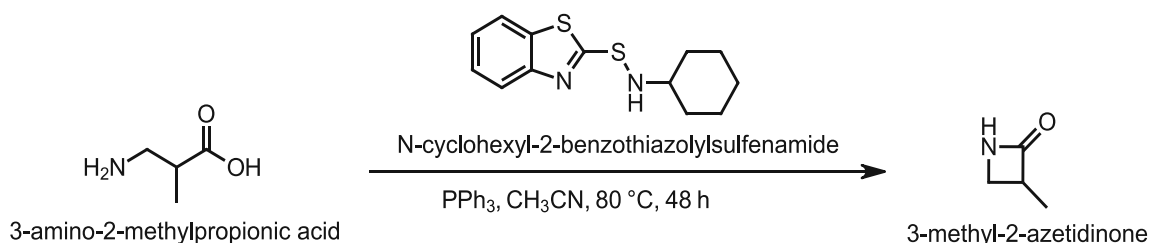
4.1.3 Photo-DSC Study of 1-Benzyl-2-Azetidinone

A formulation containing 2 mol% WPBG 266, 2 mol% N-acetylcaprolactam, and 0.02 mol% DBA was prepared. The mixture was thoroughly homogenized using a vortex mixer and an ultrasonic bath. The samples were then exposed to irradiation for 300 s under an intensity of 80 mW cm^{-2} using a light source operating in the 320–500 nm range. All measurements were conducted under a nitrogen atmosphere at $70 \text{ }^\circ\text{C}$.

4.2 N-Unsubstituted 2-Azetidinone Derivative

4.2.2 Synthesis of 3-Methyl-2-Azetidinone

2nd Attempt



The synthesis of 3-methyl-2-azetidinone was carried out following a procedure published by Murayama et al.¹³⁴ In a three-necked round-bottom flask set under an argon atmosphere using a Schlenk technique, 3-amino-2-methylpropanoic acid (1 equiv., 8 mmol, 0.84 g) and N-cyclohexyl-2-benzothiazolylsulfenamide (1.1 equiv., 9 mmol, 2.26 g) were suspended in 18 mL acetonitrile and stirred at $80 \text{ }^\circ\text{C}$. In parallel, triphenylphosphine (1.1 equiv., 9 mmol, 2.24 g) was dissolved in 2 mL toluene in a separate glass vial set under an argon atmosphere and added dropwise to the reaction mixture over a period of 20 min using a syringe. The reaction mixture was then stirred for 48 h at $80 \text{ }^\circ\text{C}$. At least, the solvent was evaporated under reduced pressure, and the crude product was purified by column chromatography (DCM:EE=1:1). The purified product was obtained as a slightly yellow liquid with 29 % of the theory (0.2 g).

Yield: 0.2 g (29 % of the theory)

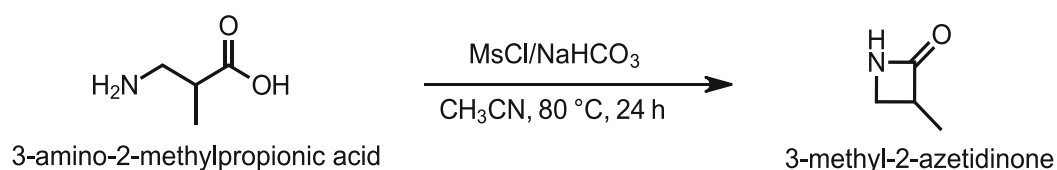
Appearance: pale yellow liquid

$^1\text{H-NMR}$ δ (ppm, 400 MHz, CDCl_3): 7.01-6.49 (s, 1H), 3.42 (m, 1H), 3.35-3.08 (m, 1H), 2.97 (dd, 1H), 1.33 (d, 3H).

$^{13}\text{C-NMR}$ δ (ppm, 100 MHz, CDCl_3): 172.76 (CO), 45.72 (CH_2), 43.33 (CH), 13.34 (CH_3).

NMR data were in accordance with literature.¹⁴¹

3rd Attempt



The synthesis of 3-methyl-2-azetidinone was adapted from an already reported procedure.¹³⁵ In a three-necked round-bottom flask set under an argon atmosphere using a Schlenk technique, NaHCO_3 (6 equiv., 21.2 mmol, 1.78 g) was suspended in 19.5 mL acetonitrile. The resulting suspension was heated to 80 °C. Methanesulfonyl chloride (1.1 equiv., 3.9 mmol, 0.44 g) was then added to the hot suspension using a syringe, and the reaction mixture was stirred vigorously at 80 °C for 24 h. At least, the fine suspension was cooled to 0 °C and filtered. The solvent was removed under reduced pressure, and the crude product was purified by column chromatography (PE:EE=1:5). The desired product was obtained as a slightly yellow liquid with 67 % of the theory (0.2 g).

Yield: 0.2 g (67 % of the theory)

Appearance: pale yellow liquid

¹H-NMR δ (ppm, 400 MHz, CDCl_3): 7.01-6.49 (s, 1H), 3.42 (m, 1H), 3.35-3.08 (m, 1H), 2.97 (dd, 1H), 1.33 (d, 3H).

¹³C-NMR δ (ppm, 100 MHz, CDCl_3): 172.76 (CO), 45.72 (CH_2), 43.33 (CH), 13.34 (CH_3).

NMR data were in accordance with literature.¹⁴¹

4.2.3 Photo-DSC Study of 3-Methyl-2-Azetidinone

Photo-DSC analysis of 3-methyl-2-azetidinone was performed using a formulation containing 2 mol% WPBG-266, 2 mol% N-acetylcaprolactam as the co-initiator, and 0.02 mol% DBA serving as the sensitizer. The measurements were conducted at 70 °C, with each sample being irradiated for 300 s under a light intensity of 80 mW cm⁻².

4.2.4 Optimizing the Model System

4.2.4.1 Temperature Screening

AROP reactions were performed according to the general procedure described in the Materials and Methods section. The experiments employed an equimolar mixture of WPBG-266 and N-acetylcaprolactam (2 mol%) as well as 0.02 mol% of ITX as the photosensitizer. The samples were irradiated for 300 s under an irradiation intensity of 80 mW cm⁻². Experiments were performed at temperatures of 50, 70, 80, 90, and 100 °C.

4.2.4.2 PBG Concentration Screening

AROP reactions were carried out following the general procedure described in the Materials and Methods section. All reactions were carried out at 70°C using different concentrations of WPBG-266, i.e. 1, 2 and 3 mol%. The irradiation intensity was set at 80 mW cm⁻².

4.2.4.3 Co-Initiator Concentration Screening

AROP reactions were conducted in agreement with the general procedure described in the Materials and Methods section. The concentration of N-acetylcaprolactam was varied between 1 and 3 mol%, while the concentration of WPBG-266 was maintained at 3 mol%. All experiments were carried out at 70 °C under irradiation with a light intensity of 80 mW cm⁻².

4.2.5 Gravimetric Analysis

After completion of the reaction, the cured samples described in Section 4.2.3.1 were dissolved in formic acid and subsequently precipitated into cold ethanol under vigorous stirring. The resulting precipitate was collected by centrifugation and left to stand for a prolonged period. The obtained polymer was then isolated, washed with additional portions of cold ethanol, and dried in an oven to a constant weight.

Conclusion

Photopolymerization has emerged as one of the most promising technologies for the advanced manufacturing of polymers. In general, radical photopolymerization has been greatly used in additive manufacturing, while the use of ionic photopolymerization is still underexplored. Over the last decades, however, there is a growing interest in ionic photopolymerization based on their resistance to oxygen inhibition, accurate control over polymer structure, and broader choice of monomers. A central element of any photopolymerization process is the photoactive compound, which absorbs light and forms reactive species to initiate polymerization, and thus determines the properties of the material. Among the recent developments in photoinitiators, photobase generators (PBGs) have attracted significant interest due to several advantages over conventional radical or acid-based initiators, such as oxygen insensitivity, monomer compatibility scope, reduced volumetric shrinkage in the cured material, and metal substrate corrosion prevention.

In this work, the focus was placed on the anionically initiated, photobase-mediated ring-opening polymerization of cyclic monomers, including both cyclic esters and amides. Initially, commonly known cyclic esters and amides, which are shown in Figure 37, were examined to evaluate their temperature dependent reactivity. For this purpose, three photobase generators known from the literature were selected (Figure 37).

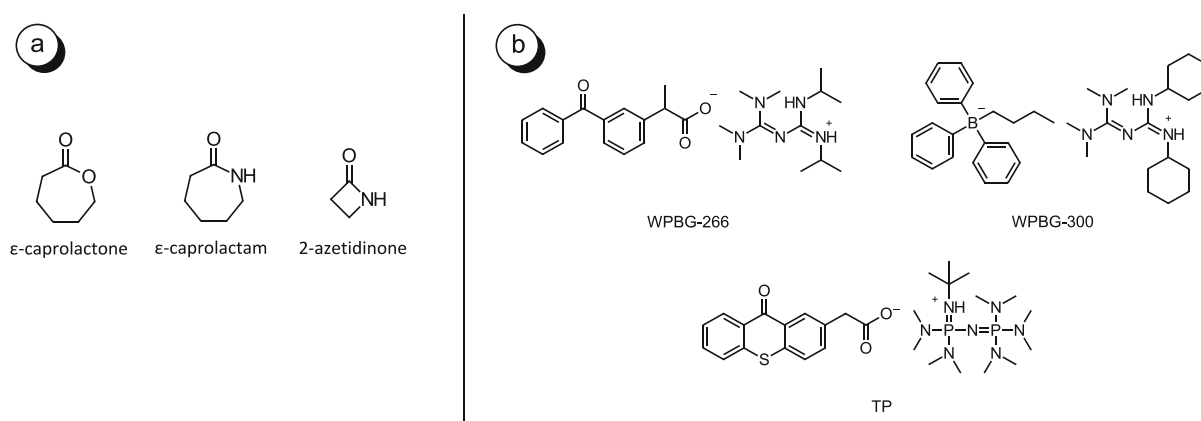


Figure 37: Chemical structures of a) cyclic esters and amides and b) photobase generators examined in PBG-mediated AROP reactions

Compared to ϵ -caprolactam, which showed no successful polymerization with any of the tested photobase generators, ϵ -caprolactone revealed good results in PBG-mediated anionic ring-opening polymerization with all three photobases. Among them, WPBG-266 outperformed the other two PBGs, demonstrating the highest efficiency. All three photobase systems revealed a very strong dependence on temperature, which pointed to the main importance of thermal activation in AROP of ϵ -caprolactone. However, since the anionic approach did not provide improved results compared to PAG-mediated cationic ring-opening polymerization of ϵ -caprolactone, the focus of this work was subsequently shifted entirely to the more reactive lactam, 2-azetidinone, which demonstrated similarly good reactivity as ϵ -caprolactone.

Although 2-azetidinone exhibited promising reactivity, its solid state at room temperature restricts its practical applicability in certain processes, such as 3D printing. To overcome this restriction, two liquid analogues which were structurally closely related to the parent compound were successfully synthesized (Figure 38). Their reactivity in PBG-mediated AROP at different temperatures was systematically evaluated with WPBG-266, which had been shown the most efficient among the tested photoinitiators.

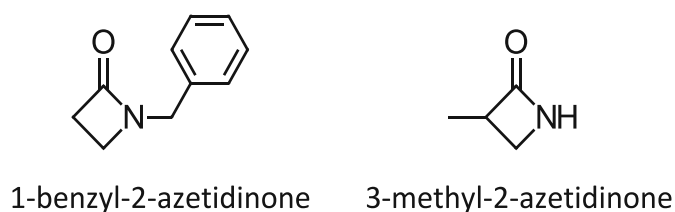


Figure 38: Chemical structures of liquid 2-azetidinone derivatives examined in PBG-mediated AROP reactions

The results obtained for 1-benzyl-2-azetidinone indicated poor polymerization performance: GPC analysis registered only low molecular weights, while photo-DSC measurements obtained only a very weak exothermic response, thus suggesting that ring-opening polymerization under the applied conditions was ineffective. In contrast, 3-methyl-2-azetidinone showed significantly higher reactivity, achieving efficient polymerization with slightly reduced performance compared to unsubstituted 2-azetidinone, yet still demonstrating relatively high efficiency.

Finally, optimization was performed on model systems employing either 2-azetidinone or 3-methyl-2-azetidinone as monomers, with WPBG-266 as the photobase generator, and N-acetylcaprolactam as the co-initiator. The impact of temperature, PBG concentration, and co-initiator concentration was then assessed. In agreement with the conclusions obtained in Chapters 3 and 4, it was found that temperature is an important factor influencing the polymerization to the greatest extent. Performing the ROP reaction at elevated temperature (above 50 °C) was necessary for satisfactory product formation. Increasing the concentrations of both WPBG-266 and the co-initiator to 3 mol% led to an overall reactivity enhancement. In both model systems, higher temperatures and increased concentrations of WPBG-266 and co-initiator resulted in higher polymerization efficiency, faster reaction rates and better overall curing performance.

In summary, PBG-mediated anionic ring-opening polymerization of ϵ -caprolactone, 2-azetidinone, and 3-methyl-2-azetidinone has been successfully shown in this research. Although the results do support the feasibility of this approach, they also emphasise the need for more thorough and extensive research. Nonetheless, the work presented in this thesis provides a foundation for future studies aimed at advancing the development and practical application of PBG-mediated polymerization systems.

Materials and Methods

Commercial chemicals: all commercially obtained chemicals were used as received without further purification, unless specified otherwise. Pure solvents were all obtained from Donau Chemie and dried with a PureSolvsystem (Inert, Amesbury, MA).

Photo-DSC studies were conducted on a Photo-DSC 204 F1 equipped with an autosampler from Netzsch, using 25 μL aluminum crucibles and glass lids. An Exfo Omnicure 2000 Spot Curing System with a 200 W Hg lamp and glass fiber light waveguides was used as a light source, calibrated *via* an Omnicure R2000 radiometer before each measurement sequence. All measurements were conducted under N_2 -atmosphere (flow rate: 20 mL min^{-1}) at the respective temperature. The analyzed formulations contained the respective monomer, 2 mol% PBG, 2 mol% BzOH or N-Acetylcaprolactam as CI and 0.02 mol% ITX or DBA as photosensitizer unless otherwise noted. A completely homogenous solution was produced using a Vortex mixer and/or an ultrasonic bath. The formulations ($12 \pm 2 \text{ mg}$) were then heated to the respective temperature, equilibrated for 4 minutes and irradiated twice for 5 minutes. The light intensity was set to 2 W cm^{-2} at the tip of the light guide corresponding to $\sim 80 \text{ mW cm}^{-2}$ on the surface of the sample. The heat flow of the polymerization reaction was recorded as a function of time. All measurements were performed in triplicates. The data analysis was performed with the Netzsch Proteus Thermal Analysis program in version 8.0.1.

Calorimetric and conversion analysis

Three samples were measured for each formulation and parameter. Before irradiation, each sample was conditioned during an isothermal period of 4 min at the selected temperature. Then, the samples underwent two successive irradiation sessions, each lasting 300 seconds at the selected temperatures. The results represent the polymerization enthalpy of the respective formulation as a function of time. The second irradiation phase was conducted to eliminate background signals during evaluation, achieved by subtracting the second irradiation segment from the first. These results were then used to determine the polymerization heat (area in J g^{-1}), t_{max} (time to maximum heat development) and t_{95} (time until 95% of the heat is developed). The rate of polymerization R_p was determined using Equation 1:

$$R_p \text{ (mmolL}^{-1}\text{s}^{-1}\text{)} = \frac{h \cdot \rho}{\Delta H_0} \cdot 1000$$

Equation 1: Calculation of R_p ($\text{mmolL}^{-1}\text{s}^{-1}$)

- h height of the photo-DSC signal [mW mg^{-1}]
 ρ density of the monomer [g L^{-1}]
 ΔH_0 theoretical polymerization heat of the monomer [J mol^{-1}]

The polymerized samples were analyzed immediately after irradiation *via* NMR and GPC analysis. For the GPC analysis, the samples in the aluminum crucibles were dissolved in THF containing 0.5 mg mL^{-1} BHT as a flow marker and transferred into GPC vials *via* syringe filters. For NMR analysis of the systems in which PAG was used as the initiator to trigger the CROP mechanism, the samples were dissolved in CDCl_3 containing 0.3 wt% pyridine and measured directly, while all other samples were analyzed using only CDCl_3 as the solvent.

Gel permeation chromatography (GPC) measurements were performed on a Malvern VISCOTEK TDA system equipped with a VISCOTEK SEC MALS 9 light scattering detector, a Viscotek TDA 305-021 RI + Visc detector, and a UV Detector Module 2550 for TDA 305. The cured samples were dissolved in tetrahydrofuran (yielding concentrations of about 2.5 mL min^{-1}) containing 0.5 mg mL^{-1} butylated hydroxytoluene (BHT) as a flow marker unless otherwise noted and transferred into GPC vials *via* syringe filters. Conventional calibration was conducted with polystyrene (PS) standards (MW = 474 – 177 000 Da) supplied by PSS. Separation was conducted through three consecutive PSS SDC columns (100 \AA , 1.000 \AA , and 100.000 \AA) using THF as solvent at a flow rate of 0.8 mL min^{-1} . Analysis was conducted with the OmniSEC Software V5.12.461 (Malvern) to evaluate the elugrams.

ATR-FTIR experiments of the cured specimens were carried out on a PerkinElmer Spectrum 65 FT-IR Spectrometer, using a Specac MKII Golden Gate Single Reflection ATR System and evaluated with PerkinElmer Spectrum 10.03.07.0112.

Thin-layer chromatography (TLC) was carried out on aluminum-backed unmodified Merck silica gel 60 F_{254} plates, and the spots were visualized under UV irradiation.

Column chromatography was performed with a Büchi MPLC-system equipped with the control unit C-620, fraction collector C-660, RI detector and UV-photometer C-635. As stationary phase Merck silica gel 60 (0.040 – 0.063 mm) was used as stationary phase.

Ultra-High-Pressure Liquid Chromatography-mass spectroscopy (UHPLC-MS): HPLC analysis was performed on a Nexera X2[®] UHPLC system by Shimadzu[®] equipped with LC-30AD pumps, SIL-30AC autosampler, CTO-20AC column oven, and DGU-20A5/3 degasser module. Detection was achieved using an SPD-M20A photodiode array, an RF-20Axs fluorescence detector, and ELS-2041 evaporative light scattering detector (JASCO[®]) and an LC-MS-2020 mass spectrometer (ESI/APCI). Unless stated otherwise, separations were conducted using a Waters[®] XSelect[®] CSHTM C18 2,5 μm (3.0 x 50 mm) column XP at 40 °C with a flowrate of 1.7 mL min⁻¹ with water/acetonitrile + 0.1 % formic acid gradient elution.

Orange light lab: All weigh-ins, reactions and measurements of light-sensitive substances were performed in an orange light laboratory. Windows were laminated with Asmetec metolight SF-UV foils (type ASR-SF-LY5) to block UV radiation, and the lighting was provided by Osram Lumix lamps equipped with chip-controlled light color 62.

Nuclear magnetic resonanz (NMR) spectra were obtained on a Bruker Avance DRX-400 FT-NMR spectrometer at 400 MHz for ¹H and 100 MHz for ¹³C. Chemical shifts were given in ppm relative to trimethyl silane (d = 0 ppm) and referenced on the respective NMR-solvent. Reactions showing dark polymerization were quenched with pyridine (0.3 wt%) before the measurement. The spectra were analyzed using the software *MestreNova*.

Dynamic light scattering (DLS) experiments were carried out on an ALV/LSE-5004 Light Scattering Electronics and Multiple Tau Digital Correlator at 25 °C. The wavelength of the laser was 633 nm and the scattering angle was 90° with respect to the incoming beam. Acquisition time was varied between 30 seconds to 60 seconds. For evaluation of the data, the software ALV-7004 Correlator was used.

Software: *Graphs and plots* were generated using Microsoft Excel. *Chemical drawings*, marked as Schemes, were created using ChemDoodle. ChatGPT was used for *language refinement*, including improvements in *word choice, grammar, syntax, paraphrasing and copyediting*. *Interpretation and visualization of NMR spectra* was generated with the help of the software

MestreNova. To evaluate *photo-DSC graphs*, NETZSCH-Proteus-80 was utilized. For processing *ATR-FTIR spectra* Proteus Analysis was used.

Abbreviations

AMT	Additive manufacturing technology
Ar	Argon
AROP	Anionic ring-opening polymerization
ATR-FTIR	Attenuated total reflectance-fourier transform spectroscopy
BzOH	Benzyl alcohol
CI	Co-initiator
CDCl ₃	Deuterated chloroform
εCL	ε-caprolactone
CROP	Cationic ring-opening polymerization
DBA	9,10-Dibutoxyanthracene
DCM	Dichloromethane
DLP	Digital light processing
DLS	Dynamic light scattering
DSC	Differential scanning calorimetry
3D	Three Dimensional
EE	Ethyl acetate
GPC	Gel permeation chromatography
HPLC	High performance liquid chromatography
ITX	2-Isopropylthioxanthone
M _n	Number average molecular weight
mol%	Mole percent
M _w	Weight average molecular weight
NMR	Nuclear magnetic resonance
PAG	Photoacid generator
PBG	Photobase generator
PCL	Poly(caprolactone)
PDI	Polydispersity
PE	Petroleum ether
PI	Photoinitiator

ROP	Ring-opening polymerization
RP	Rapid prototyping
rt	Room temperature
t	Time
T	Temperature
THF	Tetrahydrofuran
TLC	Thin layer chromatography
TP	Bis(dimethylamino)[tris(dimethylamino)phosphorylamino]phosphoryl(<i>tert</i> -butyl)azanium
t ₉₅	Time where conversion reaches 95%
UHPC-MS	Ultra-high-pressure liquid chromatography-mass spectroscopy
UV	Ultraviolet
WPBG-266	1,2-Diisopropyl-3-[bis(dimethylamino)methylene]guanidium 2-(3-benzoylphenyl)propionate
WPBG-300	1,2-Dicyclohexyl-4,4,5,5-tetramethylbiguanidium n-butyltriphenylborate
wt%	Weight percent

Literature

1. Wong K V., Hernandez A. A Review of Additive Manufacturing. ISRN Mechanical Engineering. 2012;2012:1-10. doi:10.5402/2012/208760
2. Abdulhameed O, Al-Ahmari A, Ameen W, Mian SH. Additive manufacturing: Challenges, trends, and applications. Advances in Mechanical Engineering. 2019;11(2). doi:10.1177/1687814018822880
3. Butt J, Hewavidana Y, Mohaghegh V, Sadeghi-Esfahlani S, Shirvani H. Hybrid manufacturing and experimental testing of glass fiber enhanced thermoplastic composites. Journal of Manufacturing and Materials Processing. 2019;3(4). doi:10.3390/jmmp3040096
4. Ahn JH, Ham NH, Kim JH, Kim JJ. Additive Manufacturing Oriented Parametric Design Automation of Adaptive Joint System for an Irregular Form Gridshell Structure. Applied Sciences (Switzerland). 2024;14(23). doi:10.3390/app142311038
5. Gebhardt A. Understanding Additive Manufacturing: Rapid Prototyping, Rapid Tooling, Rapid Manufacturing. Carl Hanser Verlag; 2011. ISBN 978-3-446-41715-0.
6. Ligon SC, Liska R, Stampfl J, Gurr M, Mülhaupt R. Polymers for 3D Printing and Customized Additive Manufacturing. Chem Rev.American Chemical Society. 2017;117(15):10212-10290. doi:10.1021/acs.chemrev.7b00074
7. Zivanovic ST, Popovic MD, Vorkapic NM, Pjevic MD, Slavkovic NR. An overview of rapid prototyping technologies using subtractive, additive and formative processes. FME Transactions. 2020;48(1):246-253. doi:10.5937/fmet2001246Z
8. Narowski P, Wilczyński K. A Global Approach to Modeling Injection Molding. Polymers (Basel). 2024;16(1). doi:10.3390/polym16010147
9. Deboer B, Nguyen N, Diba F, Hosseini A. Additive, subtractive, and formative manufacturing of metal components: a life cycle assessment comparison. doi:10.1007/s00170-021-07173-5/Published
10. Thomas DS, Gilbert SW. Costs and Cost Effectiveness of Additive Manufacturing.; 2014. doi:10.6028/NIST.SP.1176
11. Krimpenis AA, Iordanidis DM. Design and Analysis of a Desktop Multi-Axis Hybrid Milling-Filament Extrusion CNC Machine Tool for Non-Metallic Materials. Machines. 2023;11(6). doi:10.3390/machines11060637
12. Blakey-Milner B, Gradl P, Snedden G, et al. Metal additive manufacturing in aerospace: A review. Mater Des. 2021;209:110008. doi:10.1016/J.MATDES.2021.110008
13. Blakey-Milner B, Gradl P, Snedden G, et al. Metal additive manufacturing in aerospace: A review. Mater Des. 2021;209. doi:10.1016/j.matdes.2021.110008
14. Schiller G1. Additive Manufacturing for Aerospace; 2015. doi:10.1109/AERO.2015.7118958
15. Mohanavel V, Ashraff Ali KS, Ranganathan K, Allen Jeffrey J, Ravikumar MM, Rajkumar S. The roles and applications of additive manufacturing in the aerospace and automobile sector. In: Materials Today: Proceedings. Vol 47. Elsevier Ltd; 2021:405-409. doi:10.1016/j.matpr.2021.04.596
16. Sandgren J, Nilsson J, Olivella J. Additive Manufacturing in the Automotive Industry A Review on the Future Prospects; 2023.

17. Schuhmann D, Rockinger C, Merkel M, Harrison DK. A Study on Additive Manufacturing for Electromobility. *World Electric Vehicle Journal*.MDPI. 2022;13(8). doi:10.3390/wevj13080154
18. Drstvensek I, Pal S, Ihan Hren N, eds. *Additive Manufacturing in Multidisciplinary Cooperation and Production*. Springer International Publishing; 2024. doi:10.1007/978-3-031-37671-9
19. Li C, Pisignano D, Zhao Y, Xue J. Advances in Medical Applications of Additive Manufacturing. *Engineering*. 2020;6(11):1222-1231. doi:10.1016/j.eng.2020.02.018
20. Singh S, Ramakrishna S. Biomedical applications of additive manufacturing: Present and future. *Curr Opin Biomed Eng*.Elsevier B.V. 2017;2:105-115. doi:10.1016/j.cobme.2017.05.006
21. Bhargav A, Sanjairaj V, Rosa V, Feng LW, Fuh YH J. Applications of additive manufacturing in dentistry: A review. *J Biomed Mater Res B Appl Biomater*.John Wiley and Sons Inc. 2018;106(5):2058-2064. doi:10.1002/jbm.b.33961
22. Medellín-Castillo HI, Esau J, Torres P. (2009). Rapid prototyping and manufacturing: A review of current technologies. *American Society of Mechanical Engineers*. doi:10.1115/IMECE2009-11750
23. Saleh Alghamdi S, John S, Roy Choudhury N, Dutta NK. *polymers Additive Manufacturing of Polymer Materials: Progress, Promise and Challenges*. Published online 2021. doi:10.3390/polym13
24. Huang J, Qin Q, Wang J. A review of stereolithography: Processes and systems. *Processes*.Multidisciplinary Digital Publishing Institute (MDPI). 2020;8(9). doi:10.3390/PR8091138
25. Hull CW, Arcadia C. Apparatus for production of three-dimensional objects by stereolithography (U.S. Patent No. 4,575,330). United States Patent and Trademark Office; 1986.
26. Voet VSD, Guit J, Loos K. Sustainable Photopolymers in 3D Printing: A Review on Biobased, Biodegradable, and Recyclable Alternatives. *Macromol Rapid Commun*.Wiley-VCH Verlag. 2021;42(3). doi:10.1002/marc.202000475
27. Pfaffinger M. Hot Lithography – New Possibilities in Polymer 3D Printing. *Laser Technik Journal*. 2018;15(4):45-47. doi:10.1002/latj.201800024
28. Pezzana L, Wolff R, Melilli G, et al. Hot-lithography 3D printing of biobased epoxy resins. *Polymer (Guildf)*. 2022;254. doi:10.1016/j.polymer.2022.125097
29. Wolff R, Ehrmann K, Knaack P, et al. Photo-chemically induced polycondensation of a pure phenolic resin for additive manufacturing. *Polym Chem*. 2022;13(6):768-777. doi:10.1039/d1py01665b
30. Mete Y, Seidler K, Gorsche C, Koch T, Knaack P, Liska R. Cationic photopolymerization of cyclic esters at elevated temperatures and their application in hot lithography. *Polym Int*. 2022;71(9):1062-1071. doi:10.1002/pi.6430
31. Schandl S, Koch T, Stampfl J, Ehrmann K, Liska R. Pure aliphatic polycarbonate networks via photoinduced anionic ring-opening polymerization at elevated temperature. *React Funct Polym*. 2023;182. doi:10.1016/j.reactfunctpolym.2022.105460
32. Steyrer B, Neubauer P, Liska R, Stampfl J. Visible light photoinitiator for 3D-printing of tough methacrylate resins. *Materials*. 2017;10(12). doi:10.3390/ma10121445

33. Corrigan N, Yeow J, Judzewitsch P, Xu J, Boyer C. Seeing the Light: Advancing Materials Chemistry through Photopolymerization. *Angewandte Chemie*. 2019;131(16):5224-5243. doi:10.1002/ange.201805473
34. Zivic N, Kuroishi PK, Dumur F, Gignes D, Dove AP, Sardon H. Organische Photosäuren- und Photobasenbildner für Polymerisationen: Jüngste Fortschritte und Herausforderungen. *Angewandte Chemie*. 2019;131(31):10518-10531. doi:10.1002/ange.201810118
35. Ganster B, Fischer UK, Moszner N, Liska R. New photocleavable structures. Diacylgermane-based photoinitiators for visible light curing. *Macromolecules*. 2008;41(7):2394-2400. doi:10.1021/ma702418q
36. Fouassier JP, Allonas X, Burget D. Photopolymerization reactions under visible lights: Principle, mechanisms and examples of applications. *Prog Org Coat*. 2003;47(1):16-36. doi:10.1016/S0300-9440(03)00011-0
37. Lang M, Hirner S, Wiesbrock F, Fuchs P. A Review on Modeling Cure Kinetics and Mechanisms of Photopolymerization. *Polymers (Basel)*. 2022;14(10). doi:10.3390/polym14102074
38. Dadashi-Silab S, Doran S, Yagci Y. Photoinduced Electron Transfer Reactions for Macromolecular Syntheses. *Chem Rev.American Chemical Society*. 2016;116(17):10212-10275. doi:10.1021/acs.chemrev.5b00586
39. Gruber HF. Photoinitiators for free radical polymerization. Vol. 17; 1992.
40. Andrzejewska E. Photopolymerization Kinetics of Multifunctional Monomers. *Progress in Polymer Science*, Vol. 26, 2001, str. 605–665. doi:10.1016/S0079-6700(01)00004-1
41. Kaur M, Srivastava AK. Photopolymerization: A review. *Journal of Macromolecular Science - Polymer Reviews*. Marcel Dekker Inc. 2002;42(4):481-512. doi:10.1081/MC-120015988
42. Mete Y.D. Novel initiators and green monomers for ionic photopolymerization; 2021.
43. Sipani V, Scranton AB. Dark-Cure Studies of Cationic Photopolymerizations of Epoxides: Characterization of the Active Center Lifetime and Kinetic Rate Constants.; 2003.
44. Decker C, Moussa K. Kinetic Study of the Cationic Photopolymerization of Epoxy Monomers.
45. Zivic N, Kuroishi PK, Dumur F, Gignes D, Dove AP, Sardon H. Organische Photosäuren- und Photobasenbildner für Polymerisationen: Jüngste Fortschritte und Herausforderungen. *Angewandte Chemie*. 2019;131(31):10518-10531. doi:10.1002/ange.201810118
46. Sangermano M, Roppolo I, Chiappone A. New horizons in cationic photopolymerization. *Polymers (Basel)*. MDPI AG. 2018;10(2). doi:10.3390/polym10020136
47. Dadashi-Silab S, Doran S, Yagci Y. Photoinduced Electron Transfer Reactions for Macromolecular Syntheses. *Chem Rev.American Chemical Society*. 2016;116(17):10212-10275. doi:10.1021/acs.chemrev.5b00586
48. Crivello J V, Lam JHW. Diaryliodonium Salts 1307 Diaryliodonium Salts. A New Class of Photoinitiators for Cationic Polymerization. Vol 10. UTC; 2025. <https://pubs.acs.org/sharingguidelines>
49. Crivello J V., Lam JHW. Photoinitiated cationic polymerization with triarylsulfonium salts. *J Polym Sci A Polym Chem*. 1996;34(16):3231-3253. doi:10.1002/pola.1996.873

50. Crivello J V. The discovery and development of onium salt cationic photoinitiators. *J Polym Sci A Polym Chem.* 1999;37(23):4241-4254. doi:10.1002/(SICI)1099-0518(19991201)37:23<4241::AID-POLA1>3.0.CO;2-R
51. Fouassier JPierre, Lalevée Jacques. *Photoinitiators.* Wiley-VCH; 2021.
52. Noon A, Hamieh T, Toufaily J, et al. Phenothiazine-based oxime ester as a photobase generator for thiol-acrylate reactions. *Eur Polym J.* 2024;204. doi:10.1016/j.eurpolymj.2023.112679
53. Zheng Y, Yang Y, Yang H, Han F, Li Z. Thioxanthone-based amidine: An efficient nonionic photobase generator for thiol-based click polymerization under visible LED light. *Prog Org Coat.* 2020;148. doi:10.1016/j.porgcoat.2020.105842
54. Cameron, J. F.; Frechet, J. M. J. Base Catalysis in Imaging Materials. 1. Design and Synthesis of Novel Light-Sensitive Urethanes as Photoprecursors of Amines. *Journal of Organic Chemistry*, 1990, 55(23), 5919–5922. doi: 10.1021/jo00310a028
55. Sarker AM, Lungu A, Mejiritski A, Kaneko Y, Neckers DC. Tetraorganylborate Salts as Convenient Precursors for Photogeneration of Tertiary Amines.; 1998.
56. Sun X, Gao JP, Wang ZY. Bicyclic guanidinium tetraphenylborate: A photobase generator and a photocatalyst for living anionic ring-opening polymerization and cross-linking of polymeric materials containing ester and hydroxy groups. *J Am Chem Soc.* 2008;130(26):8130-8131. doi:10.1021/ja802816g
57. Arimitsu K, Endo R. Application to photoreactive materials of photochemical generation of superbases with high efficiency based on photodecarboxylation reactions. *Chemistry of Materials.* 2013;25(22):4461-4463. doi:10.1021/cm4022485
58. Suyama K, Shirai M. Photobase generators: Recent progress and application trend in polymer systems. *Progress in Polymer Science (Oxford).* 2009;34(2):194-209. doi:10.1016/j.progpolymsci.2008.08.005
59. Russo S, Casazza E. Ring-Opening Polymerization of Cyclic Amides (Lactams). In: *Polymer Science: A Comprehensive Reference, 10 Volume Set. Vol 4.* Elsevier; 2012:331-396. doi:10.1016/B978-0-444-53349-4.00109-6
60. Varghese M, Grinstaff MW. Beyond nylon 6: polyamides via ring opening polymerization of designer lactam monomers for biomedical applications. *Chem Soc Rev.Royal Society of Chemistry.* 2022;51(19):8258-8275. doi:10.1039/d1cs00930c
61. Liu R, Chen X, Falk SP, et al. Structure-activity relationships among antifungal nylon-3 polymers: Identification of materials active against drug-resistant strains of *Candida albicans*. *J Am Chem Soc.* 2014;136(11):4333-4342. doi:10.1021/ja500036r
62. Ravve A. Ring-Opening Polymerizations. In: *Principles of Polymer Chemistry.* Springer New York; 2012:253-327. doi:10.1007/978-1-4614-2212-9_5
63. Bestian H. Poly- β -amides. *Angewandte Chemie International Edition in English.* 1968;7(4):278-285. doi:10.1002/anie.196802781
64. Sebenda J. Lactams. *Makromol Chem.* 74(1):1–10; 1964.
65. Sibikin I, Karger-Kocsis J. Toward industrial use of anionically activated lactam polymers: Past, present and future. *Advanced Industrial and Engineering Polymer Research.KeAi Communications Co.* 2018;1(1):48-60. doi:10.1016/j.aiepr.2018.06.003
66. Hashimoto K. Ring-Opening Polymerization of Lactams. *Living Anionic Polymerization and Its Applications.* Springer; 2012:1–40.

67. Ageyeva T, Sibikin I, Karger-Kocsis J. Polymers and related composites via anionic ring-opening polymerization of lactams: Recent developments and future trends. *Polymers (Basel)*. MDPI AG. 2018;10(4). doi:10.3390/polym10040357
68. Frunze TM, Kurashv V V, Kotel'nikov VA, Volkova T V. Activators of the Anionic Polymerisation of Lactams. Vol 48.; 1979.
69. Merna J, Chromcová D, Brožek J, Roda J. Polymerization of lactams: 97. Anionic polymerization of ϵ -caprolactam activated by esters. *Eur Polym J*. 2006;42(7):1569-1580. doi:10.1016/j.eurpolymj.2006.01.003
70. Wu J, Yu TL, Chen CT, Lin CC. Recent developments in main group metal complexes catalyzed/initiated polymerization of lactides and related cyclic esters. *Coord Chem Rev*. 2006;250(5-6):602-626. doi:10.1016/j.ccr.2005.07.010
71. Zhang X, Fevre M, Jones GO, Waymouth RM. Catalysis as an Enabling Science for Sustainable Polymers. *Chem Rev*. American Chemical Society. 2018;118(2):839-885. doi:10.1021/acs.chemrev.7b00329
72. Bogaert JC, Coszach P. Poly(lactic acids): A potential solution to plastic waste dilemma. In: *Macromolecular Symposia*. Vol 153. John Wiley and Sons Ltd; 2000:287-303. doi:10.1002/1521-3900(200003)153:1<287::AID-MASY287>3.0.CO;2-E
73. Drumright RE, Gruber PR, Henton DE. Polylactic acid technology. *Advanced Materials*. 2000;12(23):1841-1846. doi:10.1002/1521-4095(200012)12:23<1841::AID-ADMA1841>3.0.CO;2-E
74. Houk KN, Jabbari A, Hall HK, Alemán C. Why δ -valerolactone polymerizes and γ -butyrolactone does not. *Journal of Organic Chemistry*. 2008;73(7):2674-2678. doi:10.1021/jo702567v
75. Hong M, Chen EY -X. Towards Truly Sustainable Polymers: A Metal-Free Recyclable Polyester from Biorenewable Non-Strained γ -Butyrolactone. *Angewandte Chemie*. 2016;128(13):4260-4265. doi:10.1002/ange.201601092
76. Albertsson AC, Varma IK. Recent developments in ring opening polymerization of lactones for biomedical applications. *Biomacromolecules*. 2003;4(6):1466-1486. doi:10.1021/bm034247a
77. Odian G. *Principles of Polymerization*. 4th ed. John Wiley & Sons, Inc.; 2004. ISBN 0-471-27400-3.
78. Guy N, Giani O, Blanquer S, Pinaud J, Robin JJ. Photoinduced ring-opening polymerizations. *Prog Org Coat*. Elsevier B.V. 2021;153. doi:10.1016/j.porgcoat.2021.106159
79. Jerome R, Teyssie P. Kinetics of polymerization initiated by charged nucleophiles 502 34.2.1 P-Propiolactone 502 34.2.2 OL,OL-Disubstituted Fi.
80. Baško M, Kubisa P. Cationic copolymerization of ϵ -caprolactone and L,L-lactide by an activated monomer mechanism. *J Polym Sci A Polym Chem*. 2006;44(24):7071-7081. doi:10.1002/pola.21712
81. Kojic D. *Diploma Thesis Spirocyclic Monomers for Hot Lithography Technology*; 2021. doi:10.34726/hss.2021.76701
82. Dubois P, Jérôme R. Recent Advances in Ring-Opening Polymerization of Lactones and Related Compounds. *Journal of Macromolecular Science, Part C*. 1995;35(3):379-418. doi:10.1080/15321799508014594

83. Basko M. Activated monomer mechanism in the cationic polymerization of L,L-lactide. *Pure and Applied Chemistry*. 2012;84(10):2081-2088. doi:10.1351/PAC-CON-11-10-19
84. Kaur P. Anionic, cationic and co-ordination insertion ring-opening polymerization mechanisms of polylactide using various initiators. *International Journal of Creative Research Thoughts (IJCRT)*, Vol 11.; 2023.
85. Shakaroun R. Synthesis of Original PHAs by ROP of Functional β -Lactones : Mechanistic Insights and Stereoselectives Catalysis. <https://theses.hal.science/tel-03847885v1>
86. Dubois Philippe, Coulembier Olivier, Raquez JMarie. *Handbook of Ring-Opening Polymerization*. Wiley-VCH; 2009.
87. Duda A, Kowalski A. *Handbook of Ring-Opening Polymerization*; 2009.
88. Penczek S. On the mechanism of polymerization of cyclic esters induced by Tin(II) Octoate. *Macromolecular Symposia*, 157, 61–70; 2000.
89. Uhrich KE, Cannizzaro SM, Langer RS, Shakesheff KM. Polymeric Systems for Controlled Drug Release. *Chem Rev*. 1999;99(11):3181-3198. doi:10.1021/cr940351u
90. Arbaoui A, Redshaw C. Metal catalysts for ϵ -caprolactone polymerisation. *Polym Chem*. 2010;1(6):801-826. doi:10.1039/b9py00334g
91. Chisholm MH, Zhou Z. New generation polymers: The role of metal alkoxides as catalysts in the production of polyoxygenates. In: *Journal of Materials Chemistry*. Vol 14. 2004:3081-3092. doi:10.1039/b405489j
92. Serhan M, Sprowls M, Jackemeyer D, et al. Total iron measurement in human serum with a smartphone. In: *AIChE Annual Meeting, Conference Proceedings*. Vol 2019-November. American Institute of Chemical Engineers; 2019. doi:10.1039/x0xx00000x
93. Roda J, Kmfnek I, Krhlieek J. Polymerization of Lactams, 23*) Non-Activated Polymerization of 2-Pyrrolidone Initiated with Potassium Tert-Butoxide. Vol 179.; 1978.
94. Sangermano M, Tonin M, Yagci Y. Degradable epoxy coatings by photoinitiated cationic copolymerization of bisepoxide with ϵ -caprolactone. *Eur Polym J*. 2010;46(2):254-259. doi:10.1016/j.eurpolymj.2009.10.023
95. Barker IA, Dove AP. Triarylsulfonium hexafluorophosphate salts as photoactivated acidic catalysts for ring-opening polymerisation. *Chemical Communications*. 2013;49(12):1205-1207. doi:10.1039/c2cc38114a
96. Suyama K, Shirai M. Photobase generators: Recent progress and application trend in polymer systems. *Progress in Polymer Science (Oxford)*. 2009;34(2):194-209. doi:10.1016/j.progpolymsci.2008.08.005
97. Kuroishi PK, Dove AP. Photoinduced ring-opening polymerisation of L-lactide: Via a photocaged superbase. *Chemical Communications*. 2018;54(49):6264-6267. doi:10.1039/c8cc01913d
98. Placet E, Pinaud J, Gimello O, Lacroix-Desmazes P. UV-Initiated Ring Opening Polymerization of L-Lactide Using a Photobase Generator. *ACS Macro Lett*. 2018;7(6):688-692. doi:10.1021/acsmacrolett.8b00251
99. Pei HW, Ye K, Shao Y, et al. Photopolymerization activated by photobase generators and applications: from photolithography to high-quality photoresists. *Polym Chem.Royal Society of Chemistry*. 2024;15(4):248-268. doi:10.1039/d3py00992k

100. Yu S, Reddy O, Abaci A, et al. Novel BODIPY-Based Photobase Generators for Photoinduced Polymerization. *ACS Appl Mater Interfaces*. 2023;15(38):45281-45289. doi:10.1021/acsami.3c09326
101. Honda S. Organocatalytic vat-ring-opening photopolymerization enables 3D printing of fully degradable polymers. *Commun Chem.Nature Research*. 2023;6(1). doi:10.1038/s42004-023-00985-4
102. WPBG-266|CAS:1632211-89-2|FUJIFILM Wako Chemicals Europe GmbH. Accessed April 19, 2025. <https://specchem-wako.fujifilm.com/europe/de/photo-base-generators/WPBG-266.htm>
103. WPBG-300|CAS:1801263-71-7|FUJIFILM Wako Chemicals Europe GmbH. Accessed April 19, 2025. <https://specchem-wako.fujifilm.com/europe/de/photo-base-generators/WPBG-300.htm>
104. Glasovac Z, Eckert-Maksić M, Maksić ZB. Basicity of organic bases and superbases in acetonitrile by the polarized continuum model and DFT calculations. *New Journal of Chemistry*. 2009;33(3):588-597. doi:10.1039/b814812k
105. Penczek S, Pretula J, Slomkowski S. Ring-opening polymerization. *Chemistry Teacher International.Walter de Gruyter GmbH*. 2021;3(2):33-57. doi:10.1515/cti-2020-0028
106. Munzeiwa WA, Omondi BO, Nyamori VO. A perspective into ring-opening polymerization of ϵ -caprolactone and lactides: effect of, ligand, catalyst structure and system dynamics, on catalytic activity and polymer properties. *Polymer Bulletin.Springer Science and Business Media Deutschland GmbH*. 2024;81(11):9419-9464. doi:10.1007/s00289-024-05149-5
107. Alamri H, Zhao J, Pahovnik D, Hadjichristidis N. Phosphazene-catalyzed ring-opening polymerization of ϵ -caprolactone: Influence of solvents and initiators. *Polym Chem*. 2014;5(18):5471-5478. doi:10.1039/c4py00493k
108. Crivello J V., Jang M. Anthracene electron-transfer photosensitizers for onium salt induced cationic photopolymerizations. *J Photochem Photobiol A Chem*. 2003;159(2):173-188. doi:10.1016/S1010-6030(03)00182-5
109. Wloka T, Gottschaldt M, Schubert US. From Light to Structure: Photo Initiators for Radical Two-Photon Polymerization. *Chemistry - A European Journal.John Wiley and Sons Inc*. 2022;28(32). doi:10.1002/chem.202104191
110. Idacavage - The Use of Anthracene Derivatives in UV-LED Curing Additives.
111. Fouassier JP, Morlet-Savary F, Lalevée J, Allonas X, Ley C. Dyes as photoinitiators or photosensitizers of polymerization reactions. *Materials*. 2010;3(12):5130-5142. doi:10.3390/ma3125130
112. Su WF. Ring-Opening Polymerization. In: 2013:267-299. doi:10.1007/978-3-642-38730-2_11
113. Olsén P, Odelius K, Albertsson AC. Thermodynamic Presynthetic Considerations for Ring-Opening Polymerization. *Biomacromolecules.American Chemical Society*. 2016;17(3):699-709. doi:10.1021/acs.biomac.5b01698
114. Photo curing|FUJIFILM Wako Chemicals Europe GmbH. Accessed April 19, 2025. <https://labchem-wako.fujifilm.com/us/category/00203.html>
115. Ito, K. Radiation-curable composition by anionic polymerization. European Patent Application EP19179164.9; 2020.

116. Ibrahim A, Stefano L Di, Tarzi O, Tar H, Ley C, Allonas X. High-performance photoinitiating systems for free radical photopolymerization. Application to holographic recording. *Photochem Photobiol.* 2013;89(6):1283-1290. doi:10.1111/php.12132
117. Kumar A, Von Wolff N, Rauch M, et al. Hydrogenative Depolymerization of Nylons. *J Am Chem Soc.* 2020;142(33):14267-14275. doi:10.1021/jacs.0c05675
118. Iwamoto R, Murase H. Infrared Spectroscopic Study of the Interactions of Nylon-6 with Water. Vol 41.; 2003.
119. Oshiro M, Takashima K, Furukawa Y. Infrared Stark spectra for a Nylon 6 film. *Chem Phys Lett.* 2019;728:32-36. doi:10.1016/j.cplett.2019.04.068
120. Farias-Aguilar JC, Ramírez-Moreno MJ, Téllez-Jurado L, Balmori-Ramírez H. Low pressure and low temperature synthesis of polyamide-6 (PA6) using NaO as catalyst. *Mater Lett.* 2014;136:388-392. doi:10.1016/j.matlet.2014.08.071
121. Yang H, Zhao J, Yan M, Pispas S, Zhang G. Nylon 3 synthesized by ring opening polymerization with a metal-free catalyst. *Polym Chem.* 2011;2(12):2888-2892. doi:10.1039/c1py00334h
122. Motiwala HF, Armaly AM, Cacioppo JG, et al. HFIP in Organic Synthesis. *Chem Rev.American Chemical Society.* 2022;122(15):12544-12747. doi:10.1021/acs.chemrev.1c00749
123. Dworak C, Kopeinig S, Hoffmann H, Liska R. Photoinitiating monomers based on di- And triacryloylated hydroxylamine derivatives. *J Polym Sci A Polym Chem.* 2009;47(2):392-403. doi:10.1002/pola.23156
124. Dane EL, Grinstaff MW. Poly-amido-saccharides: Synthesis via Anionic Polymerization of a β -Lactam Sugar Monomer. *J Am Chem Soc.* 2012;134(39):16255-16264. doi:10.1021/ja305900r
125. Tran H, Toland A, Stellmach K, Paul MK, Gutekunst W, Ramprasad R. Toward Recyclable Polymers: Ring-Opening Polymerization Enthalpy from First-Principles. *Journal of Physical Chemistry Letters.* 2022;13:4778-4785. doi:10.1021/acs.jpcllett.2c00995
126. Kanwar S, Sharma SD. (Chloromethylene)Dimethylammonium Chloride: A Highly Efficient Reagent for the Synthesis of β -Lactams from β -Amino Acids.
127. Fang Y, Rogness DC, Larock RC, Shi F. Formation of acridones by ethylene extrusion in the reaction of arynes with β -lactams and dihydroquinolinones. *Journal of Organic Chemistry.* 2012;77(14):6262-6270. doi:10.1021/jo3011073
128. Dzygiel P, Monti C, Piarulli U, Gennari C. Efficient resolution of racemic N-benzyl β -amino acids by iterative liquid-liquid extraction with a chiral (salen)cobalt(iii) complex as enantioselective selector. *Org Biomol Chem.* 2007;5(21):3464-3471. doi:10.1039/b711477j
129. Odian G. Principles of Polymerization (4th ed.). New York: John Wiley & Sons. ISBN 0-471-27400-3; 2004.
130. Pandey RK, Gupta M, Rajput CS, Singh AS. Synthesis of N-acyl-benzotriazole using Mukaiyama reagent. *Arkivoc.* 2023;2023(7). doi:10.24820/ark.5550190.p012.042
131. Huang H, Iwasawa N, Mukaiyama T. Convenient Method for the Construction of β -Lactam Compounds from β -Amino Acids Using 2-Chloro-1-Methylpyridinium Iodide as Condensing Reagent. *Chem. Soc. Jpn;* 1984.136. Mukaiyama T, Usui M, Saigo K. The Facile Synthesis of Lactones; 1976.

132. Mukaiyama T, Usui M, Saigo K. The facile synthesis of lactones; 1976.
133. Kulikov O V., Incarvito C, Hamilton AD. Hydrophobic side-chain interactions in a family of dimeric amide foldamers-potential alpha-helix mimetics. *Tetrahedron Lett.* 2011;52(29):3705-3709. doi:10.1016/j.tetlet.2011.05.004
134. Murayama T, Kobayashi T, Miura T. A Convenient Preparative Method for β -Lactams from [3-Amino Acids Using Sulfenamide/Triphenylphosphine. Vol 36.; 1995.
135. Loewe MF, Cvetovich RJ, Hazen GG. S-Amino Acid Cyclodehydration Using Methanesulfonyl Chloride to Thienamycin Intermediate 3-[l-Hydroxyethyl]-4-[Methoxycarbonylmethyl]-Azetidin-2-One. Volume 32, 1991.
136. Gabbott P. A Practical Introduction to Differential Scanning Calorimetry. 2nd Edition; John Wiley & Sons: Chichester, UK, 2008.
137. Balushev S, Miteva T, Yakutkin V, Nelles G, Yasuda A, Wegner G. Up-conversion fluorescence: Noncoherent excitation by sunlight. *Phys Rev Lett.* 2006;97(14). doi:10.1103/PhysRevLett.97.143903
138. Aguirre-Soto A, Lim CH, Hwang AT, Musgrave CB, Stansbury JW. Visible-light organic photocatalysis for latent radical-initiated polymerization via 2e-/1H+ transfers: Initiation with parallels to photosynthesis. *J Am Chem Soc.* 2014;136(20):7418-7427. doi:10.1021/ja502441d
139. Lalevée Jacques, Fouassier JPierre. Dyes and Chromophores in Polymer Science. Wiley; 2015.
140. Więckowska A, Wichur T, Godyń J, et al. Novel Multitarget-Directed Ligands Aiming at Symptoms and Causes of Alzheimer's Disease. *ACS Chem Neurosci.* 2018;9(5):1195-1214. doi:10.1021/acchemneuro.8b00024
141. Huang H, Iwasawa N, Mukaiyama T. β -Lactam Analogues of Oxotremorine. 3-and 4-Methyl-Substituted 2-Azetidinones. Vol 33.; 1990.